ISTANBUL TECHNICAL UNIVERSITY ★ GRADUATE SCHOOL OF SCIENCE ENGINEERING AND TECHNOLOGY

INVESTIGATION OF POLY(DIMETHYLSILOXANE) ADDITIVES ON POLYETHYLENE BLEND BASED NANOCOMPOSITES

M.Sc. THESIS

Duygu ÇAKIR

Department of Polymer Science and Technology

Polymer Science and Technology Program

MAY 2014

ISTANBUL TECHNICAL UNIVERSITY ★ GRADUATE SCHOOL OF SCIENCE ENGINEERING AND TECHNOLOGY

INVESTIGATION OF POLY(DIMETHYLSILOXANE) ADDITIVES ON POLYETHYLENE BLEND BASED NANOCOMPOSITES

M.Sc. THESIS

Duygu ÇAKIR
(515111037)

Department of Polymer Science and Technology

Polymer Science and Technology Program

Thesis Advisor: Prof. Dr. Nurseli UYANIK

MAY 2014

İSTANBUL TEKNİK ÜNİVERSİTESİ ★ FEN BİLİMLERİ ENSTİTÜSÜ

POLİ(DİMETİLSİLOKSAN) KATKISININ POLİETİLEN HARMAN MATRİSLİ NANOKOMPOZİTLERE ETKİSİNİN ARAŞTIRILMASI

YÜKSEK LİSANS TEZİ

Duygu ÇAKIR
(515111037)

Polimer Bilim ve Teknolojileri Bölümü

Polimer Bilim ve Teknolojileri Programı

Tez Danışmanı: Prof. Dr. Nurseli UYANIK

MAYIS 2014

To my mother,

FOREWORD

Words stay short in expressing my sincere appreciation and gratitude to my thesis supervisor, Prof. Dr. Nurseli UYANIK for her infinite support, guidance and helpful suggestions throughout my research. It was a great honour and pleasure to work with her and benefit from her experience.

I would like to express my deepest thanks and appreciation to Dr. Tolga GÖKKURT, Technical Manager of Polipro Plastic, for his endless endevours and invaluable support during this difficult period. I could not accomplish this work without him.

I also would like to express my thanks to Assoc. Prof. Dr. Güralp ÖZKOÇ from Kocaeli University, Department of Chemical Engineering, for providing me an opportunity to make my contact angle measurements at Kocaeli University, Polymer Laboratory.

I would like to thank Tuğba UÇAR DEMİR from Eczacıbaşı ESAN Company for providing me XRD analysis of my samples.

My personal thanks are to Buket ŞENTÜRK, Mert Emre ÖZTOKSOY, Hilal GÜNEYSU and Hakan GÖKÇE from ITU for their friendship and support.

I would like to thank my childhood friend Buse FIRAT for all her emotional assist and motivation during this extremely difficult accomplishment.

Most of all, I would like to thank my family, especially my mother Ayşe Sema OĞUZ and my father Dr.Sabahattin ÇAKIR for supporting me all my life. For all those times they stood by me and heartedly supported. I was able to accomplish everything in my life thanks to their eternal love and trust.

May 2014

Duygu ÇAKIR

Chemical Engineer

TABLE OF CONTENTS

Page

ABBREVIATIONS

C	**:** Compatibilizer
DSC	**:** Differential scanning calorimetry
EMA	**:** Ethylene-co-methylacrylate
HDPE	**:** High density polyethylene
L/D	**:** Length to diameter ratio
LDPE	**:** Low density polyethylene
LLDPE	**:** Linear low density polyethylene
MFI	**:** Melt flow index
MFR	**:** Melt flow rate
MMT	**:** Montmorillonite
mPE	**:** Metallocene polyethylene
MWD	**:** Molecular weight distribution
O-MMT	**:** Organomodified montmorillonite
PA6	**:** Polyamide-6
PA66	**:** Polyamide-66
PDMS	**:** Poly(dimethylsiloxane)
PE	**:** Polyethylene
PE-g-MA	**:** Polyethylene-grafted maleic anhydride
PEO	**:** Polyethylene oxide
PET	**:** Polyethylene terephthalate
PI	**:** Polyimide
PS	**:** Polystyrene
PU	**:** Polyurethane
RPM	**:** Revolutions per minute
SEM	**:** Scanning electron microscopy
SiO_2	**:** Silicon dioxide, silica
TEM	**:** Transmission electron microscopy
TGA	**:** Thermal gravimetric analysis
UV	**:** Ultraviolet light
XRD	**:** X-ray diffraction

LIST OF SYMBOLS

E	**:** Modulus of elasticity
Tc	**:** Crystallization temperature
Tg	**:** Glass transition temperature
Tm	**:** Melting temperature
To	**:** Onset temperature
Tp	**:** Significant peak temperature
ΔH_c	**:** Crystallization enthalpy
ΔH_f	**:** Heat of fusion
ΔH_m	**:** Melting enthalpy
Xc	**:** Degree of crystallinity
θ	**:** Contact angle
θ_{PE}	**:** PE fraction in composition
σ_M	**:** Tensile strength
σ_B	**:** Strength at break
ε_M	**:** Elongation at break

LIST OF TABLES

Page

LIST OF FIGURES

Page

INVESTIGATION OF POLY(DIMETHYLSILOXANE) ADDITIVES ON POLYETHYLENE BLEND BASED NANOCOMPOSITES

SUMMARY

Polymeric materials have been filled with natural or synthetic materials (calcium carbonate, glass fibers, mica etc.) in order to improve their properties or reduce cost. Although conventional filled or reinforced polymers are widely used in various applications, there are some drawbacks such as increase in weight, opacity and brittleness.

Nanocomposites are a new class of composites which at least one dimensions of the dispersed particles is in the nanometer scale (nanotubes, nanowhiskers, layered crystals, layered clays etc.). Clay and layered-silicate materials have been widely investigated because of the ease of their accessibility and their intercalation chemistry has been studied for a long time.

Research in layered-silicate based polymer nanocomposites has progressed rapidly in the last couple of decades due to the fact that the addition of small amounts of nanoclays may produce properties equivalent to those of traditional composites and their potential as a low-cost alternative for applications ranging from automotive and food packaging to biomedical engineering applications. Generally, the mechanical performance, thermal stability, barrier properties, chemical resistance, and flame retardancy of the polymers are enhanced with the addition of layered-silicates, without sacrificing processability, density and ease of recycling.

Polymer-clay nanocomposites are generally produced by solution dispersion, in situ polymerization and melt intercalation. Among the other methods, melt intercalation has become a mainstream for the preparation of polymer-clay nanocomposites. One of the main difficulties in the production is the dispersion of the filler in the polymeric matrix, especially when the matrix is a non-polar polyolefin, because of the intrinsic incompatibility of hydrophilic layered silicates and hydrophobic polymer. Two actions are taken in order to overcome this problem, the modification of the hydrophilic nature of clay (organo-modified clay) and the addition of a small amount of compatibilizer. Montmorillonite is a natural layer-silicate clay with an aspect ratio higher than 100 frequently used in polymer nanocomposites. Its modification is generally done by the exchange of small surface cations with alkylammonium cations. Maleic anhydride-grafted polyolefins are introduced in the formulations as interfacial agents or compatibilizers in the polyolefin based nanocomposites. In the case of nanocomposites based on polyethylene, ethylene copolymers and functionalized polymers such as grafted polyethylene are frequently used to enhance the filler–matrix compatibility.

Polyethylene (PE) is one of the most consumed polymers in the world. The use of this polymer is highly extended because of its extraordinary versatility in properties, applications, and low cost. Due to the nature and characteristics of PE, it can be

found in variety of applications, such as electrical wires and cables, adhesives, films and bags, blow and injection molded articles etc. In the last years, its use in packaging applications, where mechanical, barrier properties, and transparency are important, has increased. Eventhough polyethylenes are versatile and offer wide range of applications, they have some shortcomings such as high permability to gases, low stress crack resistance and low temperature toughness. There has been an attempt to improve mechanical, thermal and barrier properties of polyethylene by incorporation of conventional fillers. But in the last decade, a great interest in polyethylene based polymer-layered silicate nanocomposites has emerged.

The development of metallocene catalyst technology has enabled new polyolefins with enhanced structural uniformity, mechanical, and optical properties, resulting from improved control of chain branching and narrower molecular weight distribution during polymerization. This combination of properties enables the extension of mPE applications into areas traditionally dominated by other thermoplastic materials. As a result, global consumption of metallocence polyethylene (mPE) resins has been virtually doubling every year since their commercialization in 1995. mPE has been widely used in film and molding products although its cost is higher than the traditional PE. On the other hand, the poor melt strength and high melting temperature cause it difficult to process mPE melt into high quality products, so that some traditional PE such as LDPE (low density polyethylene) and conventionally produced LLDPE (linear low density polyethylene), are blended with mPE to not only improve the rheology properties but also lower the cost of the final product.

Polysiloxanes or silicones, the most important of the inorganic backbone polymers, are very interesting materials in a large variety of applications ranging from microelectronics to building materials. They have quite unique properties such as high chemical and thermal stability, low temperature toughness, very low glass transition temperature (Tg), low surface energy (high hydrophobicity), good optical clarity, UV resistance and electrical-insulation. While polymer layered-silicate nanocomposites have generated over a thousand publications, only a few deal with polysiloxanes. In some researches, the evidence of intercalation or exfoliation by the addition of silicones in clay nanocomposites has motivated the use of polysiloxanes as swelling or intercalating agent in layered-silicate nanocomposites.

In this study, the effects of the poly(dimethylsiloxane) (PDMS) additives and the composition of the low density polyethylene/metallocene polyethylene (LDPE/mPE) blends, on the morphology, thermal and the mechanical properties of the organo-modified montmorillonite (O-MMT) containing nanocomposites were investigated. LDPE was blended with mPE at varying compositions by melt blending via extrusion. The extruder was an intermeshing co-rotating 27 mm diameter twin-screw extruder with L/D ratio of 48 consisted of one main volumetric feeder, two side volumetric feeders, thirteen heating zones, and degassing unit before the die segment and a strand die with five holes. The screws have contained different screw elements such as nine conveying blocks and seven kneading blocks. The polymer melt leaving the extruder from the die segment cooled down into a water bath and obtained as spaghettis that are cut into small pieces by the granulating unit. A commercial maleic anhydride grafted LLDPE (PE-g-MA) was used as a compatibilizer.

An optimization study was carried out to determine the optimum temperature profile and screw speed for processing the nanocomposites. After this optimization,

70/165/175/175/185/185/190/195/195/195/205/205/205°C temperature profile, from hopper to die, and 450 rpm screw speed have decided for the processing conditions.

Twenty different samples were prepared and the weight percents of the LDPE and mPE in the blends were varied from 0 to 100. Different composition PE blend based nanocomposites containing 5 parts per hundred resin (phr) O-MMT clay and 15 phr PE-g-MA compatibilizer with 5 and 10 phr PDMS were prepared. The samples with the same compositions of nanoclay, compatibilizer and LDPE/mPE and samples composed of neat LDPE/mPE blends were also prepared for comparison. The test specimens according to ISO standards were prepared by an injection molding machine with a special mold design. Mechanical, thermal, structural and morphological properties of the samples were analyzed by tensile tests, hardness tests, impact tests, differential scanning calorimetry (DSC) analysis, melt flow index (MFI), X-ray diffraction (XRD), and contact angle analysis, respectively. Actual filler contents of the samples were determined by the ash content test.

Mechanical property analysis of the samples showed that PDMS addition to the nanocomposites had a pronounced effect on the mechanical properties. Generally, modulus of elasticity is decreasing while the elongation at break is increasing with the increasing amount of PDMS. Izod impact strength and hardness of the samples are decreasing with the PDMS addition. The hardest samples are found to be the nanocomposites without PDMS. The varying amounts of LDPE and mPE have caused the same trends in the mechanical test results of neat PE blends and nanocomposites with/without PDMS.

Thermal properties and the crystallization behaviours of the nanocomposites were investigated by DSC analysis. The degree of crystallinies (Xc) are decreasing with increasing PDMS content. This situation is significantly observed in LDPE rich nanocomposites. In the nanocomposites composed of mPE matrices, the Xc values are higher and getting lower with the addition of LDPE into the blends.

XRD patterns of the nanocomposites showed that polyolefin chains had separated the organoclay layers by penetrating between these layers. In the 100% LDPE samples containing 5 and 10 phr PDMS, it was observed that PDMS had contributed to the separation of the clays layers. However, in the samples containing 50% LDPE and 50% mPE, the addition of PDMS did not have a significant effect on the exfoliation of the nanoclay.It was observed that the 10 phr PDMS containing 100% mPE sample, showed the best result, it can be concluded that partial exfoliation had formed.

MFI results revealed that nanoclay and compatibilizer addition causes poor flow properties. It was observed that neat PE blends have higher MFI values comparing to nanocomposites both with/without PDMS. The different PDMS adding has no significant effect on MFI values. Different PE blend formulations did not affect the flow properties of the nanocomposites and the same trend was obtained in all the samples.

Contact angle values are low in the nanocomposites containing only O-MMT and PE-g-MA. This is because of the hydrophilic nature of the clay. An increase in the contact angles and values above 90° were obtained with the addition of PDMS and higher values were observed with more PDMS content. PDMS low surface energy and hydrophobic structure is the reason of this result. mPE contact angle values measured lower than LDPE and a decrease in values was observed in mPE rich blend based samples.

POLİ (DİMETİLSİLOKSAN) KATKISININ POLİETİLEN HARMAN MATRİSLİ NANOKOMPOZİTLERE ETKİSİNİN ARAŞTIRILMASI

ÖZET

Polimerik malzemeler özelliklerinin geliştirilmesi veya maliyetlerinin düşürülmesi maksadıyla doğal ya da sentetik malzemeler kullanılarak (kalsiyum karbonat, cam elyaf, mika vb.) güçlendirilmişlerdir. Geleneksel şekilde dolgulanmış veya güçlendirilmiş polimerler birçok uygulamada kullanılmalarına rağmen ağırlık artışı, opaklık ve kırılganlık gibi bazı dezavantajlara sahiptirler.

Nanokompozitler kompozit malzemelerin yeni bir sınıfını oluştururlar ve matriste dağılmış partiküllerin en az bir boyutlarının nanometre ölçeğinde olması gerekmektedir. Günümüzde değişik araştırmalarda rastladığımız nanotüpler, tabakalı kristaller ve tabakalı killer nanokatkılara örnek olarak verilebilirler. Diğer nanokatkılara kıyasla killer ve tabakalı killer üzerinde yoğun çalışmalar yapılmaktadır. Bunun sebebi killerin kolay elde edilebilir olmaları ve katmanlar arası yapılarının uzun zamandır inceleniyor olmasıdır.

Tabakalı silikatlı polimer nanokompozit araştırmaları geçtiğimiz birkaç yıl içerisinde hızla artmıştır. Nanokillerin yapıya az miktarda eklenmesi ile geleneksel yöntemlerle hazırlanan kompozit malzemelerin özelliklerine eşdeğer özellikler elde edilmesi ve otomotivden gıda ambalajlarına ve biyomedikal mühendislik uygulamalarına kadar pek çok değişik alanda düşük maliyetli alternatifler olma potansiyalleri bu çalışmaların artmasına sebep olmuştur. Tabakalı silikatların yapıya eklenmesi ile polimerlerin mekanik özellikleri, termal dayanımları, gaz geçirgenlik özellikleri, kimyasal dayanımları ve alev geciktirici özellikleri geliştirilirken işlenebilirlik, yoğunluk ve geridönüşüm gibi özellikleri değişmeden kalmaktadır.

Polimer-kil nanokompozitler genellikle çözelti dispersiyonu, yerinde polimerizayon ve eriyik karıştırma yöntemleri ile üretilirler. Diğer yöntemlerin yanısıra eriyik dağıtma yöntemi polimer-kil nanokillerin üretiminde daha yaygın olarak kullanılmaktadır. Üretimdeki en büyük zorluklardan birisi killerin polimer matriste dağıtılmasıdır. Özellikle apolar poliolefinik matrislerde hidrofilik tabakalı silikatlar ile hidrofobik polimer arasındaki uyumsuzluk sebebiyle killeri dağıtmak daha da zorlaşır. Bu problemin üstesinden gelmek için iki yol izlenir; kilin hidrofilik yapısının modifiye edilmesi (organik modifiye kil) ve yapıya düşük miktarda uyumlaştırıcı girilmesi. Montmorillonit en-boy oranı 100'den büyük olan ve sıklıkla kullanılan bir doğal tabakalı silikat kildir. Montmorillonitin modifikasyonu genellikle yüzey katyonlarının alkilamonyum katyonları ile değiştirilmesi ile gerçekleştirilir. Maleik anhidrit aşılanmış poliolefinler, poliolefin bazlı nanokompozitlerde arayüzey ajanı veya uyumlaştırıcı olarak kullanılırlar. Polietilen bazlı nanokompozitlerde etilen kopolimerleri ve maleik anhidrit aşılanmış polietilenler dolgu ile matris arasındaki etkileşimi arttırmak için kullanılırlar.

Polietilen (PE) dünyada en çok kullanılan polimerlerden birisidir. Çok değişik özelliklere sahip olup birçok alanda kullanılması ve düşük maliyetli olması bu yaygın kullanımının sebeplerindendir. Yapısı ve karakteristik özellikleri polietileni yapıştırıcılardan elektrik kablolarına, gıda ambalajlarından alışveriş torbalarına, oyuncaklardan şampuan şişelerine kadar birçok uygulama ile günlük hayatta karşımıza çıkarmaktadır. Son yıllarda mekanik, gaz geçirgenlik ve şeffaflık gibi özelliklerin önemli olduğu ambalaj uygulamalarında kullanımı gittikçe artmıştır. Ancak polietilen birçok özelliğe ve uygulama alanına sahip olmasına rağmen yüksek gaz geçirgenlik, düşük gerilim dayanımı ve düşük sıcaklık tokluğu gibi bazı eksiklikleri bulunmaktadır. Polietilenin mekanik, termal ve gaz geçirgenlik özelliklerini geliştirmek amacıyla geleneksel dolgular ile kompozitleri çalışılmıştır. Ancak son on yılda polietilen bazlı tabakalı silikatlı nanokompozitlere ilgi artmıştır.

Metalosen kataliz teknolojisinin gelişmesi düzenli yapılara sahip, mekanik ve optik özellikleri gelişmiş poliolefinler üretilmesine olanak sağlamıştır. Bu yöntemle üretilen poliolefinlerde zincir dallanmaları kontrol edilir ve polimerizayon sırasında daha dar molekül ağırlığı dağılımı elde edilebilir. Bu özelliklerin birleşmesi metalosen polietilenin (mPE) birçok alanda diğer termoplastik polimerlerin yerini almasına imkan vermiştir. Sonuç olarak 1995 yılında ticarileşmesinden beri küresel metalosen polietilen kullanımı her yıl iki katına çıkmaktadır. Geleneksel yöntemlerle üretilen polietilenlere kıyasla daha maliyetli olmasına rağmen film ve kalıpla üretilen ürünlerde yaygınca kullanılmaktadır. Ancak öte yandan zayıf eriyik mukavemeti ve yüksek erime sıcaklığı yüksek kalitede ürünler elde edilmesini zorlaştırmaktadır. Bu nedenle geleneksel yöntemlerle üretilmiş LDPE (alçak yoğunluklu polietilen) ve LLDPE (lineer alçak yoğunluklu polietilen) ile harmanlanarak kullanımı yaygınlaşmaktadır. Bu yolla reolojik özellikleri geliştirmenin yanı sıra son ürünün maliyeti de düşürülmektedir.

Polisiloksanlar veya silikonlar inorganik yapıdaki polimerler arasında en önemlilerindendir ve mikroelektronikten yapı-inşaat sektörüne kadar pek çok değişik alanda kullanılmaktadırlar. Yüksek kimyasal ve ısıl dayanım, düşük sıcaklık tokluğu, oldukça düşük camsı geçiş sıcaklığı, düşük yüzey enerjisi (yüksek hidrofobik yapı), optik şeffaflık, UV dayanımı ve elektrik yalıtımı gibi oldukça özgün özelliklere sahiptirler. Tabakalı silikatlı polimerik nanokompozitlerle ilgili birçok çalışma bulunmasına rağmen çok az bir kısmı polisiloksanlarla ilgilidir. Bazı araştırmalarda silikon ilavesi ile sıralı tabakalı ve tabakaları dagıtılmış yapıların elde edilmesi, polisiloksanların nanokompozitlerde şişme ajanı olarak kullanımının araştırılmasına sebep olmuştur.

Bu çalışmada poli(dimetilsiloksan) (PDMS) katkısının ve LDPE/mPE harmanlarının kompozisyonunun organik modifiye kil (O-MMT) içeren nanokompozitlerin morfolojik, termal ve mekanik özelliklerine olan etkisi incelenmiştir. Ticari bir LDPE ve ticari mPE, ekstruder kullanılarak, eriyik karıştırma yöntemiyle değişik kompozisyonlarda harmanlanmıştır. Kullanılan ekstruder, 27 mm çapında, L/D'si 48 olan, bir ana ve iki yan volümetrik dozatöre sahip, vidaları çevreleyen onüç ısıtma bölgesi, kafa bölgesinden önce vent ve beş delikli kafadan oluşan çift vidalı ekstruderdir. Vidalar dokuz adet taşıyıcı blok ve dokuz adet yoğurma blokları gibi değişik vida elemanları ile donatılmıştır. Kafadan spagetti şeklinde çıkarak ekstrüderi terk eden eriyik polimer su banyosunda soğutulduktan sonra granül makinesinde pelletize edilmiştir. Uyumlaştırıcı olarak, ticari bir maleik anhidrit aşılanmış LLDPE (PE-g-MA) kullanılmıştır.

Çalışmanın başında optimum ekstrüzyon sıcaklık profili ve vida hızının belirlenmesi amacıyla bir optimizasyon çalışması yapılmıştır. Bu çalışmanın sonucunda besleme bölgesinden kafaya 70/165/175/175/185/185/190/195/195/195/205/205/205°C sıcaklık profili ve 450 rpm vida hızı proses koşulları olarak belirlenmiştir.

Ağırlıkça LDPE ve mPE yüzdesi 0 ile 100 arasında değişen yirmi farklı örnek hazırlanmıştır. Değişik kompozisyonlarda PE harmanları bazlı, 5 toplam karışıma göre yüzde (phr) oranında O-MMT ve 15 phr PE-g-MA uyumlaştırıcı ve 5 ile 10 phr PDMS içeren nanokompozitler eriyik karıştırma yöntemi kullanılarak hazırlanmıştır. Ayrıca nanokil, uyumlaştırıcı ve LDPE/mPE oranları aynı olan nanokompozitler ve saf LDPE/mPE harmanları karşılaştırma için hazırlanmıştır. ISO standartlarına uygun şekilde test numuneleri özel bir kalıp tasarımına sahip enjeksiyon kalıplama makinesi ile elde edilmiştir. Örneklerin mekanik, termal, yapısal ve morfolojik özellikleri, sırasıyla çekme-kopma testleri, darbe ve sertlik testleri, DSC analizi, eriyik akış hızı (MFI) analizi, X-ışını kırınımı ve temas açısı ölçümleri ile incelenmiştir. Örneklerin gerçek dolgu miktarı kül testi ile belirlenmiştir.

Örneklerin mekanik karakterizasyonunda, nanokompozitlere PDMS ilavesinin ürünlerin mekanik özelliklerini belirgin bir biçimde etkilediğini ortaya koymuştur. Genel olarak, artan PDMS miktarı ile örneklerin elastisite modülü azalırken kopmada uzma değerlerinde artış gözlenmiştir. Izod darbe dayanımı ve sertlik değerleri PDMS ilavesi ile azalmaktadir. En sert örnekler PDMS içermeyen nanokompozitler olarak tespit edilmiştir. Değişen LDPE ve mPE miktarları, saf PE harmanları ve PDMS içeren/içermeyen nanokompozitlerin mekanik test sonuçlarında aynı trendi göstermiştir.

Tüm karışımların ısıl özellikleri DSC analizi ile incelenmiştir. Örneklerin kristallenme dereceleri (Xc) artan PDMS miktarı ile azalmaktadır. Bu durum LDPE zengin nanokompozitlerde daha belirgin olarak gözlenmektedir. mPE matrisli nanokompozitlerde kristallenme dereceleri daha yüksek değerlerdedir ve harmanlardaki LDPE miktarı arttıkça değerler düşüş göstermektedir.

XRD'leri çekilen nanokompozitlerde, poliolefin zincirlerinin organokilin tabakaları arasına girerek tabakaları açtığı gözlenmiştir. Sonuçlardan 100% LDPE içeren 5 phr ve 10 phr PDMS'li örneklerde PDMS'in tabakaların açılmasına katkı sağladığı anlaşılmıştır. Ancak, 50% mPE ve 50% LDPE içeren örneklerde PDMS katkısının tabakaların arasının açılmasına önemli bir etki yapmamış olduğu da görülmüştür. En iyi sonuç 100% mPE'li örneklerde 10 phr PDMS içeren örnektir. Bu örnek için tabakaların kısmen dağılmış olduğu söylenebilir.

Eriyik akış hızı (MFI) analiz sonuçları nanokil ve uyumlaştırıcı ilavesinin düşük akış özelliklerine sebep olduğunu göstermiştir. Saf PE harmanlarının PDMS içeren/içermeyen nanokompozitlere göre daha yüksek MFI değerlerine sahip oldukları gözlenmiştir. Değişik miktarlarda PDMS ilavesinin MFI değerleri üzerinde önemli bir etkisi yoktur. PE harmanlarının değişen oranlarının akış özelliklerini etkilemediği görülüp tüm örneklerde aynı eğilim elde edilmiştir.

Sadece O-MMT ve PE-g-MA içeren nanokompozitlerin temas açısı değerleri düşük çıkmıştır, bu durum kilin hidrofilik yapısıyla açıklanabilir. PDMS ilavesi ile 90°'nin üzerinde temas açısı değerleri elde edilmiş olup artan PDMS miktarı ile değerlerin daha da arttığı gözlenmiştir. PDMS'in düşük yüzey enerjisi ve hidrofobik yapısından dolayı bu sonuçlar elde edilmiştir. Yapılan testlerde mPE'in temas açısı değeri LDPE'e kıyasla daha düşük olarak elde edildiği için mPE zengin harmanlı örneklerin temas açısı değerleri daha düşüktür.

1. INTRODUCTION

Polyethylene is one of the most consumed polymers in the world. Polyethylene has various types mostly categorized by branching and density, offering different properties and applications. Although polyethylene is a low cost material and has versatile applications, it has some obstacles such as poor stiffness, high permeability to gases, and low melting behaviour. There has been an attempt to improve its mechanical, thermal and barrier properties by incorporation of fillers. Conventional fillers such as silica, glass fiber, talc, wood flour, cellulose, etc, have been used to form traditional microcomposites with enhanced properties.

In recent years, a lot of work has been concerned with nanocomposites based on a polymer matrix and layered silicates, more specifically organomodified montmorillonite clays. With the incorporation of layered nanoclays as fillers, having high aspect ratio (length/ thickness) and thickness in the nanometer range, it has been possible to improve mechanical, thermal and barrier properties at lower loadings (usually less than 10%) than for conventional fillers. These improved properties may be due to the synergic effects of nanoscaled structure and the resulting enlarged interaction of the layered inorganic materials with the polymer molecules [1].

Melt compounding or melt intercalation is one of the most convenient and common process to obtain nanocomposites. The dispersion state of the nanoplatelets depends not only extrusion parameters such as temperature, shear rate, and screw profile, but also on the interactions between silicate layers and the polymer. This is very essential to obtain a well dispersion of the platelets in the polymer matrix to get an exfoliated morphology. For polymer matrices such as polyolefins, it is very difficult to obtain the exfoliation of the clay layers, even intercalated morphologies. The hydrophobic character of polyethylene prevents the development of strong interactions with the surfaces of the montmorillonites especially the galleries in which the polymer chains need to be inserted for intercalated or exfoliated structures. Two ways are used to improve these interactions: alkyl quaternary ammonium ions are used to modify the

clays and maleic anhydride-grafted polyolefins are introduced in the formulations as interfacial agents or compatibilizers [2].

In recent years, in order to obtain the desired structures, there has been an attempt to use different types of silicone based polymers.

Although polymer/layered silicate nanocomposites have generated over a thousand publications, only a very few of them describe the use of polysiloxanes. Evidence of intercalation/delamination of silicone fluids in montmorillonite clays, without any solvent assistance or high shear, has been associated to the highly unusual surface properties of poly(dimethylsiloxane) (PDMS) and the similar structure of the PDMS backbone with that of clay layers. This result motivated the use of this polymer as swelling or intercalating agent in layered silicates, giving rise to silicone/clays systems [3].

Besides that, applications of different polymer blends matrices are an outstanding trend in current nanocomposites studies. Blending of polymers is becoming increasingly important to enhance properties, improve processing or reduce cost. Enhancement of properties of polymers; such as coefficient of friction (COF), adding color, promoting adhesion, increasing output, improving stability, and obtaining easy-opening features, can be achieved by blending.

In this study, polyethylene blend composed of low density polyethylene (LDPE) and metallocene polyethylene (mPE) based organomodified nanoclay were prepared via melt extrusion. PDMS as improving agent, and polyethylene grafted maleic anhydride (PE-g-MA) as compatibilizer were used in the nanocomposites. The effects of varying amounts of PDMS on the mechanical, thermal and morphological properties of polyethylene blend nanocomposites were investigated.

Tensile, hardness and impact tests were performed in order to obtain mechanical properties of the samples. Thermal properties and crystallization behaviours of the specimens were characterized by differential scanning calorimetry (DSC) thermograms. Actual filler contents of the samples were determined by the ash content test. Structural and morphological characterizations were made by melt flow rate (MFR), X-ray diffraction (XRD), and contact angle analysis.

2. THEORY

2.1 Polyethylene

Polyethylene has the simplest basic structure of any polymer (Figure 2.1), it is the largest tonnage plastics material and probably the polymer people see most in daily life as grocery bags, shampoo bottles, children`s toys etc.

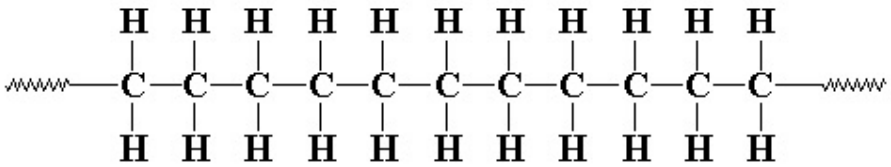

Figure 2.1 : Structure of polyethylene.

The main attractive features of polyethylene, in addition to its low price, are excellent electrical insulation properties, very good chemical resistance, good processability, toughness, flexibility, and transparency in thin films [4].

2.1.1 Types of polyethylene

Traditionally, commercial polyethylenes have been classified into three major groups based on both the manufacturing process and the polymer properties:

- Low Density, or LDPE,
- High Density, or HDPE,
- Linear Low Density, or LLDPE.

Sometimes, polyethylene with densities below 0.91 are considered to be a fourth group, the very- or ultra-low density polyethylenes (VLDPE or ULDPE). These are usually produced in an LLDPE-type process that has been modified to handle stickier, lower density polymers. They also have been made in high pressure, LDPE equipment. An additional type of polyethylene has recently been introduced that is

made with transition-metal-metallocene catalysts in conventional reactors. Properties of these materials are radically different from those of conventional resins.

According to the Society of the Plastics Industry, commercial production of polyethylene in the United States alone is approximately ten million metric tons per year, of which about 30% is LDPE, 45% is HDPE, and 25% is LLDPE. Market shares for these various polymers are approximately given in Table 2.1 [5].

2.1.1.1 Low density polyethylene (LDPE)

LDPE is produced by a free-radical catalyzed reaction using oxygen or other free radical initiators such as organic peroxides or azo compounds. Synthesis conditions are usually 250-300 °C temperature and 120-280 MPa pressure. Nominal reactor residence times are about 10-50 seconds.

Heat of polymerization is about 800 Kcal/gm, which must be removed during the short residence time available. Only a small part of this heat can be removed through the reactor walls because of their comparatively limited area and necessary thickness. In addition, the polymer tends to deposit on cool surfaces. In practice, heat is removed by recirculating excess cool monomer and the system operates essentially adiabatically. Therefore, production rates vary directly with the ethylene recirculation rate and the allowable temperature rise through the reactor. Heat balance limits conversion to ~15-20% on each pass.

Heat of polymerization is about 800 Kcal/gm, which must be removed during the short residence time available. Only a small part of this heat can be removed through the reactor walls because of their comparatively limited area and necessary thickness. In addition, the polymer tends to deposit on cool surfaces. In practice, heat is removed by recirculating excess cool monomer and the system operates essentially adiabatically. Therefore, production rates vary directly with the ethylene recirculation rate and the allowable temperature rise through the reactor. Heat balance limits conversion to ~15-20% on each pass.

Reactors are of two general types, autoclaves and high pressure tubes. Each of these types produces slightly different polymers, primarily because of differing temperature profiles through the reactors. In many cases, commercially similar polymers can be produced in either type of reactor.

Table 2.1 : Domestic market shares of polyethylene types in the United States.

Market Area	LDPE (%)	HDPE (%)	LLDPE (%)
Film	58	19	66
Extrusion coating	13	7	<1
Injection molding	6	18	10
Blow molding	<1	35	<1
Wire and cable	4	<1	3
Other	19	20	22

2.1.1.2 High density polyethylene (HDPE)

These polymers are produced as a slurry in an inert hydrocarbon diluent or in gas phase fluidized beds. There is also a solution phase process which is becoming obsolescent. To produce copolymers, a very small amount of α-olefin comonomer, usually butene-1 or hexene-1, is used to maintain the density in the 0.945-0.965 range. Both types of reactor produce similar, if not interchangeable, products.

Transition metal catalysts are used to manufacture HDPE. Chromium catalysts tend to produce broader molecular weight distributions (MWD) than Ziegler types.

2.1.1.3 Linear low density polyethylene (LLDPE)

Linear low density polyethylenes are obtained by incorporating sufficient α-olefin comonomers to yield polymers with densities in the 0.910-0.940 density range. Butene-1 is the usual comonomer, but either hexene-1, octene-1, or 4-methyl-pentene-1 is employed to give enhanced physical and optical properties, albeit at a higher production cost. Propylene has been employed as a less expensive comonomer but usually produces inferior products.

Synthesis conditions, as well as equipment, are similar to those employed for HDPE and, in fact, many commercial fluid bed installations have been designed to switch back and forth between HDPE and LLDPE as market conditions dictate. Generally, LLDPE polymer powder is significantly stickier than HDPE and downstream equipment must be designed to handle it.

LLDPE can also be produced in LDPE systems and, in fact, has been on the market for many years. Several manufacturers have announced improved processes to manufacture LLDPE in LDPE equipment. These copolymers are made with transition metals rather than with free radical catalysts [6].

2.1.1.4 Metallocene catalyzed polyethylenes (mPE)

New types of linear low density polyethylenes (LLDPE) based on the metallocene catalyst technology was introduced in the market place in 1991. There are now a number of well-established metallocene PE families commercially available and new products are constantly being introduced into the market. Because of its versatile mechanical and thermal properties, it has received a lot of interest both industrially and academically since its synthesis.

These resins are unique because metallocene catalysts are homogeneous, unlike heterogeneous transition metal catalysts used in conventional low-pressure processes. Nor are they like free-radical catalysts which produce polymers with a wide range of chain lengths and chain spacing. Because they are homogeneous (single site), metallocene catalysts produce polymers with markedly narrower molecular weight distributions than LLDPE produced via Ziegler-Natta catalyst system. The copolymers possess very narrow compositional distributions as well [5,7] .

The development of metallocene-catalyst technology has enabled new polyolefins with enhanced structural uniformity, organoleptic, mechanical, and optical properties, resulting from improved control of chain branching and narrower molecular weight distribution during polymerization.

This combination of properties therefore enables the extension of metallocene polyethylene applications into areas traditionally dominated by other thermoplastic materials. For example, mPE was introduced as a direct and safer alternative to flexible PVC and EVA in medical devices at comparable cost, given its better processability, mechanical properties, thermal stability, optical properties, improved sealability, nontoxicity, odor neutrality, insusceptibility to post-sterilizing discoloration, and reduced permepermeability to moisture and ammonia [8].

2.1.2 Density

Polymer density is a rough measure of crystallinity and, therefore, of the physical and optical properties that are dependent on the degree of crystallinity. The relationship between density and the various properties of the polymers is illustrated in Table 2.2 .

LDPEs and LLDPEs of the same density have somewhat dissimilar properties. This difference is largely because LDPE, being free radical catalyzed, contains a range of

both long and short side chains attached to the main polymer backbone. LLDPE, on the other hand, contains only short branch lengths, those of the comonomer. Although the degree of crystallization may be the same, the morphology of the crystal is dissimilar. LLDPE possesses many improved solid properties, such as strength, toughness, and draw-down, but LDPE in general is easier to process, is softer, and yields films with better optical properties [6].

Table 2.2 : Changes in polymer properties with density.

	Direction of Property Enhancement	
Density	0.910	0.965
Heat softening point		→
Yield strength		→
Tensile at break	←	
Elongation at break	←	
Stiffness		→
Resistance to shrinkage	←	
Resistance to warpage	←	
Film toughness	←	
Resistance to low temperature brittleness	←	
Resistance to environmental stress cracking	←	
Gas/liquid impermeability		→
Resistance to oil absorption		→
Transparency	←	
Freedom from haze	←	
Gloss	←	
Film draw down		→
Film hot tear resistance		→
Molding cycle time		→

2.1.3 Polyethylene-polyethylene blends

Metallocene catalysed polyethylenes exhibit the general characteristics of polyethylene. Furthermore they are more like low density polyethylenes (LDPE and LLDPE) than HDPE. The property differences largely arise from the narrow molecular weight distribution, the more uniform incorporation of the α-olefin and the low level of polymerization residues.

Narrow molecular weight distribution polymers such as m-PE are less pseudoplastic in their melt flow behaviour than conventional polyethylenes. As an example, that given an m-LLDPE and a conventional LLDPE of similar melt index, the mPE will have a much higher melt viscosity at the high shear rates involved in film processing. The polymers are also more susceptible to melt fracture and sharkskin.

An approach would be to produce bi-, tri- or other polymodal blends to overcome the inherent disadvantages of narrow molecular weight distribution polymers [4]. Multicomponent polyethylene is a term used to describe blends of two or more distinctly different polyethylene component resins. The component resins are selected in such a way as to give the resulting blend enhanced physical properties [9]. The components vary in molecular weight, molecular weight distribution, and both short-chain (comonomer content) and long-chain branching content. Blends of two components are the most common multicomponent system and are often referred to as bimodal resins [10].

A common blend is LDPE with linear low-density PE (LLDPE). Adding LLDPE can improve the toughness and elongation of LDPE, making it possible to produce a significantly thinner film (downgauging) with strength and impact properties equal to or better than a thicker LDPE film. LDPE also improves the processability of LLDPE. Blends of LDPE with 10, 20, 30, and 60% LLDPE include pallet shrink wrap, briquette bags, horticulture bags, and microirrigation pipes, respectively. Other blends manufactured by PE producers are LDPE and butyl rubber, which imparts environmental stress-crack resistance to the former [11].

Extruder or melt blending is the easiest means of producing multicomponent resins in concept and in versatility. In extruder blending, two or more polymers are simply fed to an extruder and melt blended to obtain a desired resin. The advantage of this process is in the control of blend composition. Drawbacks include the need to prepare and pelletize several different component resins commercially, the need to keep large inventories of the component resins on hand, and the ability to prepare homogeneous blends. It is difficult to blend pellets of two or more resins that differ dramatically in molecular weight [12,13].

2.2 Nanocomposites

Nanocomposite technology is a newly developed field, in which nanofillers are added to polymer to reinforce and provide novel characteristics. Nanocomposite technology is applicable to a wide range of polymers from thermoplastics and thermosets to elastomers. Two decades ago, researchers from Toyota Central Research and Development produced a new group of polymer-clay complexes or composites, and called polymer-layered silicate nanocomposites or polymer

nanocomposites. Today, there is a variety of nanofillers used in nanocomposites. The common types of fillers are natural clays (mined, refined and treated), synthetic clays, nanostructured silicas, nanoceramics, nanocalcium carbonates and nanotubes.

The property enhancements have allowed these materials to commercially compete with traditional materials. Some of the property improvements could be listed as:

- Efficient reinforcerment with minimal loss in ductility and impact strength
- Thermal endurance
- Flame retardance
- Improved liquid and gas barrier properties
- Improved abrasion resistance
- Reduced shrinkage and residual loss
- Altered electrical, electronic and optical properties [14].

2.2.1 Morphology of polymer layered-silicate nanocomposites

Type of silicate material, type of organic material used to tender hydrophilic silicates organophilic, the nature of polymer matrix, the preparation technique of the nanocomposites and the mechanical factors depending on the technique such as mechanical shear, residence time, type of mixer etc., are all important factors determining the morphology of the nanocomposites.Depending on these factors, three morphologies are possible: phase-separated, intercalated and exfoliated (Figure 2.2) [15].

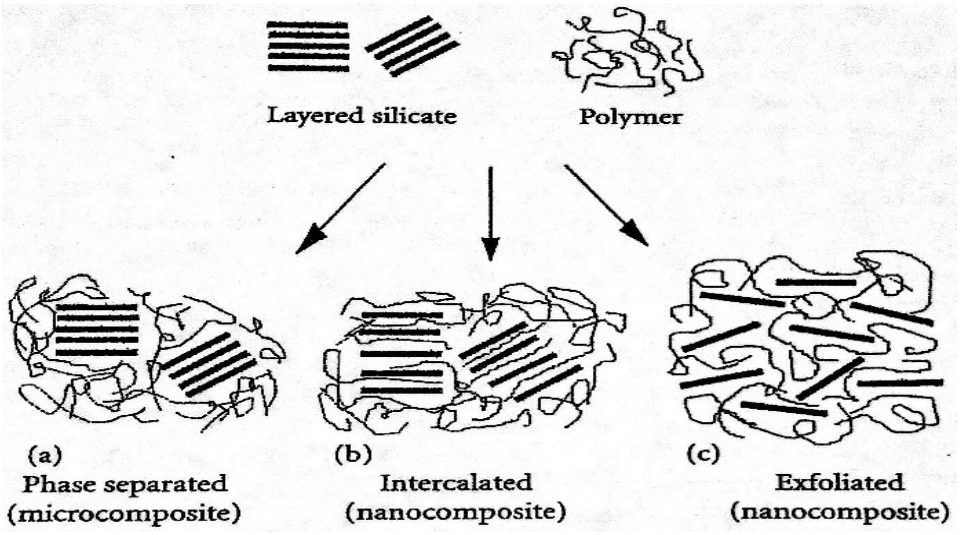

Figure 2.2 : Different types of morphologies of nanocomposites.

Phase-separated refers to composites that maintain immiscibility between the polymer and the inorganic filler. In this morphology, the polymer chains do not penetrate into the clay layers, the clay material is simply dispersed within the polymer matrix so that there is minimal reinforcement by the fillers.

Intercalated structures are obtained when polymer chains penetrate deep within the layers of silicate, while still retaining an ordered structure. The intercalation of the polymer chains into the layer galleries results in the expansion of the distance between the silicate layers. Due to mechanical shearing forces and interactions between the organo-silicates and the polymer chains, the stacks of layered silicates disperse within the matrix. Thus, increasing the interacting surface area of contact with the polymer. Intercalated structures have been reported to have regions of both high and low reinforcements [16].

Exfoliated morphologies result when individual layers (~1 nm) are well dispersed and randomly distributed throughout the polymer matrix. Once the exfoliated morphology reaches the percolation threshold, the average distance between layers becomes independent of the filler concentration or the structure turns to be a highly swollen intercalated one. The exfoliated structure facilitates maximum reinforcement due to the large surface area of contact with the matrix.

2.2.2 Types and structures of nanoclays

Layered materials such as silicates are suitable for the design of nanocomposites due to their lamellar elements that have high in-plane strength and stiffness and high aspect ratio (> 50). The clay material has a very high specific surface area of about 750 m^2/g (e.g., montmorillonite). Almost all groups of lamellar solids, especially smectite clays, are the material of choice for nanocomposites for two reasons:

- Their rich intercalation chemistry allows them to be chemically modified and made compatible with organic polymers for dispersal on a nanometer scale.
- They can be easily acquired at low costs [17, 18].

According to the relative ratio of two unit crystal sheets, the layered silicates are divided into three types:

- 1:1 type: Its unit lamellar crystal is composed of one crystal sheet of silica tetrahedron combined with one-crystal lamellae of alumina octahedron.

- 2:1 type: Its unit lamellar crystal is composed of two crystal sheets of silica tetrahedron combined with one crystal sheet of alumina octahedron between them.
- 2:2 type: Its unit lamellar crystal is composed of four crystal sheets, in which crystal sheets of silica tetrahedron and alumina or magnesium octahedron are alternaly arranged [19].

The layered silicates that are commonly used in nanocomposites belong to the 2:1 phyllosilicates family and montmorillonite (MMT) is a famous example of this family. MMT swells when contacted by water and this process of swelling is known as crystalline swelling [20]. The lattice crystal structure is comprosed of two-dimensional, ~1 nm thick layers. These are made up of two outer tedrahedral sheets of silica (SiO_4) fused onto an inner layer, which is composed of an octahedral sheet of alumina. The structure of MMT can be seen in Figure 2.3 [21, 22].

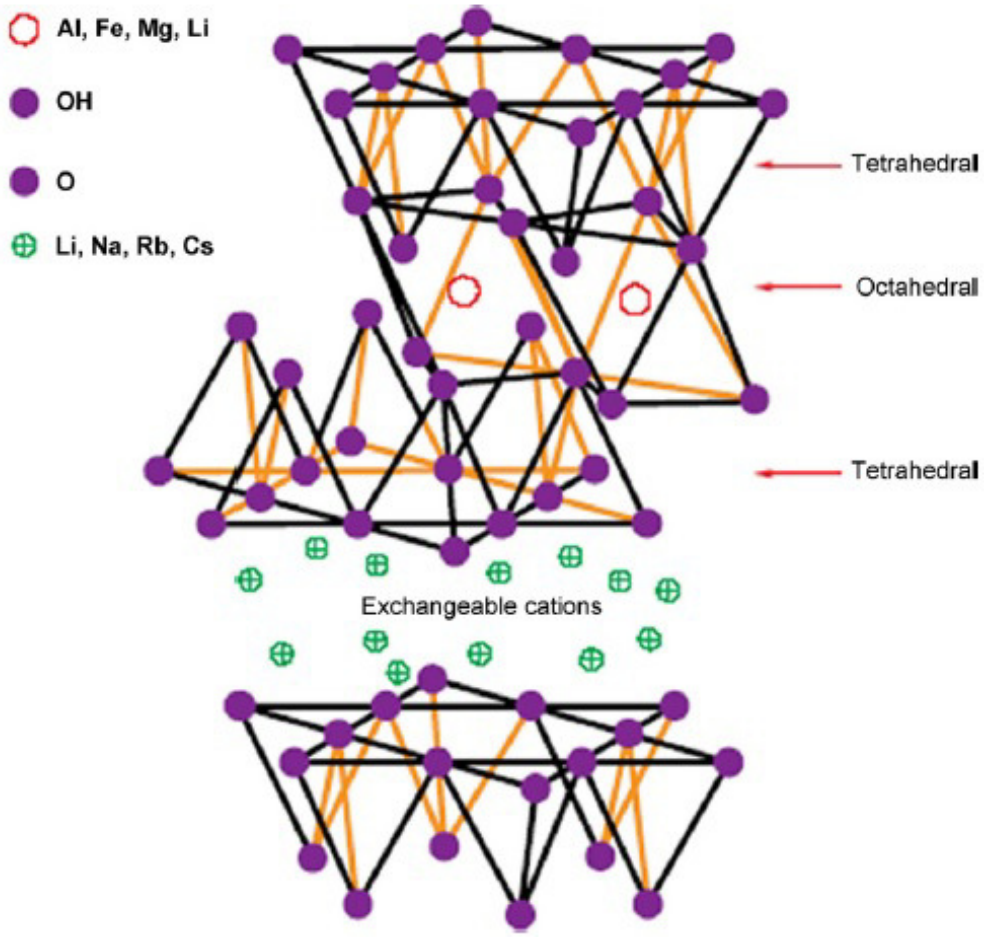

Figure 2.3 : Structure of MMT.

2.2.3 Clay modification

The layered structure of clay allows expansion after wetting, the cations in the intergallery are strongly hydrated in the presence of water. The strong polar and hydrophilic nature of montmorillonite requires modification in order to be compatible with nonpolar polymer molecules. In order to render the hydrophilic fillers more organophilic, the hydrated cations of the interlayer (Li^+, Na^+, Ca^{2+}) need to be exchanged with cationic surfactants. Long chain alkylammonium cations are the most common ions used in the modification of montmorillonite clay. The modification is called ion-exchange reaction and lowers the surface energy, hence making the clay compatible with most polymer systems and ensuring good dispersion in the polymer matrix [23].

2.2.4 Preparation of nanocomposites

There are several methods for the preparation of nanocomposites. Particle dispersion is one of the most urgent problems. Homegeneously dispersing or exfoliating the clay layers into the polymer matrix is very essential due to the fact that the morphology of dispersed particles have an inherent relationship with the final properties of the nanocomposites.

In general, nanocomposites can be formed in these ways:

- Solution dispersion
- In-situ polymerization
- Melt intercalation

2.2.4.1 Solution dispersion

This method is based on a solvent system in which the polymer is soluble and the silicate layers are swellable. The layered silicate is first swollen in a solvent (water, toluene, chloroform etc.), then the polymer and layered silicate solutions are mixed. The polymer chains intercalate and displace the solvent within the interlayer of the silicate. Later the solvent is removed and the intercalated structure remains [24].

Suitable polymers for preparing nanocomposites with this method can be listed as polyimide (PI), polyethylene oxide (PEO), polyethylene terephtalate (PET) and polyurethane (PU).

2.2.4.2 In-situ polymerization

The layered silicate is swollen within the liquid monomer or a monomer solution. The prepared mixture is polymerized under the reaction conditions similar to pure polymer, polymer formation occurs between the intercalated sheets.

This technique is suitable for polymers such as polystyrene (PS), polyamide-6 (PA6), polyamide-66 (PA66) and polyethylene terephtalate (PET) [19, 24].

2.2.4.3 Melt intercalation

Melt intercalation is the most widely used method in nanocomposite preparation and has an excellent potential for industrial application. In this method, polymer pellets and clay are directly mixed in the extruder machine and then melt-extruded together. This method is widely used for nanocomposites of polypropylene (PP), polyethylene (PE), polyamide-6 (PA6) and polystyrene (PS).

Generally, a reagent or compatibilizer with different surface affinity is used together with the organo-clay in order to match the system. For example, in the preparation of PE-MMTs nanocomposites, polyethylene grafted maleic anhydride (PE-g-MA) is also added to the blend, which improves the compatibility of organo-clay with the PE matrix [19].

2.2.5 Polyethylene nanocomposites

Polyethylene production is over 100 million tons per year worldwide as a result of its wide application. Low cost, good recycling performance, good processability, nontoxicity and biocompatibility of PE are its outstanding advantages over other similar polymers. If PE is divided according to its applications, there are PEs for special applications, such as PE for cabel application, blown-film PE, casting-film for food package, PE for pipelines or man-made skins, etc.

Although it has so many applications and advantages, PE has its disadvantages, such as poor stiffnes, low-temperature toughness, low melting behaviour, low stress crack resistance, and high permeability to gases and water vapour. All of these gave a great opportunity for investigators to improve the PE properties and modifications of PE through PE-MMTs nanocomposites have been introduced.

The introduction of nanofillers has provided opportunities to overcome the shortfalls

of plastics in general. Layered silicates provide a high surface area of interaction with the polymer chains and reinforcing them. For improving the properties, the clay should be well-dispersed and distributed in the polymer matrix. For example, a tortuous pathway can be created for the permeants such as gas and water vapour, hence decreasing the permeability. Kenig et al. reported on the production of high barrier blow molded containers with a significant reduction in permeation of hydrocarbon fluids, enhancements in stiffness and dimensional stability without loss of impact resistance. According to their results, the mass loss of xylene is highest from 10 L blow molded containers made of HDPE, rather than of HDPE-clay nanocomposites [25].

Lee et al. presented results on the flammability of HDPE nanocomposites and they proved that incorporation of <1 wt.% clay decreased the burning rate by 10-15% of the exfoliated nanocomposites compared with the intercalated HDPE nanocomposites. This was caused by the formation of a high performance carbonaceous-silicate char that insulates the underlying material during burning. This makes HDPE suitable for applications such as petrol tanks and containers that hold flammable materials [26].

PE degredation is a currently researched topic. The degradation takes place in two steps, first the abiotic degradation due to thermal oxidation takes place, then microbial consumption or biodegradation occurs. Reddy et al. have demonstrated the incorporation of layered silicates increased the rate of thermo-oxidation in the LDPE nanocomposites. They showed that when the nanocomposites exposed to oven-aging at 70°C, a much higher carbonil index is produced, which is a measure of carbonyl compounds in a material and a sign of oxidation [27].

2.2.5.1 Compatibilizer

Compatibilizers are often used as additives to improve the compatibility of immiscible polymers and thus improve the morphology and resulting properties of the blend. Similarly, it is often challenging to disperse fillers effectively in the matrix polymer of a composite, or to adhere layers of polymers to each other or to other substrates, such as glass or metals, in laminates.

The largest number of polymeric compatibilizers are the modified polyolefins. Most types of modified polyolefins contain polar groups that enhance their compatibility

with polar polymers, and their abilities to couple to (and disperse) inorganic fillers more effectively and to adhere to substrates [28].

Polyethylene and polyolefins in general have a non-polar backbone, because of that there is an inherent poor adhesion between the polar clay and the polymer. It has been attempted to enhance the interaction between clay and polyethylene by modifying clay surface with alkylammonium salts as mentioned in section 2.2.3 and using compatibilizers in the mixing process. Better dispersion is achieved using polyethylene grafted maleic anhydride (PE-g-MA) as compatibilizer, which can enhance the intercalation of the polymer chains within the silicate gallery [1].

Many scientific groups and researchers had studied the effect of PE-g-MA in various polyethylene nanocomposites. Bula and co-workers studied the effect of PE-g-MA on the mechanical properties and morphology of HDPE/silica (SiO_2) composites. Various SiO_2 content (2, 4, and 6 wt%) composites were melt blended in a co-rotating twin screw extruder and PE-g-MA was added (2 wt%) as a compatibilizer. Mechanical properties and composite microstructure were determined by tensile tests and scanning elctron microscopy (SEM). PE/SiO_2 and PE/PE-g-MA/SiO_2 properties were discussed and Young`s modulus of the PE-g-MA containing composites showed highest values. This increase was associated with the compatibility and improvement of interfacial adhesion between the PE matrix and nanoparticles. This finding was verified on the basis of SEM migrographs [29].

Durmus and co-workers studied LLDPE/clay nanocomposites with carious clay content and two different compatibilizers, PE-g-MA and oxidized polyethylene (OxPE) and the nanocomposites were prepared by melt processing. Effects of structure and physical properties of the compatibilizers on the clay dispersion and clay amount on the microstructure and physical properties of the nanocomposites were investigated. Lower percolation and higher aspect ratio values were obtained for the sample series prepared with the PE-g-MA than that prepared with the OxPE. It was found that the PE-g-MA yielded better clay dispersion and more exfoliated structure compared to the OxPE [30].

Reddy et al. had prepared LDPE nanocomposites by melt intercalating PE-g-MA and MMT clay. They have found that maleic anhydride has promoted strong interactions between PE and MMT which is leading to the homogeneous dispersion of clay

layers. According to rheological experiment results, nanocomposites exhibited shear thinning behaviour and and increase in steady shear viscosities comparing to virgin PE. The tensile strength of nanocomposites was improved but elongation at break decreased [31].

Ranade and his friends had investigated non-linear time dependent creep of PE/MMT nanocomposites and PE-g-MA was used as a compatibilizer in their blends. The creep and tensile response of maleated and non-maleated PE nanocomposites were determined. Tensile properties of maleated PE nanocomposites were higher than the non-maleated nanocomposites [32].

In addition to the usage of PE-g-MA in PE nanocomposites, some scientists were studying on PE bio-composites with natural materials such as lignin, eggshell, bloodmeal, etc. and PE-g-MA is used as a compatibilizer in these blends. Li et al. studied on acorn shell and LDPE composites prepared via a twin-screw extruder. Three different compatibilizers (ethylene acrylic acid, ethylene-vinyl acetate and PE-g-MA) were used to increase the interaction between PE and acorn shell. The results showed that the three compatibilizers improved the mechanical properties of composites at different levels, and PE-g-MA showed the best mechanical strength, about 80% from that of the non-compatibilized one. Dynamic mechanical anaylises further confirmed that the addition of PE-g-MA significantly improved the compatibility of the components and changed the properties of LDPE matrix [33].

Supri and co-workers studied the effects of PE-g-MA on the tensile properties, morphology and thermal properties of LDPE/eggshell powder composites and LDPE/chicken feather fiber composites. The tensile strength, elongation at break and thermal stability of LDPE/eggshell powder composites with PE-g-MAH were greater than non-compatibilized composites, and their differences became more pronounced at higher filler content. The interfacial adhesion between eggshell powder and LDPE was improved with the addition of PE-g-MAH as evidenced by the morphological study. LDPE/chicken feather fiber/PE-g-MA composites exhibit higher tensile strength, Young's modulus, and final decomposition temperature, but lower mass swell percentage and elongation at break than non-compatibillized composites. SEM morphology showed that the chicken feather fiber more widely dispersed in the LDPE matrix with the addition of PE-g-MA as a coupling agent. It was also found that the addition of PE-g-MA offers better thermal stability [34, 35].

2.3 Polysiloxanes

Polymeric materials composed of a (Si-O) backbone with two monovalent organic radicals attached to each silicon atom (R_2Si-O) are generallycalled “silicone” polymers. The (Si-O) repeat unit is also called as the “siloxane” bond or linkage and therefore other terms used to describe these types of polymers also include siloxane polymers and polysiloxanes. Since the polymer backbone is “inorganic” in nature, while the substituents attached to the silicon atom are generally “organic” radicals, silicones form an important bridge between inorganic and organic polymers. Because of the dual nature of their backbones another widely used name to describe silicone polymers is polyorganosiloxanes.

One of the major advantages offered by the flexible chemistry of silicone polymers is the possibility of introducing a wide selection of substituents onto the silicon atom in the backbone. These substituents can be inert, such as methyl, phenyl and 3,3,3-trifluoropropyl or reactive such as vinyl, hydrogen, epoxy or amino groups. For the preparation of silicone containing block or segmented copolymers inert backbones are preferred. On the other hand for crosslinked systems silicone backbones with reactive substituents may be more suitable.

The most common silicone polymer is poly(dimethylsiloxane) (PDMS) (Figure 2.4). Thermodynamic calculations and spectroscopic studies have shown that in PDMS, the methyl groups rotate with unusual ease around the (Si-O) bonds. A large molar volume (75.5 cm^3/mol) and a low cohesive energy density (intermolecular forces) of PDMS are consequences of the ease of rotation of the methyl groups. Low intermolecular forces and the flexibility are also responsible for many unique properties of the PDMS.

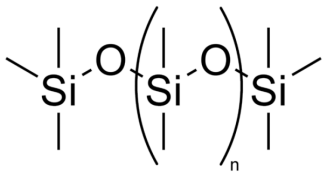

Figure 2.4 : Chemical backbone structure of PDMS.

In addition to its ease of commercial production, PDMS also displays an interesting combination of physical properties such as very low Tg(−120°C), high gas

permeability, low dielectric constant, very low solubility parameter of 15.5 $(J/cm^3)^{1/2}$, a fairly low surface tension of 21–22 mN/m and excellent biocompatibility. High molecular weight PDMS (usually with Mn> 5000 g/mol) also displays crystallinity with a melting point around −50°C, which may limit its flexibility at very low temperatures [36].

PDMS is transparent to visible and UV light, very resistant to ozone and corona discharge, stable against atomic oxygen an even oxygen plasmas. Moreover, these properties show only a very small variation over a wide temperature range. Other outstanding properties include film forming ability, high permeability to various gases, hydrophobic behaviour, release action, surface activity and chemical and physiological inertness.

Despite their many outstanding properties, PDMS rubbers require extremely high molecular weights to develop useful mechanical properties. Even at a molecular weight of 500,000 g/mol they exhibit cold flow and very weak rubbery properties. Therefore, PDMS must generally be chemically crosslinked in order to be used in an elastomer. However, unfilled PDMS vulcanizates still have very low tensile and tear strengths and elongations. Polysiloxanes can not bring about compatible mixtures with the numerous organic polymers due to their low solubility-parameter. In addition, they have high gas permeability, chemically and physically inert and hydrophobic properties [37].

2.3.1 Contact angle and surface properties

The contact angle is defined as the angle formed by the intersection of the liquid-solid interface and the liquid-vapor interface. The interface where solid, liquid, and vapor co-exist is referred to as the “three phase contact line”. Figure 2.5 shows that a small contact angle is observed when the liquid spreads on the surface, while a large contact angle is observed when the liquid beads on the surface. More specifically, a contact angle less than 90° indicates that wetting of the surface is favourable (hydrophilic in case of water), and the fluid will spread over a large area on the surface; while contact angles greater than 90° generally means that wetting of the surface is unfavourable (hydrophobic in case of water) so the fluid will minimize its contact with the surface and form a compact liquid droplet. For example, complete wetting occurs when the contact angle is 0°, as the droplet turns into a flat puddle.

For superhydrophobic surfaces, water contact angles are usually greater than 150°, showing almost no contact between the liquid drop and the surface, which can rationalize the “lotus effect” [38].

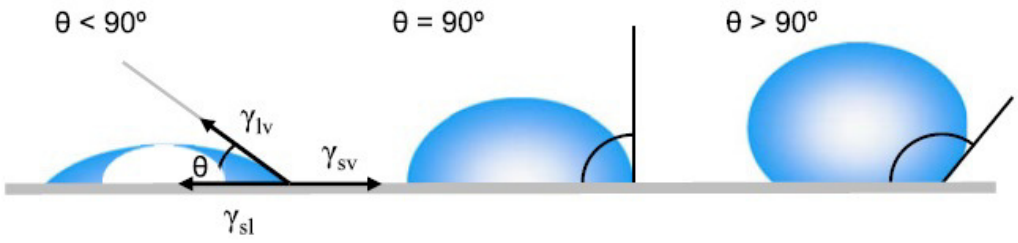

Figure 2.5 : Illustration of contact angles by sessile drops on smooth solid surface.

When compared with other polymeric materials, with the exception of highly fluorinated systems, one of the most interesting phenomena displayed by poly(dimethylsiloxane) containing systems is their very low surface energies around 20–22 mN/m. Silicone rich surfaces provide interesting properties, which include hydrophobicity (contact angle >90°), water repellency, lubricity, reduced coefficient of friction, improved biocompatibility and antifouling or foul release properties [36].

2.4 Literaure Review

2.4.1 Polyethylene/nanoclay

Polyethylene offers many advantages such as low cost, good processability and versatile applications. Due to its some disadvantages and shortcomes, there has been an attempt by many research groups to improve its film barrier, mechanical, rheological and thermal properties.

Arunvisut and co-workers studied LDPE/clay nanocomposites containing modified organoclay and PE-g-Ma as compatibilizer. They prepared the nanocomposites by melt-mixing in a twin-screw extruder and then blown-filmed them. D-spacing of clay and thermal behaviour of nanocomposites were characterized by wide-angle X-ray diffraction and differential scanning calorimetry (DSC), respectively. XRD results confirmed the increase in PE-g-MA exhibited better dispersion of clay. According to DSC analysis, the increased PE-g-MA contents caused the decrease in the degree of crystallinity. Mechnical properties of blown film specimens were tested in two directions of tensile tests, in transverse tests and in machine direction tests. Tensile

modulus and tensile strength at yield when clay amount increased because of the reinforcing behaviour of clay on both test directions. However, elongation at yield decreased with increasing clay loading. Oxygen permeability tests of LDPE/clay nanocomposites also decreases by 24% as the clay amount increased to 7 wt% [39].

Khalili et al. worked on the effect of organo-modified MMT on mechanical and gas barrier properties od LLDPE/LDPE blend based nanocomposite films. They used PE-g-MA to obtain better dispersion of the nanoclay. They had melt compounded and then blown filmed the blend samples which contain various amounts of the clay. Mechanical properties of the films were studied in machine and transverse directions. Addition of 4 phr nanoclay improved the tensile modulus about 59% in machine direction and about 100% in transverse direction. It further reduced the oxygen permeability ca.38% [40].

Jacquelot and co-workers investigated the morphology and gas barrier properties of nanocomposites with two different PE reference matrices, mPE and LDPE-g-MA, and containing organo-modified MMT. HDPE-g-MA compatibilizer was used as a compatibilizer to improve the clay ddispersion in mPE based nanocomposites. Increasing the MMT content let to a significant increase of the barrier properties. It was also shown that replacing in the reference/compatibilizer/montmorillonite systems the mPE by a more polar reference matrix (a LDPE-g-MA) leads to only small enhancement of the clay dispersion and barrier properties. For these two nanocomposite series, the morphology was quite complex: individual platelets, intercalated structures, and even microdomains were observed in all the films [2].

Horst et al. prepared HDPE/clay nanocomposites with PE-g-MA as a compatibilizer by melt mixing. Concentrations between 2 and 15 wt% of MMT and concentration ratios of 1:1, 2:1 and 3:1 pf PE-g-MA/MMT were employed. The materials were characterized using X-ray diffraction, scanning electron microscopy (SEM) and thermogravimetry. The SEM images show that the presence of PE-g-MA results in a large degree of exfoliation at all clay concentrations. For 5 wt% MMT, the best degree of exfoliation is obtained for a 2:1 ratio of PE-g-MA/MMT. This ratio results in higher increase in the elastic modulus, mainly at low frequencies, with respect to that of the corresponding matrix. As the clay concentration increases, for a 2:1 ratio of PE-g-MA/MMT, the dynamic moduli increase showing pseudo solid-like behaviour at clay concentrations higher than 8 wt%. Moreover, the nanocomposites

show rheological properties that are affected by annealing at 200°C signaling further exfoliation or improved platelet and tactoid distributions. The oxygen permeability of PE decreases gradually with the clay concentration, reaching a maximum reduction of ca.30% for 15 wt% MMT [41].

Stoefler and co-workers studied the effect of clay dispersion on the properties of LLDPE/MMT nanocomposites. They used three different grafting contents and molecular weights LLDPE-g-MA as a coupling agent in preparation of LLDPE/MMT nanocomposites with various morphologies. The clay dispersion was analyzed by SEM, TEM and XRD. It was found that coupling agents having intermediate molecular weights led to the highest exfoliation extents, whereas the coupling agent presenting the highest molecular weight led to a poor delamination of the clay platelets. It was shown that the best improvements in mechanical and barrier properties are not necessarily achieved for the nanocomposites, exhibiting the highest exfoliation extents. The length of the tactoids also plays a crucial role on the macroscopic properties. In addition, a high level of delamination could result in a loss of reinforcement effect, due to the inherent flexibility of the individual clay platelets [42].

Liu et al. investigated mechanical properties of LDPE/MMT nanocomposites using two kinds of compatibilizers (PE-g-MA and thermoplastic polyolefin elastomers, TPO) prepared by twin-screw extruder. They added 1, 3, and 5 %wt MMT and 2:1 ratio of PE-g-MA (or TPO) to LDPE matrix. The morphology of these nanocomposites were determined by XRD and SEM. Tensile, hardness, impact and wearing tests were performed in order to obtain mechanical properties of the samples. It was found that in the blends containing TPO, the following had the best test results: 1 wt% MMT in the tensile test (3.08% increase), 3 wt% MMT in the impact test (11.53% increase), 5 wt% MMT in the hardness test (2.60% increase), and 5 wt% MMT in the wearing test (6.98% increase). In addition, the specimens containing PE-g-MA, the following had the best test results: 1 wt% MMT in the tensile test (5.39% increase), 3 wt% MMT in the impact test (19.71% increase), 5 wt% MMT in the hardness test (10.85% increase), and 5 wt% MMT in the wearing test (44.19% increase). It was concluded that PE-g-MA had a better effect on mechanical properties comparing to TPO [43].

Liang and co-workers studied the nonisothermal crystallization kinetics of nanocomposites containing HDPE, PE-g-MA and organo-modified MMT by DSC at various cooling rates. The difference in the exponent *n*, *m*, and *a* between HDPE and the nanocomposite indicated that nucleation mechanism and dimension of spherulite growth of the nanocomposite were different from that of HDPE to some extent. The values of half-time, K(T), and F(T) showed that the crystallization rate increased with the increase of cooling rates for HDPE and composite, but the crystallization rate of composite was faster than that of HDPE at a given cooling rate. Moreover, the method proposed by Kissinger was used to evaluate the activation energy of the mentioned samples. It was 223.7 kJ/mol for composite, which was much smaller than that for HDPE (304.6 kJ/mol). Overall, the results indicated that the addition of O-MMT and PE-g-MA could accelerate the overall nonisothermal crystallization process of PE [44].

Morawiec et al. prepared LDPE based nanocomposites containing 3 or 6 wt% organomodified MMT and LDPE-g-MA compatibilizer by melt mixing. They obtained exfoliated morphologies observed from XRD and TEM. The compatibilized nanocomposites exhibit improved thermal stability in air as compared to neat polyethylene and nonexfoliated O-MMT composite. The crystallinity and crystallization kinetics of polyethylene matrix is not affected significantly by the presence of O-MMT clay. Drawability of the compatibilized nanocomposite with 6 wt% of O-MMT is similar to neat polyethylene, whereas the composition having the same amount of O-MMT, without compatibilizer, exhibits poorer drawability. Scanning electron microscopy and density measurements of drawn samples indicate the existence of pores in noncompatibilized composite while no pores and good adhesion to O-MMT are found in compatibilized nanocomposites [45].

Lew and co-workers produced synthetic tetrasilisic fluoromica containing nanocomposites from conventional Ziegler-Natta-catalyzed and metallocene-catalyzed LLDPE by melt-compounding. The effects of compatibilizer (PE-g-MA) level, clay concentration, and blending procedure were investigated and compared. Morphology and structural analysis using TEM and XRD suggested the clay exfoliation was more intense in the metallocene LLDPE matrix, conceivably because of the controlled short-chain branching and viscosity effects. When exfoliated, these silicate sheets were shown to restrict the lamellar crystallization, as seen by the

decrease in crystallinity using DSC analysis. The dynamic mechanical thermal analysis study suggested that the three α, β, and γ-relaxations of the LLDPE were affected by polymer chain branching and clay exfoliation level [8].

Wang et al. prepared PE-g-MA and clay nanocomposites by melt compounding and investigated their morphological properties. They found out that the exfoliation and intercalation behaviours depend on the hydrophilicity of PE-g-MA and the chain length of the organic modifier in the clay. When the number of methylene groups in alkylamine (organic modifier) was larger than 16, the exfoliated nanocomposite was obtained, and the maleic anhydride grafting level was higher than about 0.1 wt% for the exfoliated nanocomposite with the clay modified with dimethyl dihydrogenated tallow ammonium ion or octadecylammonium ion. The pure LLDPE showed only the intercalation, which does not depend on the initial spacing between clay layers [46].

2.4.2 Polysiloxanes/nanoclay

Silocone polymers have been widely studied due to their unique combination of properties such as very low glass transition temperature, high chemical and thermal stability, low surface energy, good optical clarity, and UV resistance. Although there are a lot of polymer/nanoclay studies, the application of polysiloxanes are very few. Recently, they have taken attention also in the nanocomposite researches because of the intercalation/delamination of clay layers by the addition of silicone polymers were observed in some studies.

Burnside et al. prepared poly(dimethylsiloxane) (PDMS)/organomodified MMT nanocomposites by melt processing. After the silicate delamination in the polymer matrix, they have cross-linked the nanocomposites. They performed XRD and thermal gravimetric analysis (TGA) to the samples. They accomplished delamination by fine-tuning organosilicate-polymer interactions, properly matching the organomodified MMT with the polymer matrix. Also they add water to optimize delamination, the addition of water corresponded to about a monolayer coverage on the surface. The nanocomposites exhibited decreased solvent uptake and increased thermal stability. The increased swelling resistance was attributed to strong reinforcement/matrix interactions and the large surface area attainable by delamination and dispersion of the silicate in the polymer matrix [47].

Camenzind and co-workers admixed silica nanoparticles having specific surface area 50-300 m^2/g into vinyl-terminated dimethylsiloxy monomer with a dual asymmetric centrifuge (planetary mixer) and cured to form PDMS-based nanocomposites containing up to 12vol% SiO_2. They analyzed nanocomposites by TEM and small and ultra small X-ray scattering to determine their structure, basicly filler primary particle, aggregate (chemically or sinter-bonded particles) and agglomerate (physically-bonded particles) size as a function of mixing duration and filler concentration. More aggregated silicas with higher specific surface area exhibited denser crosslinking than less aggregated ones regardless of crosslinker content as determined by swelling nanocomposites in toluene at equal filler content. The nanocomposite strength was determined by tensile tests (Young's modulus and elongation at break). Consistent with "bound rubber" theory, the Young's modulus of the nanocomposites increased non-linearly with increasing filler volume fraction [48].

Ma et al. used a novel method in preparating exfoliated/intercalated nanocomposites. They used in situ polymerization method, dimethyldichlorosilane was polymerized between silica layers and blended the treated-MMT solution with several polymers yielding exfoliated/intercalated nanocomposites. The in situ polymerization destroys the strong electrostatic attraction between the silicate layers and the inter-gallery cations. PDMS grafted onto MMT layer surface via condensation of hydroxyl groups of PDMS and those hydroxyl groups existed on MMT layer surface prevents nanolayers of MMT re-aggregating, which could be proved by comparison of storage stability and relaxation time. When the treated-MMT solution was blended with other polymers, exfoliated or intercalated nanocomposites were obtained according to the discrepancy of compatibility between polymer and MMT as well as alkyl ammonium and PDMS grafted on the layer surface [49].

Schmidt and co-workers reported a multi-system study of layered-silicate dispersion in polysiloxane/layered-silicate nanocomposites. A variety of layered silicates (montmorillonite, synthetic fluoromica, laponite, and fluorohectorite) and cationic modifiers (single-, twin-, and triple-tailed surfactants with tails of varying lengths and both primary and quaternary head-groups) were combined to form organically modified layered silicates, which are then screened for compatibility with low-molecular-weight silanol-terminated PDMS. They found that the PDMS backbone is

generally incompatible with the layered silicates, regardless of modification type, and that dispersion in PDMS systems results from the presence of polar end-groups. They applied a new epoxy/amine PDMS curing chemistry to PDMS-nanocomposite production and show higher levels of layered-silicate dispersion than observed in comparable silanol-terminated PDMS-based systems. Their results indicated that an otherwise incompatible polymer could be made compatible by the inclusion of the appropriate number of dispersion enhancing functional groups, either at the chain-ends or elsewhere in the polymer [50].

Ma and co-workers developed a new strategy to prepare disorderly exfoliated silicone rubber/MMT nanocomposites by the use of a siloxane surfactant with a weight-average molecular weight of 1900 adopted to modify the clay. The modified Na^+-MMT clay slurry was then mixed with silicone rubber by hand, and exfoliation was achieved. The proposed mechanism thereof was verified by TEM and XRD. Both the tensile strength and the tear strength of the silicone rubber were increased by the addition of siloxane surfactant modified clay. The physical entanglement of the soft siloxane surfactant plays a vital role in the diffusion and intercalation of the matrix molecules during the compounding of the slurry-polymer mixture [51].

Wang et al. prepared room-temperature vulcanized silicone rubber/organomodified MMT nanocomposites by solution dispersion method. They modified Na^+-MMT by an ion-exchange reaction using di(2-oxyethyl)-12 alkane-3 methyl-amine chloride as the intercalation agent and formed a new kind of O-MMT. Four types of nanocomposites were synthesized with different amounts of O-MMT. Properties such as tensile strength, DSC and TGA were measured and compared. Fourier transform infrared spectroscopy, XRD, and TEM results showed the in corporation of O-MMT into polymer matrix and exfoliated nanocomposites were formed. The enhanced mechanical and physical properties demonstrated the efficient reinforcing and thermal stability properties of the O-MMT [52].

Kong et al. worked on silicone rubber/clay nanocomposited prepared by melt intercalation process. They used two kinds of clays, synthetic Fe-MMT and natural Na-MMT which were modified by cetyltrimethyl ammonium bromide, in order to determine whether the presence of iron (Fe) in the matrix enhance thermal stability and affect the crosslinking degree and elongation. They characterized the nanocomposites by XRD and TEM and observed that they obtained exfoliated and

intercalated structures. They also applied mechanical tests and TGA to the samples. According to the mechanical test results, while the effect of two clays on the tensile strength was similar, elongation at break values were different. They observed that elongation at break results were coinciding with the gel fraction and crosslinking degree. When the crosslinking degree was low, elongation at break increases and Fe acted as antioxidant and decreased the crosslinking degree. They also concluded that the presence of iron significantly increased the onset temperature of thermal degradation in Fe-MMT nanocomposites [53].

Wang and co-workers studied on silicone rubber/organomodified MMT hybrid nanocomposites and aerosilica-filled silicone rubber prepared by melt intercalation process. They used XRD, TEM and TGA to characterize their samples. Their results proved that O-MMT could be exfoliated into ca. 50 nm and thickness and uniformly dispersed in the PDMS matrix. The mechanical properties and thermal stability of the nanocomposites were very closed to those of aerosilica-filled silicon rubber and higher than unfilled PDMS [54].

Kaneko and co-workers were prepared nanocomposites by using MMT and organomodified MMT clay masterbatches and PDMS. They produced masterbatches by compounding MMT and O-MMT with siloxane-polyether surfactant in a mechanical stirrer. They characterized the nanocomposites by XRD, small angle/wide angle X-ray scattering, TEM and tensile tests. The results showed that masterbatch compounding with O-MMT improved the dispersion of the clay into the PDMS matrix. The morphology of the resulting nanocomposite showed a combination of intercalated and partially exfoliated clay layers with occasional clay aggregates. The addition of only 5 phr of O-MMT into the PDMS matrix, via masterbatch compounding, improved the tensile strength as much as that obtained with the nanocomposite filled with 30 phr of O-MMT clay prepared by the direct addition of the clay [3].

2.4.3 Polysiloxanes/polyethylene

Poly(dimethylsiloxane) popularly known as silicone rubber possesses excellent thermal stability, dielectric property, ozone and corona resistance property. However, it has limited applications because of its lower green strength, lower mechanical

strength, handling difficulties and high cost. Therefore, blending PDMS with cheaper polyolefins such as LDPE has become popular.

Jana et al. studied on curing reactions of LDPE and PDMS rubber blends prepared by melt processing. They investigated the properties of the samples by DSC and rheometry, and calculated the kinetic parameters by DSC thermograms. The order of reaction had been found to be first order. They found the optimum level of dicumyl peroxide as 1.5 part by weight. It was observed that tensile strength of the blends decrease with an increase in the PDMS proportion in the blend. This may be explained as to the lower tensile strength of PDMS comparing to LDPE [55].

Jana, Bhattacharya and their co-workers investigated the rheological characterization of PDMS and LDPE blends compatibilized with ethylene-co-methylacrylate (EMA). They had carried out the tests at different temperatures, shear rates and varying amounts of the compatibilizer and found out that the die swell increases with an increase in shear rate, temperature and compatibilizer content. Surface finish of the extrudates deteriorated with increasing shear rat and the temperature but improves with increasing compatibilizer content. The SEM studies of the blends gave co-continuous phase morphology at 6 wt% of ethylene-co-methylacrylate and that was found to be the optimum compatibilizer loading [56].

Jana et al. investigated the rheological behaviour of LDPE and PDMS blends at different temparatures and shear rates. They added varying amounts of ethylene methylacrylate copolymer (compatibilizer) and silica filler to the blends. The flow behaviour index of the blends decreased with the increase in the PDMS proportion and the silica filler loading but increased with the increase in the EMA proportion and the temperature. SEM analysis showed an improved dispersion for a 50/50 blend of LDPE–PDMS and it further improved with the incorporation of 6wt% of EMA as well as the blend containing 10 wt% of silica filler loading. The surface finish of the extrudate for the blend containing 10 wt% of silica filler was better compared to that with 20 wt% of silica filler [57].

Giri et al. studied the effect of electron beam irradiation on the blends of LLDPE and PDMS prepared over a wide range of compositions starting from 70:30 to 30:70 (LLDPE: PDMS) by varying the radiation doses from 50 to 300 kGy. The dynamic modulii and dielectric strength of the blends increased on irradiation at 100 kGy as

compared to that for the unirradiated blends. Degree of crystallinity and melting behaviour remained unchanged upon irradiation upto a dose of 100 kGy, beyond which it decreases. Thermal stability increased with increase in the proportion of PDMS rubber in the blend as well as on irradiation at 100 kGy. The phase morphology of the blends examined under the SEM exhibited two phase morphology before electron beam irradiation, whereas single phase morphology was observed after electron beam irradiation due to intra- as well as inter-molecular crosslinking leading to a miscible system [58].

Zhu and co-workers prepared PE and PDMS blends by in situ cationic polymerization using supercritical carbon dioxide because of the two polymers usually being immiscible and obtaining of phase-separated morphology. Differential scanning calorimetry, wide-angle X-ray diffraction, and small-angle X-ray scattering measurements showed that PE and PDMS were blended at the nanometer level. The PDMS generated in the amorphous region of PE did not affect its crystallinity. The presence of PDMS in the amorphous regions significantly affected the viscoelasticity and mechanical properties of the PE/PDMS blend. Dynamic viscoelastic analyses and tensile tests were used to measure the mechanical properties of the samples. Mechanical properties such as Young's modulus, tensile strength, and elongation at break of the PE/PDMS blend could be controlled by the mass gain of PDMS. Also, PDMS formed on the surface of PE improved its hydrophobicity [59].

3. EXPERIMENTAL

3.1 Materials

3.1.1 Low density polyethylene (LDPE)

Low density polyethylene (LDPE) was the commercial DOW^{TM} LDPE 780E supplied by The Dow Chemical Company. The melt flow rate (190 °C/2.16 kg) and Vicat softening temperature are 20 g/10min and 93 ºC, respectively. The density is 0.923 g/cm^3.

3.1.2 Metallocene polyethylene (mPE)

Metallocene polyethylene (mPE) was the commercial Eltex® PF1320AA (C_6 m-LLDPE) supplied by Ineos O&P Europe. The melt flow rate (190 °C/2.16 kg) and Vicat softening temperature are 20 g/10min and 89 ºC, respectively. The density is 0.913 g/cm^3.

3.1.3 Poly(dimethylsiloxane) (PDMS)

DOW CORNING MB50-002 masterbatch in a pelletized formulation containing 50% of an ultra high molecular weight (UHMW) siloxane polymer dispersed in LDPE which supplied by Dow Corning, Inc. used as poly(dimethylsiloxane) (PDMS) in the polymer matrix.

3.1.4 Polyethylene-grafted maleic anhydride (PE-g-MA)

Bondyram® 4108 was the commercial maleic anhydride grafted LLDPE obtained from Polyram used as a compatibilizer in the nanocomposites. The melt flow rate (190 °C/2.16 kg) and melting point are 1.5 g/10 min and 122 ºC, respectively. The density is 0.919 g/cm^3 and and the maleic anhydrite level is ca.1%. PE-g-MA is abbreviated as “C” in the following tables and graphs.

3.1.5 Organomodified nanoclay (O-MMT)

Nanomer® I.44P was the commercial nanoclay spesifically designed for polyolefin

applications obtained from Nanocor, Inc. and has contained 35–45% quaternary ammonium compounds, bis(hydrogenated tallow alkyl) dimethyl chlorides; 55–65% montmorillonite (MMT). The nanoclay is fine free flowing powder and mean typical particle sizes are in the range of 15-20 μm.

Table 3.1 : Material characteristics.

Material	Trade Name	Supplier	Characteristics
LDPE	DOW™ LDPE 780E	The Dow Chemical Company	Density=0.923 g/cm^3 MFI=20 g/10min Vicat Soft.Temp=93 ºC
mPE	Eltex® PF1320AA	Ineos O&P Europe	Density=0.913 g/cm^3 MFI=20 g/10min Vicat Soft.Temp=89 ºC
PDMS	DOW CORNING MB50-002	Dow Corning, Inc.	Siloxane content=50%
PE-g-MA	Bondyram® 4108	Polyram	Density=0.919 g/cm^3 MFI=1.5 g/10min Melting Temp=122 ºC
Nanoclay	Nanomer® I.44P	Nanocor, Inc.	Particle size=15-20 μm

3.2 Equipments

3.2.1 Twin-screw extruder

In this study, in order to obtain well-mixed PE nanocomposites, an intermeshing co-rotating twin-screw extruder with a diameter of 27 mm and L/D ratio 48:1 (shaft length/screw diameter) was used to prepare blends by melt mixing method.

The twin-screw extruder POEX T-27 from Polimer Teknik consisted of one main volumetric feeder, two side volumetric feeders, thirteen heating zones, and degassing unit before the die segment is shown in Figure 3.1. Electrical resistances and water cooling channels controlled by thermoregulator which are connected to each modular

barrel zone to ensure play important role to control the set temperature. The control panel was manually driven computer system. Technical specifications of the extruder are given in Table 3.2.

Figure 3.1 : POEX T-27 Twin-screw extruder.

Table 3.2 : POEX T-27 Twin-screw extruder technical specifications.

	Units	POEX T-27
Screw diameter	mm	27
Maximum screw speed	rpm	1200
L/D (shaft length/screw diameter)	-	48:1
Working length	mm	1296
Maximum capacity	kg/h	5-100
Motor power	kW	30
Heating power	kW	12
Average water requirement	lt/min	30
Height	mm	1000
Total weight	kg	950
Maximum pressure	bar	300
Vacuum pump	kW	0.75
Cooling unit(pump)	kW	0.50
Granulating motor	kW	2.2

The polymer melt leaving the extruder from the die segment cooled down into a water bath and obtained as spaghettis that are cut into small pieces called granules by

the fixed length pelletizer or chopper. This system is also known as the classical way of spaghettis pelletizing. Figure 3.2 shows the granulating unit.

Figure 3.2 : The granulating unit.

3.2.1.1 Screw configuration

POEX T-27 twin-screw extruder had specially designed for well mixing and melting with the ability of achieving high shear and high residence time that are required for compounding process. The special twin-screw configuration consists of six different zones, which are solid conveying zone, plasticizing zone, melt conveying zone, homogenization zone, degassing zone and pressure built up zone from feeding to die section, respectively. The picture of the screws can be seen in Figure 3.3.

The screws have contained different screw elements such as nine conveying blocks and seven kneading blocks. Raw material was fed into the extruder's first conveying zone by the main feeder, then the material was plasticized along the plasticizing zone. The molten polymer was obtained through three kneading and four conveying blocks and it was homogenized by another three kneading and four conveying blocks in the homogenization zone. Finally the gases formed during compounding process were removed via the vent in the degassing zone.

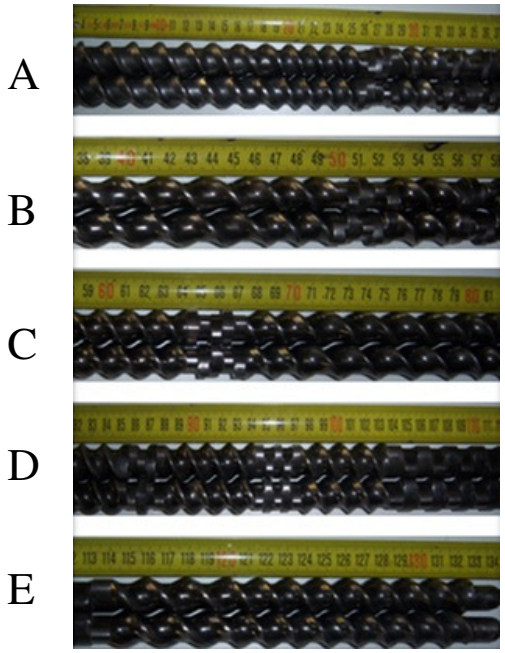

Figure 3.3 : Screw configuration of POEX T-27 twin-screw extruder.
A, B, C, D, and E are sections from hopper to die, respectively.

3.2.2 Injection molding machine

Specimens according to ISO standards were prepared by an Arburg injection molding machine with a specific mold design. Injection unit consists hopper, heat controlled barrels-cylinder, screw, molding and clamping unit, and motor, as shown in Figure 3.4.

Figure 3.4 : Injection molding machine.

3.2.3 Density determination

Radwag Analytical Balance AS 220/X equipped with a special density determination kit as shown in Figure 3.5 was used to measure the densities of the specimens.

Figure 3.5 : Density determination kit.

3.2.4 Melt flow index machine

The melt flow rate test is a method used to characterise polymer melts. Melt flow index (MFI) was measured by using Ceast Modular Base Model testing machine which consists of a standard die of 2.095 ± 0.005 mm diameter and 8.000 ± 0.025 mm, shown in Figure 3.6.

Figure 3.6 : Melt flow index machine.

3.2.5. X-ray diffraction (XRD)

X-ray diffraction analysis (XRD) is a nondestructive method for the structure analysis of crystals. The sample is irradiated with monochromatic X-ray light and the stray radiation recorded. An important field of application is the identification of crystalline fractions in samples. X-ray diffraction analysis of clays and nanocomposites were made by Panalytical X'Pert Powder XRD.

3.2.6 Contact angle test device

Attension Biolin Scientific AB, ThetaLite TL101 model optical tensiometer aparatus was used to measure contact angles of the samples.

3.2.7 Universal testing machine

Mechanical testing is essential in determining the final mechanical properties of the product. Tensile properties of specimens were measured by using Lloyd LC universal tensile testing machine equipped with 5 kN load cell as load indicator and long stroke extensometer as extension indicator which can be seen in Figure 3.7.

Figure 3.7 : Universal testing machine.

3.2.8 Izod impact testing machine

Izod impact strength of specimens was measured by using Ceast 9050 Izod impact machine and the samples were notched by a cutting machine as shown in Figure 3.8 and 3.9, respectively.

Figure 3.8 : Izod impact testing machine.

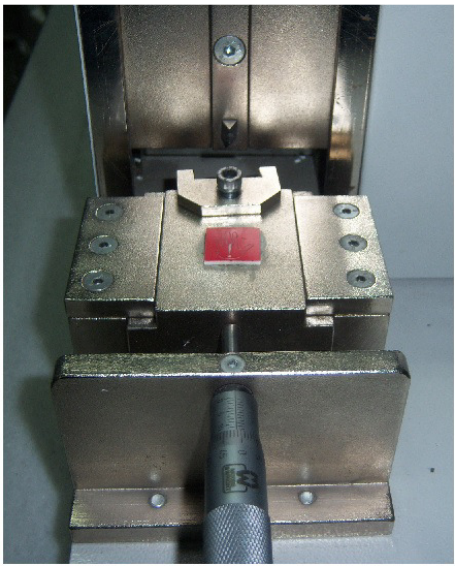

Figure 3.9 : Notch cutting machine for Izod test.

3.2.9 Durometer

The hardness (Shore D) of the samples were measured by the durometer shown in Figure 3.10.

Figure 3.10 : Shore D hardness durometer.

3.2.10 Muffle furnace

Nüve MF 120 muffle furnace as shown is Figure 3.11 was used for determining ash contents of the samples.

Figure 3.11 : Muffle furnace used for ash content test.

3.2.11 Differential scanning calorimeter (DSC)

DSC was used for determining the melting temperature (T_m), crystallization temperature (T_c), and heat of fusion values of polymers. Thermal analysis of the samples were done with TA Instruments Q20 DSC differential scanning calorimetry machine which can be seen in Figure 3.12.

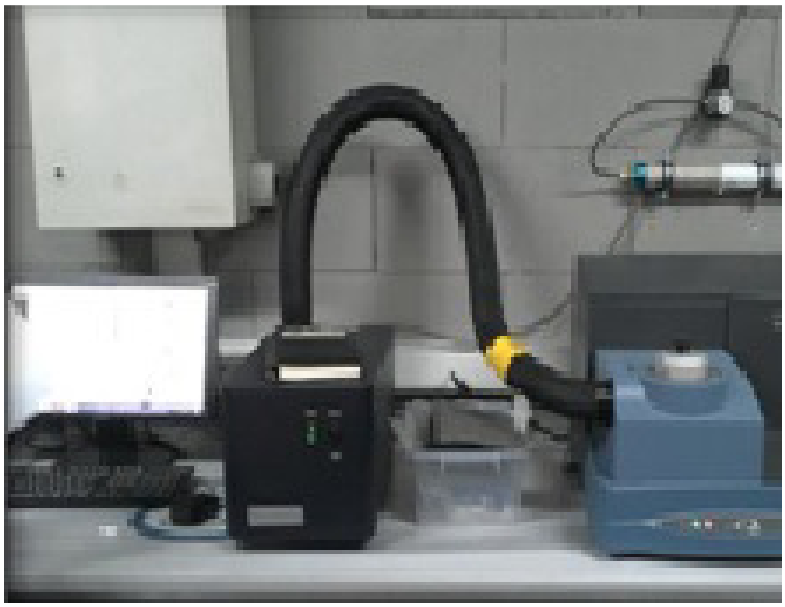

Figure 3.12 : Differential scanning calorimeter.

3.3 Experimental Procedure

3.3.1 Nanocomposites preparation procedure

LDPE, mPE, PDMS, PE-g-MA (C), and organomodified nanoclay I.44P (NC) containing nanocomposites were processed by co-rotating twin-screw extruder. The PE blend based nanocomposites were, which contain different ratios of LDPE and mPE, prepared by phr (parts per hundred parts of resin) method.

Five PE mixtures with varying weight percentages of mPE and LDPE (100% mPE, 75% mPE + 25% LDPE, 50% mPE + 50% LDPE, 25% mPE + 75% LDPE, and 100% LDPE) had taken as 100 phr, and 5 phr NC and 15 phr PE-g-MA were all mixed by shaking before feeding and then processed in the extruder. 5 phr and 10 phr PDMS containing nanocomposites were prepared for the same amounts of PE mixtures. Neat PE blends which composed of only mPE and LDPE were processed

for comparison as well. Formulations of the nanocomposites are given below in Table 3.3.

Table 3.3 : Formulations of nanocomposites containing PDMS and nanoclay.

Samples	mPE (%)	LDPE (%)	O-MMT (phr)	PE-g-MA (C) (phr)	PDMS (phr)	Definition*
1	100	--	--	--	--	100/0/0/0/0
2	100	--	5	15	--	100/0/5/15/0
3	100	--	5	15	5	100/0/5/15/5
4	100	--	5	15	10	100/0/5/15/10
5	75	25	--	--	--	75/25/0/0/0
6	75	25	5	15	--	75/25/5/15/0
7	75	25	5	15	5	75/25/5/15/5
8	75	25	5	15	10	75/25/5/15/10
9	50	50	--	--	--	50/50/0/0/0
10	50	50	5	15	--	50/50/5/15/0
11	50	50	5	15	5	50/50/5/15/5
12	50	50	5	15	10	50/50/5/15/10
13	25	75	--	--	--	25/75/0/0/0
14	25	75	5	15	--	25/75/5/15/0
15	25	75	5	15	5	25/75/5/15/5
16	25	75	5	15	10	25/75/5/15/10
17	--	100	--	--	--	0/100/0/0/0
18	--	100	5	15	--	0/100/5/15/0
19	--	100	5	15	5	0/100/5/15/5
20	--	100	5	15	10	0/100/5/15/10

* mPE/LDPE/O-MMT/PE-g-MA/PDMS

3.3.2 Nanocomposites processing conditions

During the preparation of nanocomposites by extrusion, the processing conditions play a major role. The shear stress and the residence time are two important parameters for dispersion of the clay. A high screw speed or rpm can produce higher shear stresses which causes the break-up of clay particles. Nevertheless, a high rpm also increases the viscous heating, leading to the degradation of clay. Another consequence of high rpm is the decrease of residence time, which means giving less time to polymer chains for diffusing with the clay. On the other hand, for the initial breakup of the clay, a certain amount of shear stress is required. Hence, a balance is necessary with an optimal screw speed that can provide enough shear and minimal viscous heating.

Certain processing conditions during melt blending can maximize and minimize the clay aggloromeration. A balance of processing parameters is required [60]. The clay can agglomerate when the processing temperature is high, because there is more chance of degredation of the intercalant that exists between clay sheets [61].

Above mentioned process parameters and their effects on the end products had taken into consideration and 70/165/175/175/185/185/190/195/195/195/205/205/205 °C temperature profile, from hopper to die, and 450 rpm screw speed was optimized for the extrusion process of the nanocomposites.

3.3.3 Injection molding machine and process parameters

Injection molding is defined as a process where melt polymer forced into a mold cavity and cooled down in it by taking its shape. A plastic injection machine is mainly divided into three parts which are known as mold, clamping unit and injection unit. The pellets are fed into injection machine from feeding hopper and heated until they melt. When injection process begins, the speed controlled forward movement of screw forces molten plastic into mold cavity and then holds the force for a while to minimize the shrinkage of molded part. The mold is kept closed to cool down the melted plastic and give shape after finishing injection and holding pressure. Then, mold opens and molded-shaped parts are taken.

Figure 3.13 : The special mold design of the injection molding machine.

Test specimens were produced with the injection machine according to ISO standards. The barrel temperature and the mold temperature were 210°C and 30°C, respectively. The special mold design can be seen in Figure 3.13.

3.4 Characterization

3.4.1 Structural and morphological properties

3.4.1.1 Measurement of density

The density of the samples were determined according to ISO 1183 [62]. The specimens were weighed in the air first and then placed in the water to the special density determination kit of Radwag Analytical Balance AS 220/X.

3.4.1.2 Measurement of melt flow index

The flow behaviour of molten polymer is defined as an important factor affecting the processability of polymers. The polymer sample is heated in the barrel and then extruded through a standard die using a standard weight on the piston, and the weight of polymer extruded in 10 minutes is quoted as the melt flow rate (MFR) or melt flow index (MFI) of the polymer [63].

Melt flow index (MFI) or melt flow rate (MFR) is described by flow properties of the molten polymers and measured according to ISO 1133 test standard [64]. The test temperature and weight were set to 190°C and 2.16 kg, respectively.

3.4.1.3 X-ray diffraction (XRD) analysis

X-Ray diffraction (XRD) patterns of the samples were recorded by monitoring the diffraction angles (2θ) from 10 to 150 on the apparatus by using CuKα radiation.

$$\text{Bragg equation} = \lambda\, n = 2\, d \sin\theta \; ; n=0,1,2,... \qquad \textbf{(3.1)}$$

Bragg equation (Eq.3.1) is the well-known fundamental law of X-ray crystallography. Interplanar spacing is d, the angle between the planes and the direction of the beam is θ, l is the wavelength (λ) of used light, and n is integer. The angle between reflected wave and solid surface is θ. λ=1.5405 Å is a parameter for the used apparatus. The data obtained from instrument were 2θ vs intensity and the first interlayer spacing, d_{001}, values were calculated from the plot given by using Bragg equation with given constants and taken the integer n=1.

3.4.1.4 Contact angle measurements

Contact angles were measured in order to evaluate the surface properties of the samples. The sessile drop method was performed and deionized water was used to form liquid drops. Sample surfaces were wiped by ethanol and left at room conditions for 24 hours for obtaining smooth and dirt-free (dust, oil, residues from production line etc.) test surfaces. As for accuracy and reproducibility, each sample had measured at least three times.

3.4.2 Mechanical properties

3.4.2.1 Determination of tensile properties

Tensile properties of the samples were measured according to ISO 527 [65] by Lloyd LC universal tensile testing machine Testing speed was set to 50 mm/min and gauge length (L_o) was set to 100 mm. . Tensile strength, modulus of elasticity, and elongation and strength at break were calculated from the tensile measurements. Tensile strenght is a measure of the material's strength under tensile loading. The modulus is a measure of material's resistance to deformation and can be found by the initial slope of the stress-strain curve. Strech limit of the material or deformation limit before its break is called elongation [21].

3.4.2.2 Determination of Izod impact strength

Izod impact strength values of the samples were measured according to ISO 180 [66] by Ceast 9050 Izod impact machine.

The thickness and the width of the samples were measured by electronic digital vernier calliper. Then 2 mm notch was formed as defined in ISO 180/1A.

3.4.2.3 Determination of hardness

The hardness of the samples were measured according to ISO 868 [67] and Shore D values were obtained.

3.4.3 Thermal properties

3.4.3.1 Determination of ash content and nanoclay content

Ash is the inorganic residue remaining after the water and organic matter have been

removed by heating. Ash content test provides a measure of the total amount of fillers within the tested sample.

The ash content tests were carried out by using Nüve MF 120 muffle furnace. The weight of the empty crucible (m_1) and the sample's initial weight (3.00 ± 0.20 g, m_2) were evaluated. Then the crucibles including samples were held at 800 °C for one hour in the muffle furnace.After one hour, the crucibles were cooled in desiccator for 15 minutes and reweighed (m_3). Ash content of the samples were calculated as follows (Eq.3.2):

$$\text{Ash content } \% = [\ (m_3 - m_1) / m_2\ ] \times 100 \qquad \textbf{(3.2)}$$

Since the organomodified nanoclay I.44P contains 48% organic matter, actual filler amounts within the samples were calculated according to the ash content test results.

3.4.3.2 Differential scanning calorimetry (DSC) analysis

Thermal analysis of the samples were performed by TA Instruments Q20 DSC Differential Scanning Calorimetry machine according to ISO-11357 [68].

The DSC measures the power (heat energy per unit time) differential between a small weighed sample of polymer (ea. 10 mg) in a sealed aluminum pan referenced to an empty pan in order to maintain a zero temperature differential between them during programmed heating and cooling temperature scans [69].

The samples were heated from 40 ºC to 300 ºC at a 10 ºC/min heating rate and they were cooled from 300 ºC to 25 ºC at a rate of 10 ºC/min under nitrogen atmosphere. The melting temperature (T_m), crystallization temperature (T_c), and heat of fusion values of polymers were obtained by DSC analysis.

The conversion of a measured heat of fusion was converted to percent crystallinity (%Xc) provided the heat of fusion for the 100% crystalline polymer is known. The degree of crystallinity (Xc) was calculated using the following equation (Eq.3.3):

$$Xc = \Delta H_m / (\Delta H_f \times \theta_{PE}) \times 100 \qquad \textbf{(3.3)}$$

where Xc is the degree of crystallinity %, ΔH_m is the melting enthalpy obtained from the DSC thermograms, ΔH_f is the theoretic heat of melting of a 100% crystalline polymer, and θ_{PE} is the PE fraction in composition.

The heat of fusion of pure crystalline polyethylene (the theoretic heat of melting of a

100% crystalline polyethylene) is taken to be in the range of 276.15-292.88 J/g, a commonly accepted value 279 J/g was taken in the calculations of the degree of crystallinity [70, 71, 72, 73].

4. RESULTS AND DISCUSSION

Twenty different nanocomposites containing varying ratios of LDPE, mPE, PDMS, PE-g-MA (C), and organomodified nanoclay I.44P (O-MMT) were prepared according to the procedure explained in section 3.3.1. The descriptions of the samples were given at Table 3.3. The results of the samples were evaluated and compared according to PE blend compositions.

4.1 Evaluation of structural and morphological properties

4.1.1 Measurement of density

Density measurements of the samples were performed as explained in section 3.4.1.1. The density values were ranging between 0.89-0.94 g/cm^3. There was no dramatic change in the density values of the nanocomposites with varying ratios of LDPE, mPE and PDMS. Density test results are given in Figure 4.1.

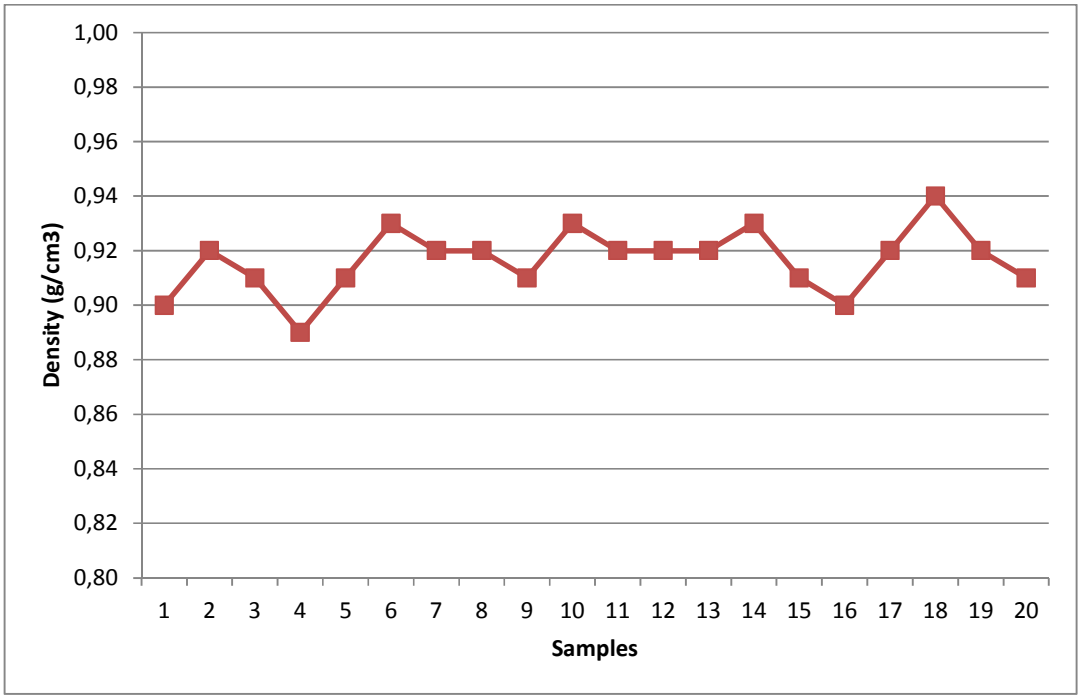

Figure 4.1 : Density measurements of the samples.

4.1.2 Measurement of melt flow index

Measurements of melt flow index were performed as explained in section 3.4.1.2. MFI results show that, neat PE blends have higher values comparing to nanocomposites containing nanoclay/PE-g-MA/PDMS and nanoclay/PE-g-MA. In addition, nanocomposites without PDMS had the lowest flow rate values. There is no important difference between 5 phr and 10 phr PDMS containing blends. Different LDPE and mPE seemed not to have a significant change in the flow behaviours. MFI test results are given in Figure 4.2.

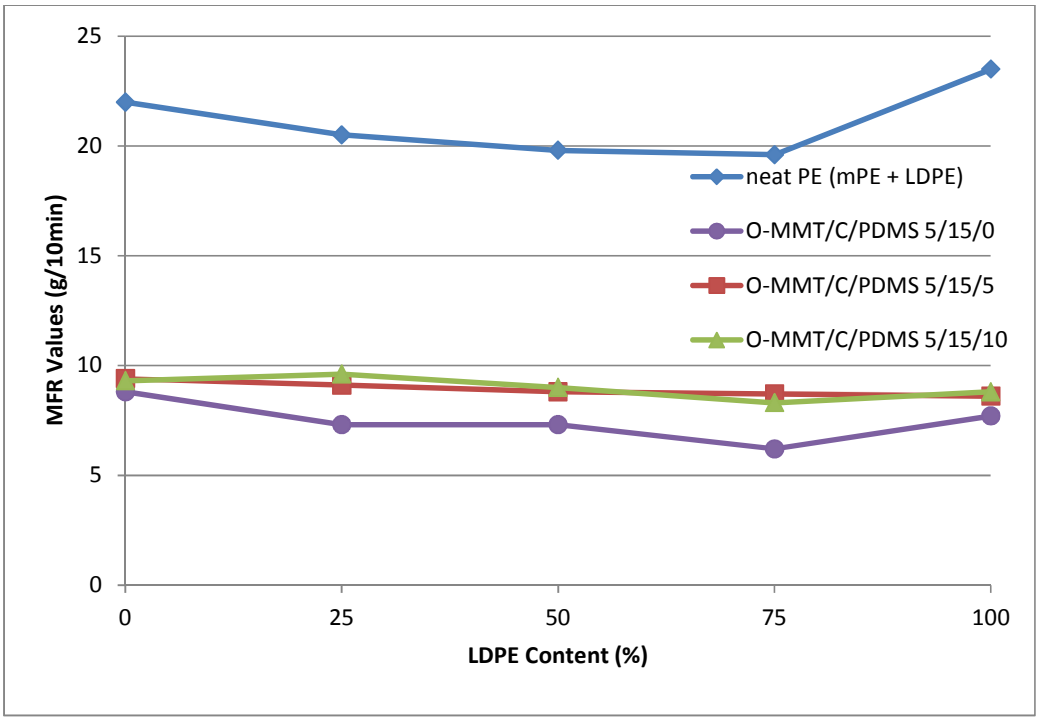

Figure 4.2 : Melt flow index results of the samples.

4.1.3 X-ray diffraction (XRD) analysis

X-ray diffraction (XRD) analysis of the samples were performed as explained in section 3.4.1.3. XRD has been used to evaluate the degree of interaction between the organoclay and the polymer matrix and the diffractograms obtained.

It is well known that the positions of diffraction peaks on the XRD patterns of nanocomposites between $2\theta=0\text{-}10^\circ$ provides some information concerning the interlayer spacing (d_{001}) of the silicate $_1$layers of the organoclay through the Bragg's equation (Eq.3.1). Table 4.1 presents the basal spacing determined from Eq.3.1 for the organoclay powder and the selected samples.

Table 4.1 : XRD measurement results of the samples.

Samples	Definition*	d_{001} (Å)
1	100/0/0/0/0	0
2	100/0/5/15/0	27.0
3	100/0/5/15/5	27.0
4	100/0/5/15/10	57.3/27.4
9	50/50/0/0/0	0
10	50/50/5/15/0	43.0/30.0
11	50/50/5/15/5	27.1
12	50/50/5/15/10	27.0
17	0/100/0/0/0	0
18	0/100/5/15/0	25.6
19	0/100/5/15/5	33.2/27.0
20	0/100/5/15/10	32.4/27.3
O-MMT	I-44P	25.82

* mPE/LDPE/O-MMT/PE-g-MA/PDMS

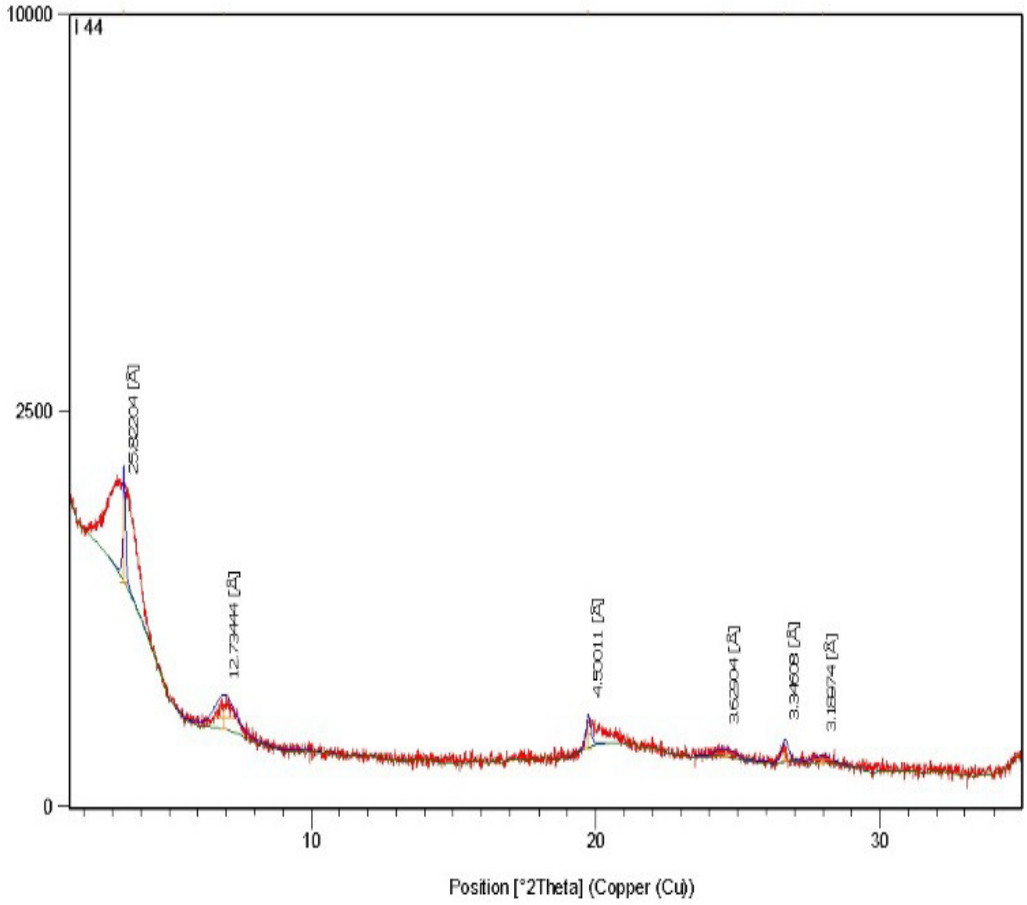

Figure 4.3 : XRD patterns of I-44 (O-MMT).

The XRD patterns of the organoclay I-44 and selected samples are given in Figure 4.3, 4.4. XRD patterns of the nanocomposites showed that polyolefin chains had separated the organoclay layers by penetrating between these layers. The reason of d_{001} values of some samples giving two peaks is having nonuniform homogenity and obtaining more exfoliation in some regions. Regarding to these results, it was observed that the 10 phr PDMS containing 100% mPE sample, Sample No.4, showed the best result. For this sample, when the peak heights had taken into consideration, it can be concluded that partial exfoliation had formed.

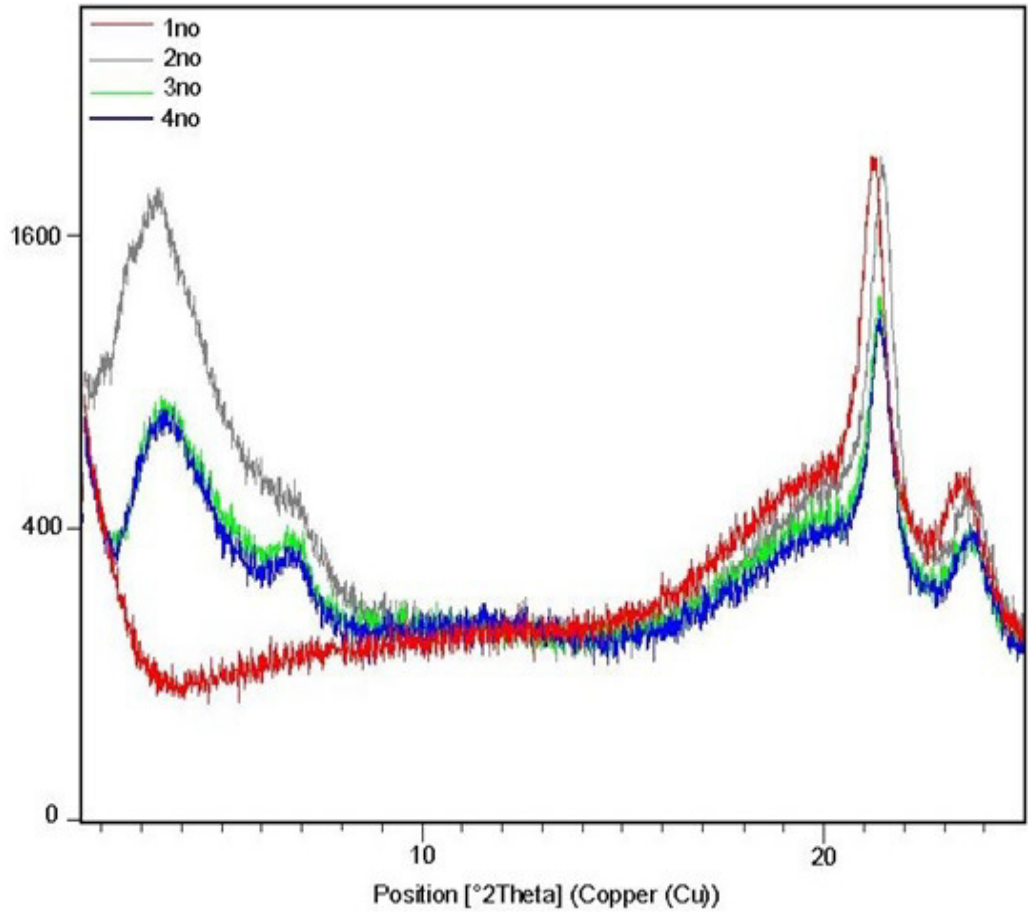

Figure 4.4 : XRD patterns of the Samples No.1, 2, 3, and 4.

In the 100% LDPE samples 19 and 20, containing 5 and 10 phr PDMS respectively, it was observed that PDMS had contributed to the separation of the clay layers in these samples. However, in the samples containing 50% LDPE and 50% mPE, the addition of PDMS did not have a significant effect on the exfoliation of the organomodified nanoclay (I44 P).

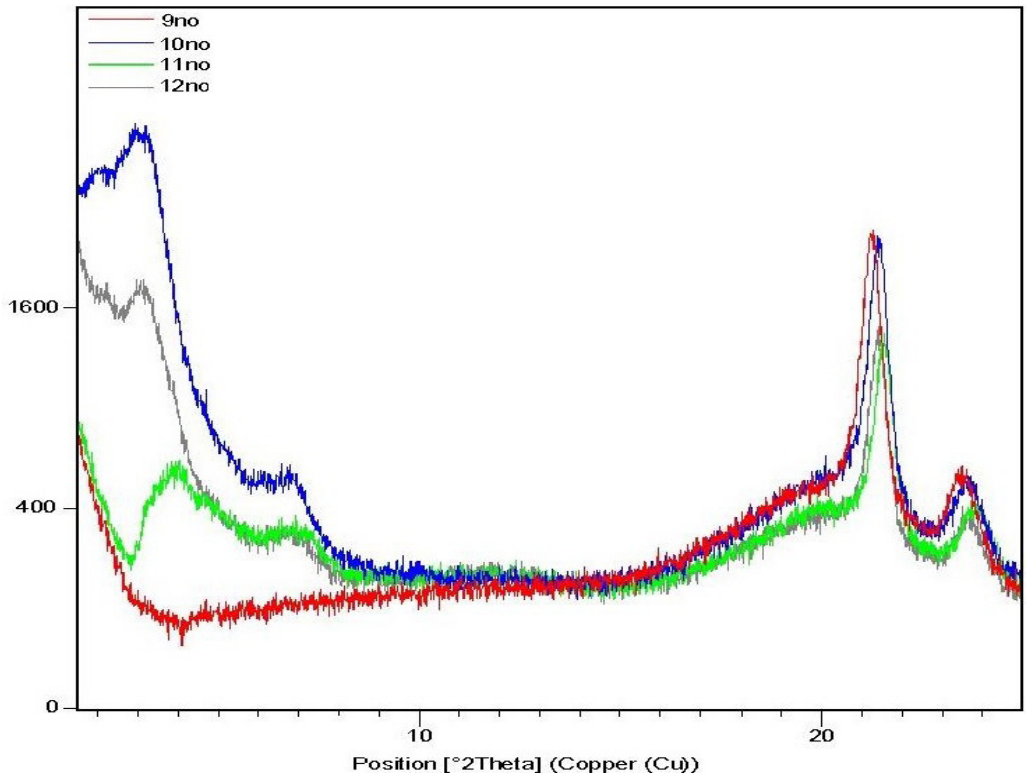

Figure 4.5 : XRD patterns of the Samples No.9, 10, 11, and 12.

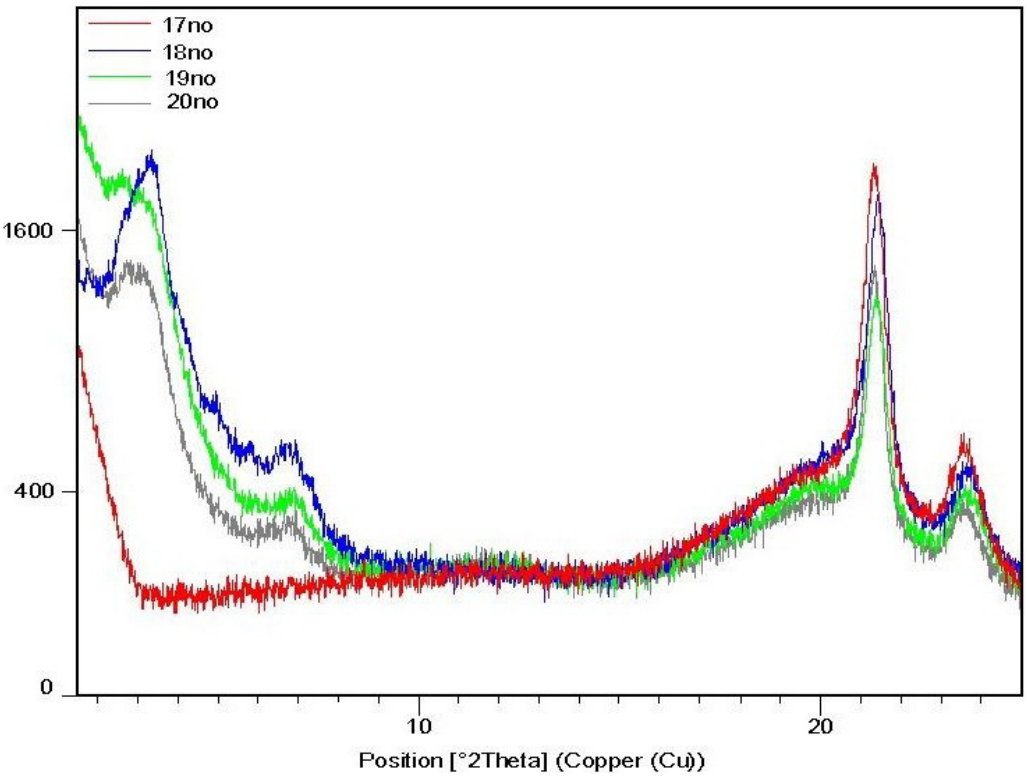

Figure 4.6 : XRD patterns of the Samples No.17, 18, 19, and 20.

4.1.4 Measument of contact angle

Contact angles of the samples were measured as explained in section 3.4.1.4. It was observed that with the addition of clay to neat PE blends, there was a decrease in contact angle values in all samples as expected due to the hydrophilic nature of O-MMT. According to the test results, it is observed that with the increasing amount of PDMS, the contact angle values were increasing and becoming higher than 90°, which means hydrophobic surfaces. In all samples, with the addition of PDMS to the clay containing nanocomposites, 5 phr and 10 phr PDMS increased the θ values around 15-20% and 25-30%, respectively. Since the θ of the mPE is low, there was a decrease in values with higher amount of mPE. Contact angle measurement results are given in Table 4.2.

Table 4.2 : Contact angle test results of the samples.

Samples*	Contact Angle (θ)
100/0/0/0/0	87.81
100/0/5/15/0	81.21
100/0/5/15/5	99.08
100/0/5/15/10	105.84
75/25/0/0/0	90.32
75/25/5/15/0	86.55
75/25/5/15/5	100.79
75/25/5/15/10	107.36
50/50/0/0/0	92.89
50/50/5/15/0	87.42
50/50/5/15/5	105.13
50/50/5/15/10	110.40
25/75/0/0/0	94.39
25/75/5/15/0	91.38
25/75/5/15/5	104.89
25/75/5/15/10	116.19
0/100/0/0/0	98.63
0/100/5/15/0	94.107
0/100/5/15/5	114.13
0/100/5/15/10	118.22

* mPE/LDPE/O-MMT/PE-g-MA/PDMS

4.2 Evaluation of mechanical properties

4.2.1 Tensile properties

Tensile tests were done as the procedure explained in section 3.4.2.1. Modulus of elasticity (E), tensile strength (σ_M), elongation at break (ε_B) and strength at break (σ_B) values are given in Table 4.3. Errors for E, σ_M , ε_B, and σ_B are %10, % 4, % 12, and % 3, respectively.

Modulus of elasticity (E) had increased almost 100% with the addition of O-MMT and PE-g-MA to neat PE blends as can be observed from Figure 4.7. However, with the addition of PDMS to nanocomposites, there was a decrease in E values and the increasing amount of PDMS lowering the values more.

Table 4.3 : Tensile test results of the samples.

Samples*	E(MPa)	σ_M (MPa)	ε_B (%)	σ_B (MPa)
100/0/0/0/0	140	10.10	240	10.10
100/0/5/15/0	290	10.20	203	7.50
100/0/5/15/5	125	9.20	315	9.10
100/0/5/15/10	105	8.30	330	8.50
75/25/0/0/0	160	10.20	292	9.60
75/25/5/15/0	322	10.40	238	8.10
75/25/5/15/5	145	9.30	310	8.50
75/25/5/15/10	125	8.50	325	8.30
50/50/0/0/0	190	10.50	345	9.20
50/50/5/15/0	358	10.50	275	8.00
50/50/5/15/5	155	9.10	365	8.10
50/50/5/15/10	125	8.10	387	7.70
25/75/0/0/0	200	10.30	390	8.50
25/75/5/15/0	392	10.90	227	8.40
25/75/5/15/5	165	9.40	410	7.90
25/75/5/15/10	135	8.50	455	7.10
0/100/0/0/0	225	10.60	450	8.40
0/100/5/15/0	394	11.30	132	8.90
0/100/5/15/5	180	9.70	552	8.10
0/100/5/15/10	165	8.90	608	7.40

* mPE/LDPE/O-MMT/PE-g-MA/PDMS

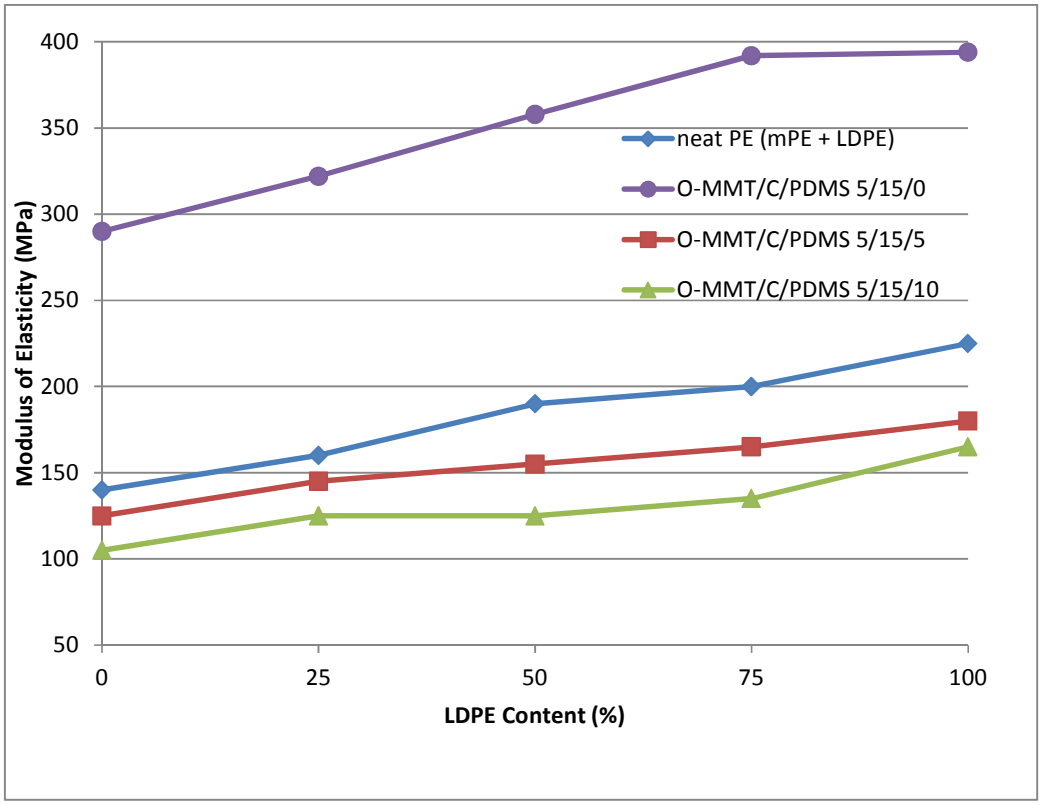

Figure 4.7 : Modulus of elasticity values of the samples.

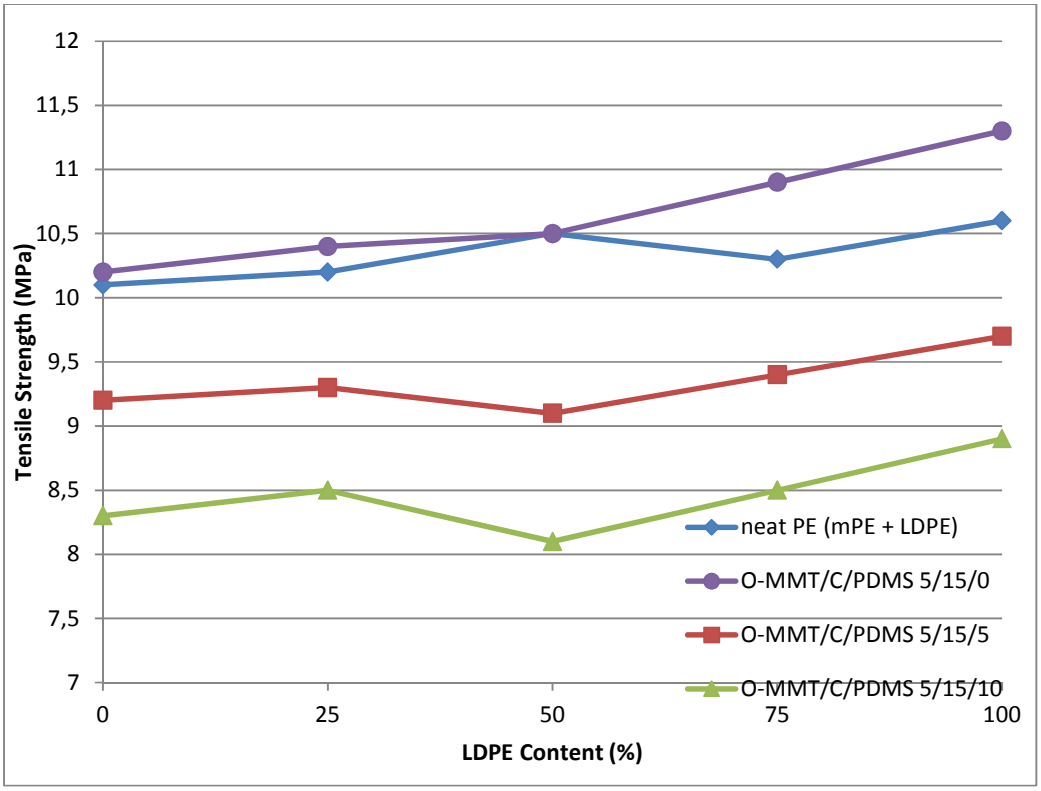

Figure 4.8 : Tensile strength values of the samples.

Tensile strength (σ_M) values of the neat PE blends almost remained the same with the addition of nanoclay and PE-g-MA. The increasing PDMS content lowered the σ_M, but this decrease is in the range of the testing errors and acceptable. In the LDPE rich nanocomposites, the effect of nanoclay is more significant.

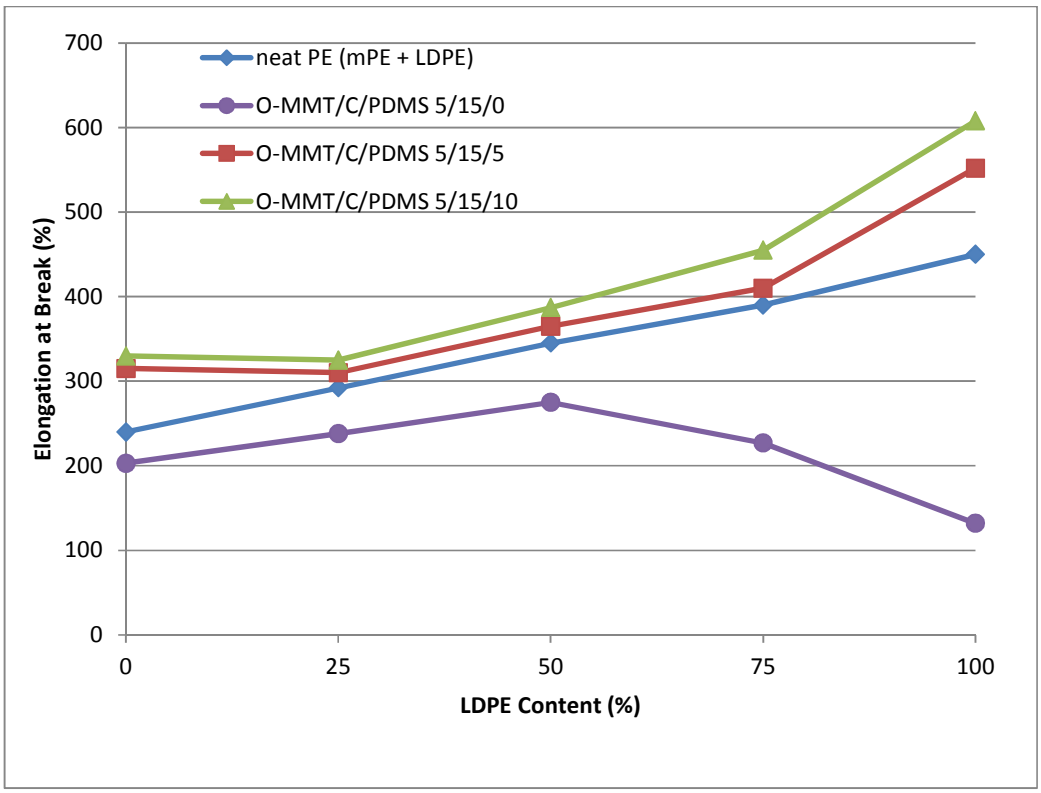

Figure 4.9 : Elongation at break values of the samples.

Elongation at break (ε_B) values of the PE blend nanocomposites containing only O-MMT and PE-g-MA are lower than neat PE. There is an increase in the elongation at break results with the increasing PDMS content. At 100% LDPE nanocomposites, addition of 10 phr PDMS to the blends increasing the ε_B up to about 35% comparing to neat PE blend, and about 360% comparing to LDPE containing only O-MMT and PE-g-MA. Also in 75% LDPE and 25% mPE containing nanocomposites, addition of 10 phr PDMS to the blends increasing the ε_B up to about 20% comparing to neat PE blend, and about 100% comparing to the nanocomposite sample without PDMS.

As can be seen from Figure 4.7, Figure 4.9 and Figure 4.10, modulus of elasticity is decreasing while the elongation at break is increasing with the increasing amount of PDMS for all test samples. Since LDPE has higher modulus compared to mPE, this

distinction became clearer with the higher amounts of LDPE. The varying amounts of LDPE and mPE have caused the same trends in the tensile test values of neat PE blends and nanocomposites with/without PDMS.

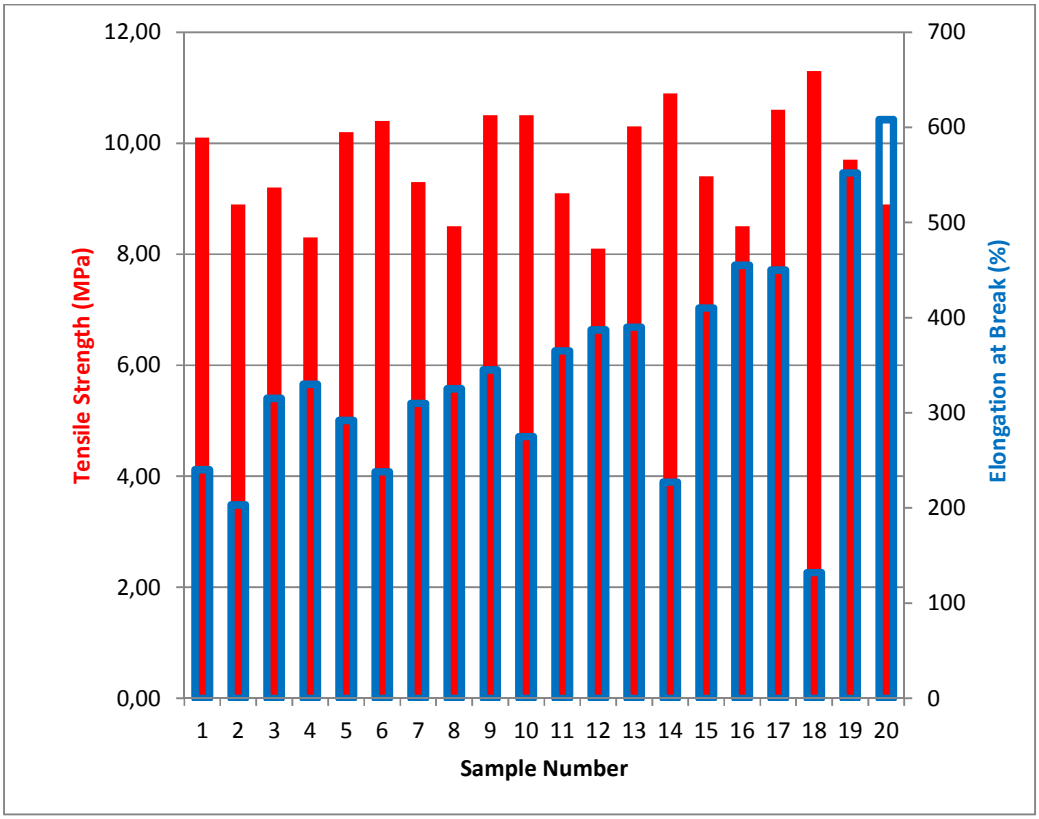

Figure 4.10 : Tensile strength and elongation at break values of the samples.

4.2.2 Izod impact properties

Izod impact tests were done according to the procedure explained in section 3.4.2.2. Izod impact test results are given in Figure 4.11. Impact resistance is decreasing with the addition of PDMS to the nanocomposites and increasing amount of PDMS is lowering the values more. The same trend is obtained for the different PE blend formulations.

4.2.3 Hardness

Shore D values of the samples were obtained as explained in section 3.4.2.3. According to the hardness test results, the blends without PDMS had higher values comparing to the ones with PDMS, and hardness was decreasing with the increasing

PDMS content as expected. Samples only containing nanoclay and PE are the hardest ones in all tested samples. Varying ratios of LDPE and mPE had not a significant effect on hardness . The test results are given in Figure 4.12.

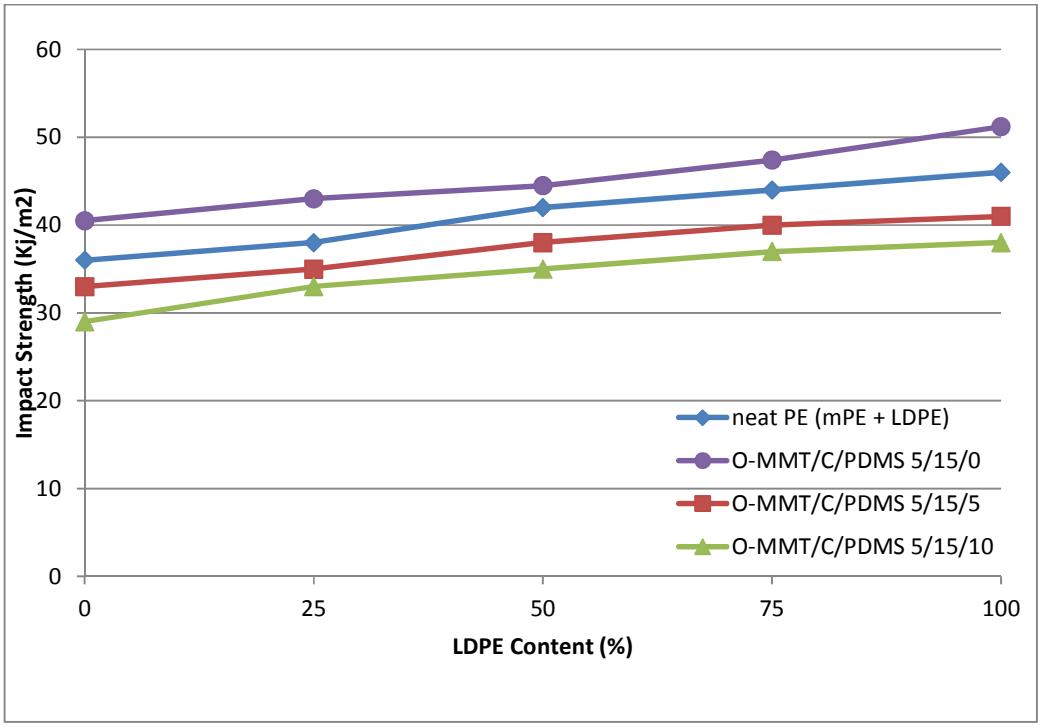

Figure 4.11 : Izod impact strength values of the samples.

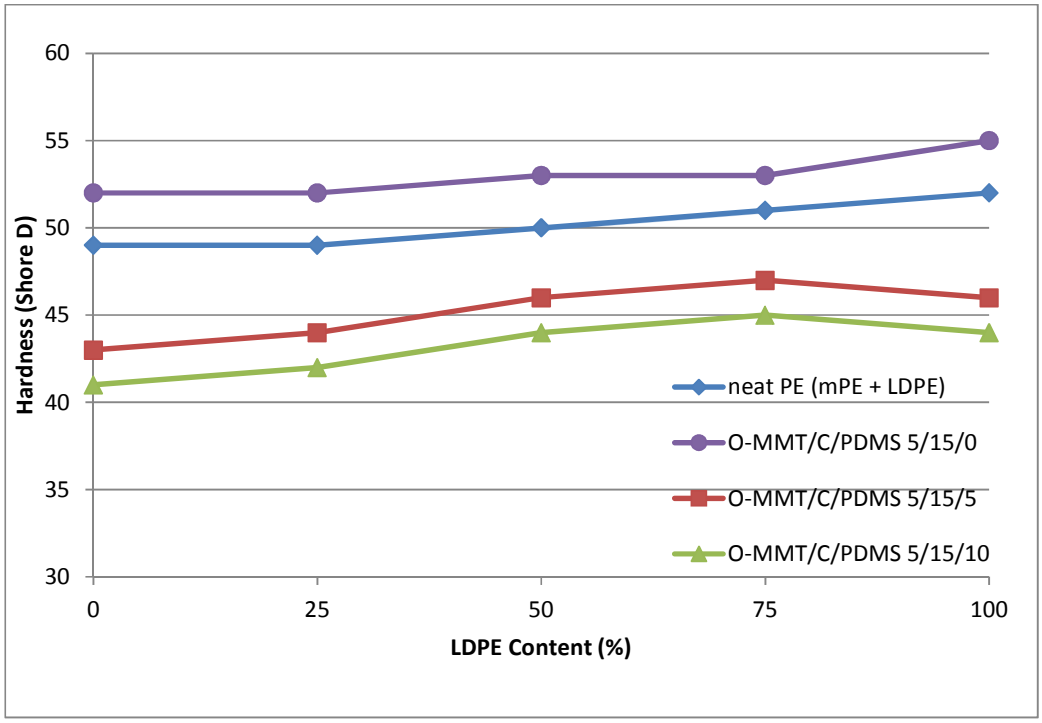

Figure 4.12 : Hardness (Shore D) values of the samples.

4.3 Evaluation of thermal properties

4.3.1 Ash content

The ash content tests were carried out and calculated according to procedure explained in section 3.4.3.1. The preparation of the nanocomposites was explained in section 3.3.1 and 5 phr organomodified nanoclay was added to each blend, except the blends containing only PE (samples 1, 5, 9, 13, and 17).

Table 4.4 : The results of the ash content tests.

Samples*	Ash Content Test Values (%)	Theoritical Filler Content (%)
100/0/0/0/0	0.00	0.00
100/0/5/15/0	1.99	2.17
100/0/5/15/5	2.26	2.08
100/0/5/15/10	1.73	2.00
75/25/0/0/0	0.00	0.00
75/25/5/15/0	2.01	2.17
75/25/5/15/5	2.10	2.08
75/25/5/15/10	1.50	2.00
50/50/0/0/0	0.00	0.00
50/50/5/15/0	1.93	2.17
50/50/5/15/5	2.03	2.08
50/50/5/15/10	1.58	2.00
25/75/0/0/0	0.00	0.00
25/75/5/15/0	2.12	2.17
25/75/5/15/5	2.16	2.08
25/75/5/15/10	1.94	2.00
0/100/0/0/0	0.00	0.00
0/100/5/15/0	1.91	2.17
0/100/5/15/5	2.16	2.08
0/100/5/15/10	1.70	2.00

* mPE/LDPE/O-MMT/PE-g-MA/PDMS

The phr values of the added nanoclay were converted into percent values to compare the ash content test results and actual filler contents. It was observed that the percentages of the nanoclay in the blends are 4.1667 % (samples 2, 6, 10, 14, and 18), 4 % (samples 3, 7, 11, 15, and 19), and 3.8462 % (samples 4, 8, 12, 16, and 20). Additionally, ash content test was performed for the organomodified nanoclay itself and it was found that 48 % of the nanoclay is organic matter and 52 % is inorganic content. The theoritical nanoclay percents in the blends were calculated by

multiplying the percent values given above by 0.52. Also, PDMS was tested as well and it was found that 10% of PDMS additive is inorganic and affecting the ash content test results. For nanocomposites containing 5 and 10 phr PDMS, the effect of PDMS to the ash content are 0.4% (samples 3, 7, 11, 15, and 19) and 0.77% (samples 4, 8, 12, 16, and 20). The ash content part of PDMS additive is subtracted from the test values and the results were compared with the theoritical filler contents.

When the results given in Table 4.4 were analysed, it could be observed that theoretical nanoclay contents according to formulations and actual nanoclay contents according to ash content test results were quite similar. These results had indicated well dosing during the production of the nanocomposites and homogenous dispersion of the nanoclays within the samples, briefly obtaining samples through a good processing.

Table 4.5 : The onset and peak melting temperature values obtained from DSC analysis.

Samples*	Melting Temperatures	
	To (°C)	Tp (°C)
100/0/0/0/0	82.03	105.38
100/0/5/15/0	80.73	105.22
100/0/5/15/5	86.11	106.54
100/0/5/15/10	84.3	103.76
75/25/0/0/0	92.67	111.38
75/25/5/15/0	90.76	109.8
75/25/5/15/5	91.62	111.64
75/25/5/15/10	98.29	113.71
50/50/0/0/0	93.99	114.33
50/50/5/15/0	93.75	112.57
50/50/5/15/5	102.86	115.14
50/50/5/15/10	94.46	110.18
25/75/0/0/0	100.29	115.53
25/75/5/15/0	99.72	113.9
25/75/5/15/5	99.62	114.39
25/75/5/15/10	97.73	110.97
0/100/0/0/0	101.99	115.15
0/100/5/15/0	99.30	113.74
0/100/5/15/5	93.69	111.08
0/100/5/15/10	103.85	114.6

* mPE/LDPE/O-MMT/PE-g-MA/PDMS

4.3.2 Differential scanning calorimetry (DSC) analysis

DSC analysis were performed as explained in section 3.4.3.2. By using the software of DSC analyzer, the first derivative of heat flow change with respect to temperature change were calculated in order to determine the start and end temperatures of the melting and crystallization regions. Linear baselines were drawn to determine the onset (To) and the peak (Tp) temperatures (Table 4.5 and Table 4.6.). The heat of melting and heat of crystallization data were obtained and the degree of crystallinity values were calculated and given in Table 4.7.

Table 4.6 : The onset and peak crystallization temperature values obtained from DSC analysis.

Samples*	Crystallization Temperatures	
	To (°C)	Tp (°C)
100/0/0/0/0	100.5	96.47
100/0/5/15/0	103.88	97.27
100/0/5/15/5	106.65	89.93
100/0/5/15/10	104.28	96.54
75/25/0/0/0	103.74	98.14
75/25/5/15/0	102.7	98.02
75/25/5/15/5	102.4	95.79
75/25/5/15/10	101.04	96.09
50/50/0/0/0	102.79	98.32
50/50/5/15/0	102.38	98.41
50/50/5/15/5	100.76	97.72
50/50/5/15/10	100.9	97.22
25/75/0/0/0	102.4	99.48
25/75/5/15/0	101.97	99.02
25/75/5/15/5	100.87	97.87
25/75/5/15/10	100.77	98.11
0/100/0/0/0	101.07	97.95
0/100/5/15/0	101.97	99.41
0/100/5/15/5	101.41	96.78
0/100/5/15/10	100.61	97.88

* mPE/LDPE/O-MMT/PE-g-MA/PDMS

Addition of O-MMT and PE-g-MA to the PE blends decreasing the onset and peak melting temperatures while increasing those of crystallization. Degree of crystallinities (Xc) of nanocomposites containing clay and compatibilizer are higher than neat PE blends and the increasing amount of PDMS is lowering Xc. This

situation is significantly observed in LDPE rich nanocomposites. In the nanocomposites composed of mPE matrices, the Xc values are higher and getting lower with the addition of LDPE into the blends eventhough LDPE alone has higher degree of crystallinity.

Table 4.7 : Melting and crystallization enthalpies and degree of crystallinities of the samples.

Samples*	ΔHm (j/g)	ΔHc (j/g)	Xc (%)
100/0/0/0/0	79.73	62.18	28.58
100/0/5/15/0	81.2	55.28	30.37
100/0/5/15/5	73.93	63.3	28.71
100/0/5/15/10	74.89	63.07	30.06
75/25/0/0/0	80.89	60.66	28.99
75/25/5/15/0	84.54	61.11	31.62
75/25/5/15/5	59.14	47.94	22.96
75/25/5/15/10	53.71	50.62	21.56
50/50/0/0/0	77.67	63.03	27.84
50/50/5/15/0	79.40	62.74	29.70
50/50/5/15/5	51.85	52.41	20.13
50/50/5/15/10	59.8	52.95	24.00
25/75/0/0/0	68.36	69.33	24.50
25/75/5/15/0	73.64	72.24	27.54
25/75/5/15/5	50.45	56.41	19.59
25/75/5/15/10	59.33	51.18	23.82
0/100/0/0/0	108.0	93.40	38.71
0/100/5/15/0	94.29	83.70	35.27
0/100/5/15/5	59.12	51.78	22.95
0/100/5/15/10	61.61	61.41	24.73

* mPE/LDPE/O-MMT/PE-g-MA/PDMS

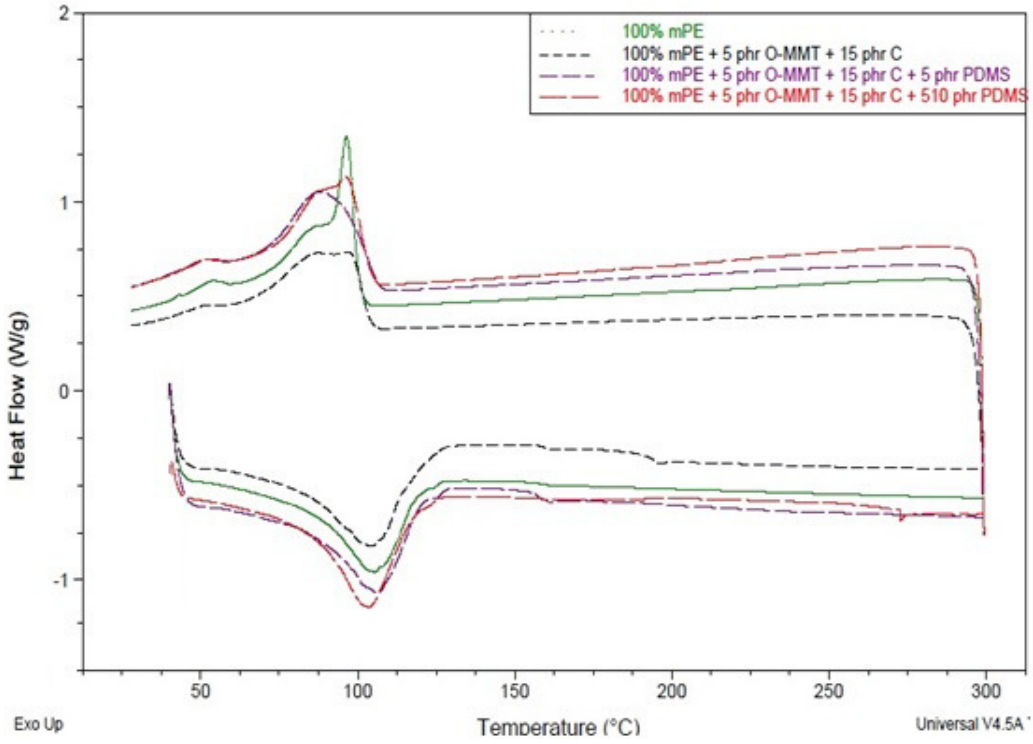

Figure 4.13 : Differential scanning calorimetry diagrams of 100% mPE containing samples (Samples 1, 2, 3 and 4).

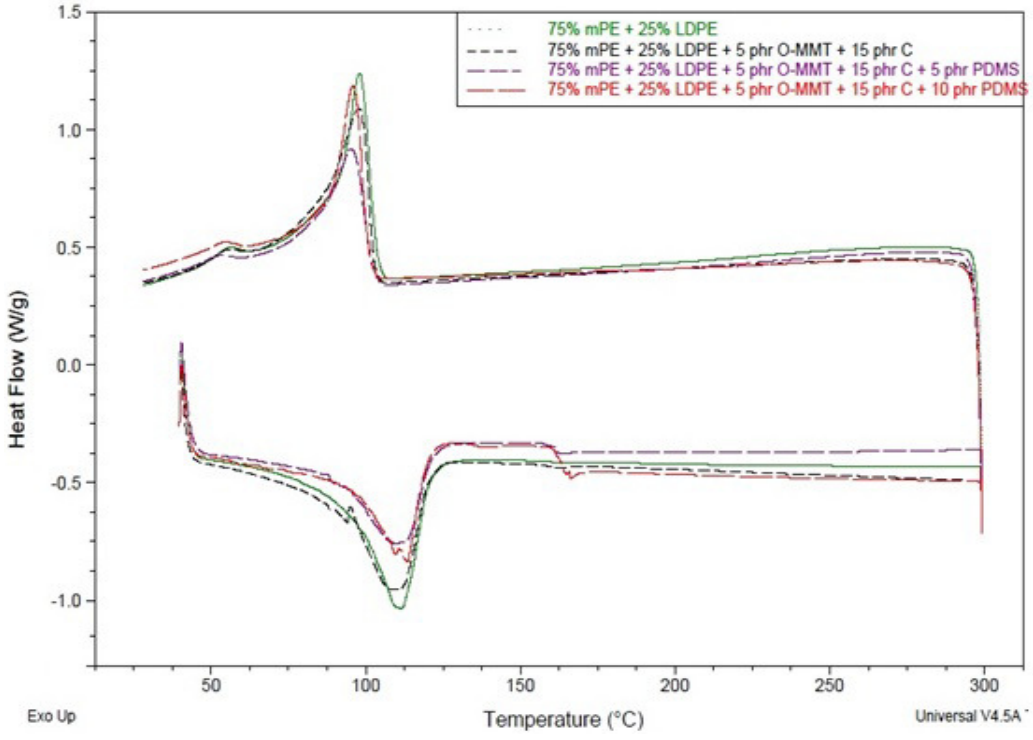

Figure 4.14 : Differential scanning calorimetry diagrams of 75% mPE and 25% LDPE containing samples (Samples 5, 6, 7 and 8).

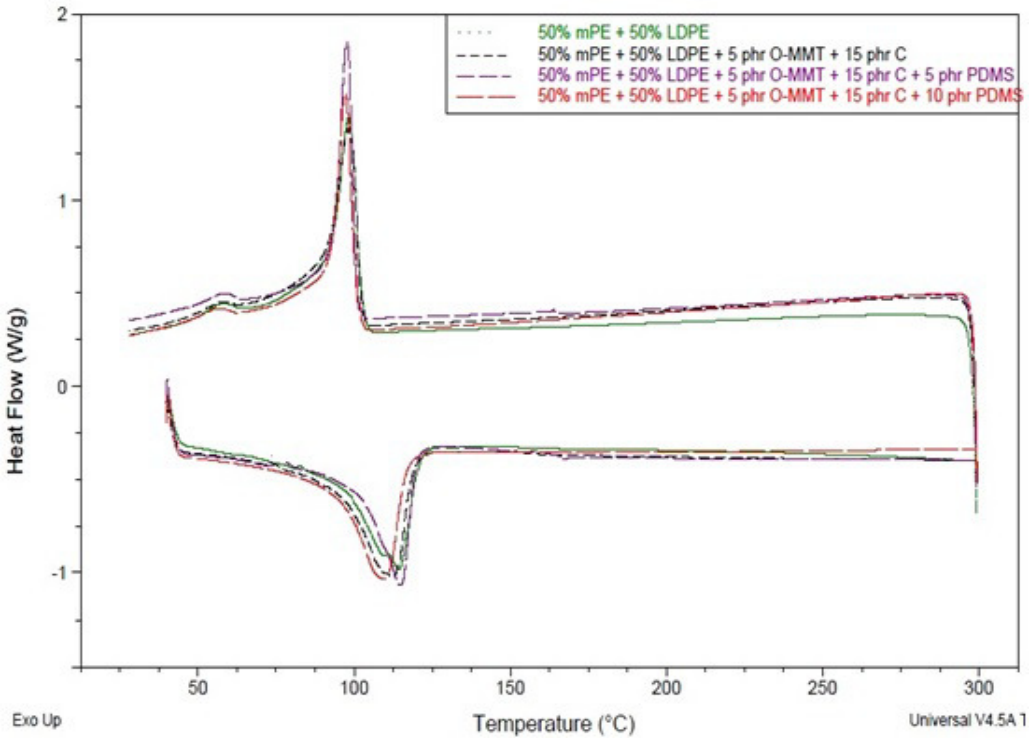

Figure 4.15 : Differential scanning calorimetry diagrams of 50% mPE and 50% LDPE containing samples (Samples 9, 10, 11 and 12).

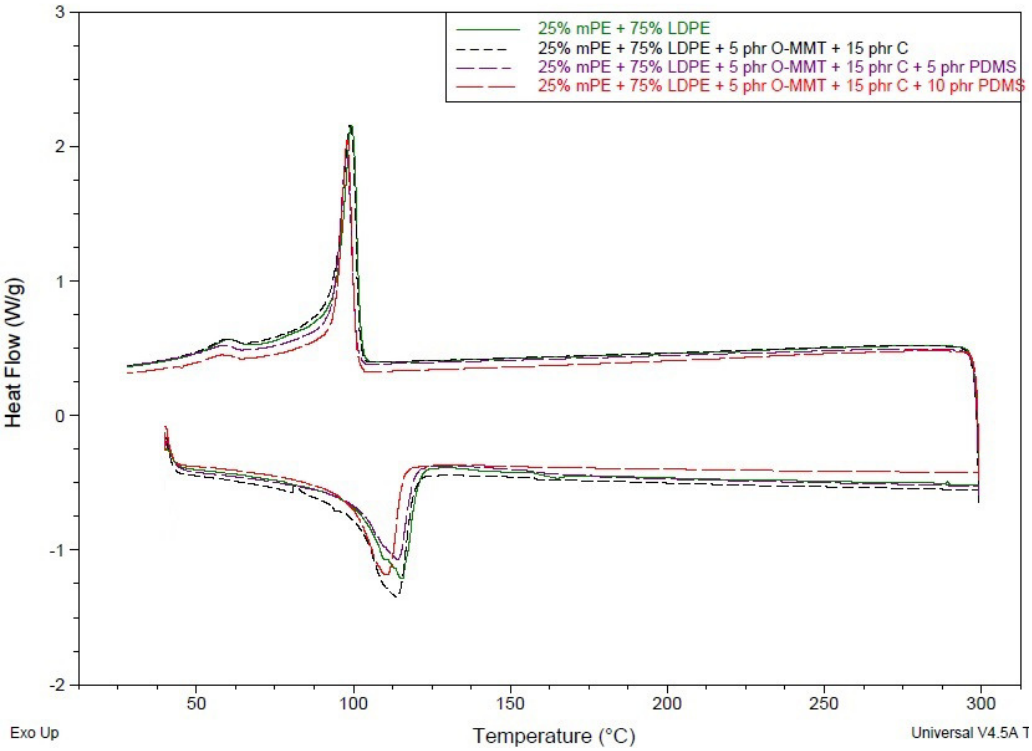

Figure 4.16 : Differential scanning calorimetry diagrams of 25% mPE and 75% LDPE containing samples (Samples 13, 14, 15 and 16).

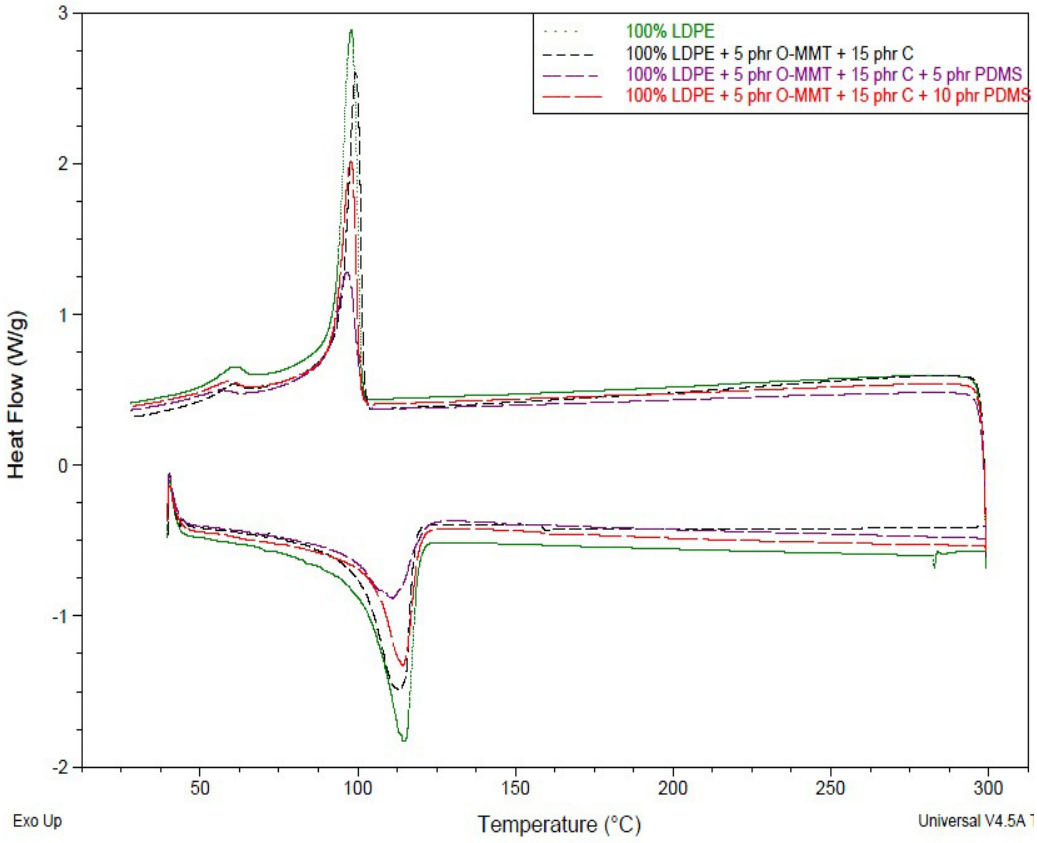

Figure 4.17 : Differential scanning calorimetry diagrams of 100% LDPE containing samples (Samples 17, 18, 19 and 20)

5. CONCLUSION

In this study, LDPE/mPE blend based nanocomposites were prepared with and without PDMS. The effects of PDMS and the composition of the blends, on the mechanical, thermal, and the morphological properties were investigated.

Different compositions of LDPE/mPE nanocomposites with and without PDMS and neat PE blends were extruded after the components were premixed before being fed to the extruder. The strands from the die were cooled in a water bath and pelletized in a granulating unit. Test specimens according to ISO standards were injection molded with a special designed mold. Actual filler contents of the nanocomposites were calculated by ash content tests and the amounts of fillers are almost the same as theoretical values.

Densities and melt flow indexes (MFI) of the samples were measured. There was no significant change in the density values of the nanocomposites with changing amounts of LDPE, mPE and PDMS. According to MFI results, the nanocomposites containing only nanoclay and compatibilizer showed the poorest flowability and neat PE blends showed better flowing properties comparing to nanocomposites both with/without PDMS. The decrease in flow behaviour with the addition of PDMS and fillers was observed in earlier studies [57]. There is no significant difference between 5 and 10 phr PDMS addition. Varying PE blend formulations did not affect the flow properties of the nanocomposites.

X-ray diffraction (XRD) analysis had been used to evaluate the degree of interaction between the organoclay and the polymer matrix and the diffractograms obtained. XRD patterns of the nanocomposites showed that polyolefin chains had separated the organoclay layers by penetrating between these layers. It was observed that the 10 phr PDMS containing 100% mPE sample, Sample No.4, showed the best result. For this sample, when the peak heights had taken into consideration, it can be concluded that partial exfoliation had formed. In the 100% LDPE samples 19 and 20, containing 5 and 10 phr PDMS respectively, it was observed that PDMS had contributed to the separation of the clays layers in these samples. However, in the samples containing

50% LDPE and 50% mPE, the addition of PDMS did not have a significant effect on the exfoliation of the nanoclay.

Contact angle test was carried out for the nanocomposites and neat PE blends. The addition of clay is decreasing the contact angle values because of the hydrophilic nature of the organomodified montmorillonite. One approach to enhance hydrophobicity of the surface is to modify the surface with materials of low surface free energy [74]. PDMS has a very low surface energy comparing to most of the polymers. The addition of PDMS to the nanocomposites was increasing the contact angle values above 90°. The higher amounts of PDMS increased the values more, 5 phr PDMS increased the contact angles around 15-20% while 10 phr PDMS addition increasing 25-30%. mPE contact angle values measured lower than LDPE and a decrease in values was observed in mPE rich blend based samples.

Mechanical property analysis of the samples showed that PDMS addition to the nanocomposites had a pronounced effect on the mechanical properties of these materials. Modulus of elasticity (E) had increased almost 100% with the addition of O-MMT and PE-g-MA to neat PE blends. On the other hand, the addition of PDMS was decreased the E values and the increasing amount of PDMS lowering the values more. This situation is similar for differently formulated PE blends.

Tensile strength (σ_M) values of the neat PE blends almost remained the same with the addition of nanoclay and PE-g-MA. The increasing PDMS content lowered the σ_M, but this decrease is in the range of the testing errors and acceptable. In the LDPE rich nanocomposites, the effect of nanoclay is more significant.

Elongation at break (ε_B) values of the PE blend nanocomposites containing only nanoclay and compatibilizer are lower than neat PE blends. There is an increase in the elongation at break results with the additon of PDMS and the higher PDMS content increased the results more. In 75% LDPE and 25% mPE based nanocomposites, the addition of 10 phr PDMS was increasing the ε_B up to about 20% comparing to neat PE blend, and about 100% comparing to the nanocomposite sample without PDMS.

Generally, modulus of elasticity is decreasing while the elongation at break is increasing with the increasing amount of PDMS. The varying amounts of LDPE and

mPE have caused the same trends in the tensile test values of neat PE blends and nanocomposites with/without PDMS.

Izod impact and hardness tests were carried out to the samples Izod impact and Shore D hardness values are decreasing with the higher PDMS content. The hardest samples are the nanocomposites without PDMS as expected. The same trend is obtained for the different PE blend formulations.

Thermal properties and the crystallization behaviours of the nanocomposites were investigated by DSC analysis. According to results obtained from DSC thermograms, there is no significant change on the onset and peak melting and crystallization temperatures with the addition of nanoclay and compatibilizer to PE matrix. The degree of crystallinies (Xc) of the nanocomposites without PDMS are higher than the neat PE samples and the ones with PDMS. The higher PDMS amounts are decreasing Xc more. This situation is significantly observed in LDPE rich nanocomposites. In the nanocomposites composed of mPE matrices, the Xc values are higher and getting lower with the addition of LDPE into the blends.

REFERENCES

[1] **Villanueva, M.P., Cabedo, L., Lagaron, J.M., and Gimenez, E.** (2010). Comperative Study of Nanocomposites of Polyolefin Compatibilizers Containing Kaolinite and Montmorillonite Organoclays, *Jour. Appl. Polym. Sci.,* 115(3), 1325-1335.

[2] **Jacquelot, E., Espuche, E., Gerard, J.F., Duchet, J., and Mazabraud, P.** (2006). Morphology and Gas Barrier Properties of Polyethylene-Based Nanocomposites, *Jour. Polym. Sci. Part B,* 44(2), 431-440.

[3] **Kaneko, M.L.Q.A, Romero, R.B., Goncalves, M.C., and Yoshida, I.V.P.** (2010). High Molar Mass Silicone Rubber Reinforced with Montmorillonite Clay Masterbatches: Morphology and Mechanical Properties, *Eur. Polym. Jour.,* 46(5), 881-890.

[4] **Brydson, J.A.** (1999). Plastics Materials, 7th Edition, *Butterworth-Heinemann,* ISBN: 978-0-7506-4132-6.

[5] **Ross, J.F. and MacAdams, J.L.** (1996). Polyethylene (Commercial), in Polymeric Materials Encyclopedia, *CRC Press,* ISBN: 978-0-8493-2470-3.

[6] **Dubois, J.H. and John, F.W.** (1981). Plastics, 6th Edition, *Van Nostrand Reinhold,* ISBN: 978-0-442-26263-1.

[7] **Chiu, F.C., Fu, Q., Peng, Y., and Shih, H.H.** (2002). Crystallization Kinetics and Melting Behavior of Metallocene Short-Chain Branched Polyethylene Fractions, *Jour. Polym. Sci. Part B*, 40 (4), 325-337.

[8] **Lew, C.Y., Murphy, W.R., and McNally, G.M.** (2004). Preparation and Properties of Polyolefin-Clay Nanocomposites, *Polym. Eng. Sci.*, 44 (6), 1027-1035.

[9] **Bailey, F.W., and Whitte, W.M.** (1984). U.S Patent 4461873, *Phillips Petroleum Company*.

[10] **Pettijohn, T.M.** (1996). Polyethylene (Multicomponent), in Polymeric Materials Encyclopedia, *CRC Press,* ISBN: 978-0-8493-2470-3.

[11] **Scheirs, J.** (1996). Polyethylene (Stabilization and Compounding), in Polymeric Materials Encyclopedia, *CRC Press,* ISBN: 978-0-8493-2470-3.

[12] **Kale, L.T. et al** (1993). U.S Patent 5210143, *the Dow Chemical Company*.

[13] **Light, R.R. and Mercer, J.W.** (1994). U.S Patent 5283295, *Eastman Kodak Chemical Company*.

[14] **Collister, J.** (2001). Commercialisation of Polymer Nanocomposites, in Polymer Nanocomposites, Synthesis Characterization and Modelling, *American Chemical Society,* ISBN: 978-0-8412-3768-1.

[15] **Alexandre, M. and Dubois, P.** (2000). Polymer-Layered Silicate Nanocomposites: Preperation, Properties and Uses of New Class of Materials, *Mater. Sci. Eng.*, 28, 1-63.

[16] **LeBaron, P.C., Wang, Z., and Pinnavaia, T.J.** (1999). Polymer-Layered Silicate Nanocomposites: An Overview, *Appl. Clay Sci.*, 15 (1), 11-29.

[17] **Dennis, H.R. et al.** (2001). Effect of Melt Processing Conditions on the Extent of Exfoliation in Organo-Clay Based Nanocomposites, *Polymer,* 42 (23), 9513-9522.

[18] **Wang, Z., Massam, J., and Pinnavaia, T.J..** (2000). Epoxy-Clay Nanocomposites, in Polymer-Clay Nanocomposites, *John Wiley and Sons,* ISBN: 978-0-471-63700-4.

[19] **Ke, Y.C. and Stroeve, P.** (2005). Polymer-Layered Silicate and Silica Nanocomposites, *Elsevier,* ISBN: 978-0-444-51570-4.

[20] **Zhu, L., Ren, X., and Yu, S.** (1998). Use of Cetyltrimethylammonium-Bromide Bentonite to Remove Organic Contaminants of Varying Polar Character from Water, *Environmental Sci. Tech.,* 32 (21), 3374-3378.

[21] **Bhattacharya, S.N., Gupta, R.K., and Kamal, M.R.** (2008) Polymeric Nanocomposites: Theory and Practice, *Carls Hanser Publishers,* ISBN: 978-3-446-40270-6.

[22] **Giannelis, E.P., Krishnamoorti, R., and Manias, E.** (1999). Polymer-Silicate Nanocomposites: Modeled Systems for Confined Polymers and Polymer Brushes, *Adv. Polym. Sci.,* 138/1999, 107-147.

[23] **Van Olphen, H.** (1977). An Introduction to Clay Colloid Chemistry: For Clay Technologist, Geologists, and Soil Scientists, *John Wiley and Sons,* ISBN: 978-0-471-01463-8.

[24] **Theng, B.K.G.** (1979). Formation and Properties of Clay-Polymer Complexes, *Elsevier,* ISBN: 978-0-444-41706-0.

[25] **Kenig, S., Ophir, A., Shepelev, O., and Weiner, F.** (2002). High Barrier Blow Molded Containers Based on Nanoclay Composites, *Antec,* 1, 1449-1455.

[26] **Lee, Y.H., Zheng, W.G., Park, C.B., and Kontopoulou, M.** (2005). Effect of Clay Dispersion on the Mechanical Properties and Flammability of Polyethylene/Clay Nanocomposites, *Antec,* 1, 1428-1432.

[27] **Reddy, M.M., Gupta, R.K., Bhacttacharya, S.N., and Parthasarathy, R.** (2006). Accelerated Environmental Degradation Studies of Polyethylene Nanocomposites, *PPS-22 Conference, Yamagata, Japan.*

[28] **Bicerano, J.** (2006). A Practical Guide to Polymeric Compatibilizers for Polymer Composites and Laminates, Ph.D. Thesis.

[29] **Bula, K. and Jesionowski, T.** (2010). Effect of Polyethylene Functionalization on Mechanical Properties and Morphology of PE/SiO_2 Composites, *Composite Interfaces,* 17(5-7), 603-614.

[30] **Durmus, A., Kasgoz, A., and Macosko, C.W.** (2007). Linear Low Density Polyethylene(LLDPE)/Clay Nanocomposites. Part I: Structural Characterization and Quantifying Clay Dispersion by Melt Rheology, *Polymer,* 48(15), 4492-4502.

[31] **Reddy, M.M., Gupta, R.K., Bhacttacharya, S.N., and Parthasarathy, R.** (2007). Structure-Property Relationship of Melt Intercalated Maleated Polyethylene Nanocomposites, *Korea-Australia Rheology Jour.,*19(3), 133-139.

[32] **Ranade, A., Nayak, K., Fairbrother, D., and D`Souza, N.A.** (2005). Maleated and Non-Maleated Polyethylene-Montmorillonite Layered Silicate Blown Films: Creep, Dispersion and Crystallinity, *Polymer,* 46(18), 7323-7333.

[33] **Li, S., Wang, C., Chu, F., Xia, L., and Xu, Y.** (2013). Effect of Compatibilizers on Composites of Acorn Shell Powder and Low Density Polyethylene, *Bioresources,* 8 (4), 5817-5825.

[34] **Supri, A.G., Ismail, H., and Shuhadah, S.** (2010). Effect of Polyethylene Grafted Maleic Anhydride (PE-g-MAH) on Properties of Low Density Polyethylene/Eggshell Powder (LDPE/ESP) Composites, *Polymer-Plastic Tech. and Eng.,* 49 (4), 347-353.

[35] **Supri, A.G., Tan, S.J., and Yeng, T.S.** (2013). Properties of Chicken Feather Fiber-Filled Low Density Polyethylene Composites: The Effect of Polyethylene Grafted Maleic Anhydride, *Polymer-Plastic Tech. and Eng.,* 52 (5), 495-500.

[36] **Yilgor, E. and Yilgor, I.** (2013). Silicone Containing Copolymers: Synthesis, Properties and Applications , *Progress in Polymer Science*.

[37] **Yilgor, I. and McGrath, J.E.** (1988). Polysiloxane Containing Copolymers: A Survey of Recent Developments, *Adv. Polym. Sci,* 86, 1-86.

[38] **Yuan, Y. and Lee, T.R.** (2013). Contact Angle and Wetting Properties, in Surface Science Techniques, *Springer,* 51, 3-34, ISBN: 978-3-642-34243-1.

[39] **Arunvisut, S., Phummanee, S., and Somwangthanaroj, A.** (2007). Effect of Clay on Mechanical and Gas Barrier Properties of Blown-Film LDPE/Clay Nanocomposites, *Adv. Polym. Sci,* 106(4), 2210-2217.

[40] **Khalili, S., Masoomi, M., and Bagheri, R.** (2012). The Effect of Organo-Modified Montmorillonite on Mechanical and Barrier Properties of LLDPE/LDPE Blend Films, *Jour.Plast. Film and Sheeting,* 29(1), 39-55.

[41] **Horst, M.F., Quinzani, L.M., and Failla, M.D.** (2014). Rheological and Barrier Properties of Nanocomposites of HDPE and Exfoliated Montmorillonite, *Jour.Thermoplastic Composite Mat.,* 27(1), 106-125.

[42] **Stoeffler, K., Lafleur, P.G., and Denault, J.** (2008). The Effect of Clay Dispersion on the Properties of LLDPE/LLDPE-g-MA/Montmorillonite Nanocomposites, *Polym. Eng. Sci,* 48(12), 2459-2473.

[43] **Liu, S.P, Lafleur, and Tu, L.C.** (2008). Studies on Mechanical Properties of Dispersing Intercalated Silane Montmorillonite in Low Density Polyethylene Matrix, *International. Communications in Heat and Mass Transfer,* 38(7), 879-886.

[44] **Liang, G, Xu, J., and Xu, W.** (2004). PE/PE-g-MAH/Org-MMT Nanocomposites. II.Nonisothermal Crystallization Kinetics, *Appl. Polym. Sci,* 91(5), 3054-3059.

[45] **Morawiec, J., Pawlak, A., Slouf, M., Galeski, A., Piorkowska, E., and Krasnikowa, N.** (2005). Preperation and Properties of Compatibilized LDPE/Organo-Modified Montmorillonite Nanocomposites, *Eur. Polym. Jour,* 41(5), 1115-1122.

[46] **Wang, K.H, Choi, M.H., Koo, C.M., Choi, Y.S., and Chung, I.J.** (2001). Synthesis and Characterization of Maleated Polyethylene/Clay Nanocomposites, *Polymer.,* 42(24), 9819-9826.

[47] **Burnside, S.D. and Giannelis, E.P.** (1995). Synthesis and Properties of New Poly(Dimethyl Siloxane) Nanocomposites, *Chem. Mater.,* 7(9), 1597-1600.

[48] **Camenzind, A., Schweizer, T., Sztucki, M., and Pratsinis, S.** (2010). Structure and Strength of Silica-PDMS Nanocomposites, *Polymer,* 51(8), 1796-1804.

[49] **Ma, J., Xu, J., Ren, J.H., Yu, Z.Z., and Mai, Y.W.** (2003). A New Approach to Polymer/Montmorillonite Nanocomposites, *Polymer,* 44(16), 4619-4624.

[50] **Schmidt, D.F., Clement, F., and Giannelis, E.P.** (2006). On the Origins of Silicate Dispersion in Polysiloxane/Layered Silicate Nanocomposites, *Adv. Func. Mat.,* 16(3), 417-425.

[51] **Ma, J., Xu, J., Yu, Z.Z., Kuan, H.C., Dasari, A., and Mai, Y.W.** (2005). A New Strategy to Exfoliate Silicone/Rubber Clay Nanocomposites, *Macro. Rapid Comm.,* 26(10), 830-833.

[52] **Wang, J., Chen, Y., and Jin, Q.** (2006). Preparation and Characteristics of a Novel Silicone Rubber Nanocomposites Based on Organophilic Montmorillonite, *High Perf. Polym,* 18(3), 325-340.

[53] **Kong, Q., Hu, Y., Song, L., Wang, Y., Chen, Z., and Fan, W.** (2006). Influence of Fe-MMT on Crosslinking and Thermal Degradation in Silicone Rubber/Clay Nanocomposites, *Polym. Adv. Tech.,* 17(6), 463-467.

[54] **Wang, S., Long, C., Wang, X., Li, Q., and Qi, Z.** (1998). Synthesis and Properties of Silicone Rubber/Organomontmorillonite Hybrid Nanocomposites, *Jour. Appl. Polym. Sci.,*69(8), 1557-1561.

[55] **Jana, R.N., Bhunia, H.P., and Nando, G.B.** (1997). An Investigation into the Mechanical Properties and Curing Kinetics of Blends of Low-Density

Polyethylene and Polydimethyl Siloxane Rubber, *Thermochimica Acta,* 302(1-2), 1-9.

[56] **Jana, R.N., Bhattacharya, A.K., Nando, G.B., and Gupta, B.R.** (2002). Compatibilized Blends of Low-Density Polyethylene and Polydimethyl Siloxane Rubber, *Kautsch. Gummi Kunstst.,* 55(12), 660-664.

[57] **Jana, R.N. and Nando, G.B.** (2005). Rheological Behaviour of Low-Density Polyethylene (LDPE) and Polydimethyl Siloxane Rubber (PDMS) Blends, *Jour. Elas. Plast.,* 37(2), 149-168.

[58] **Giri, R., Naskar, K., and Nando, G.B.** (2012). Effect of Electron Beam Irradiation on Dynamic Mechanical, Thermal and Morphological Properties of LLDPE and PDMS Rubber Blends, *Radia. Phys. Chem.,* 81(12), 1930-1942.

[59] **Zhu, R., Hoshi, T., Muroga, Y., Hagiwara, T., Yano, S., and Sawaguchi, T.** (2013). Microstructure and Mechanical Properties of a Polyethylene / Polydimethylsiloxane Composite Prepared Using Supercritical Carbon Dioxide, *Appl. Polym. Sci.,* 127(5), 3388-3394.

[60] **Fasulo, P.D., Rodgers, W.R., Ottaviani, R.A., and Hunter, D.L.** (2004). Extrusion Processing of TPO Nanocomposites, *Polym.Eng. Sci,.* 44(6), 1036-1045.

[61] **Mehrabzadeh, M. and Kamal, M.R.** (2004). Melt Processing of PA-66/Clay, HDPE/Clay and HDPE/PA-66/Clay Nanocomposites, *Polym.Eng. Sci,.* 44(6), 1152-1161.

[62] **ISO 1183** (2012). Methods for Determining Density of Non-Cellular Plastics, *International Standard Organization.*

[63] **Crawford, R.J.** (1998). Plastic Engineering, 3rd Edition, *Butterworth-Heinemann,* ISBN: 978-0-7506-3764-0.

[64] **ISO 1133** (2011). Determination of the Melt Mass-Flow Rate (MFR) and the Melt Volume-Flow Rate (MVR) of Thermoplastics, *International Standard Organization.*

[65] **ISO 527** (2012). Determination of Tensile Properties, *International Standard Organization.*

[66] **ISO 180** (2000). Determination of Izod Impact Strength, *International Standard Organization.*

[67] **ISO 868** (2003). Determination of Indentation Hardness by Means of a Durometer (Shore Hardness), *International Standard Organization.*

[68] **ISO 11357** (2009). Differenttial Scanning Calorimetry (DSC), *International Standard Organization.*

[69] **Cheremisinoff, N.P.** (1996). Polymer Characterization Laboratory Techniques and analysis, *William Andrew,* ISBN: 978-0-8155-1403-9.

[70] **Run, M., Jungang, G., and Zhiting, L.** (2005). Nonisothermal Crystallization and Melting Behaviour and of mPE/LLDPE/LDPE ternary blends, *Thermochimica Acta,* 429 (2), 171-178.

[71] **Babiker, M.E., Xi, Z., Fan, S., Wang, G., and Muhuo, Y.** (2011). The Effect of Gelation Time on UHMWPE Sheet Prepared by Gel and Pressure-Induced Flow Processes, *Jour. Sci. Tech.,* 12 (2), 170-179.

[72] **Jungang, G., Shurun, L., and Zhiting, L.** (2003). Melting Behaviour and Nonisothermal Crystallization Kinetics of Metallocene Polyethylene, *Chem. Mag.,* 5 (10), 81-87.

[73] **Flory, P.J. and Vrij, A.** (1963). Melting Points of Linear-Chain Homologs, The Normal Paraffin Hydrocarbons, *Jour. American Chem. Soc.,* 85 (22), 3548-3553.

[74] **Lu, X., Zhang, C., and Han, Y.** (2004). LDPE Superhydrophobic Surface by Control of Its Crystallization Behaviour, *Macro. Rapid Comm.,* 25 (18), 1606-1610.

APPENDICES

APPENDIX A: Differential scanning calorimetry (DSC) diagrams of samples.

APPENDIX A

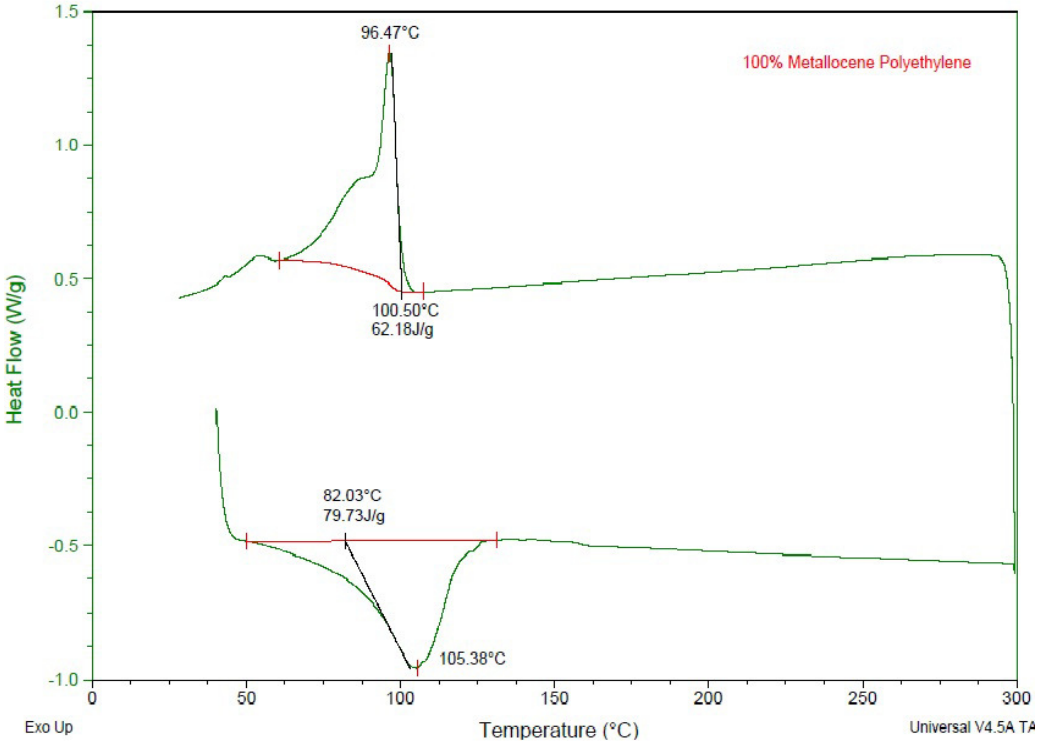

Figure A.1 : DSC diagram of 100% mPE containing sample (Sample 1).

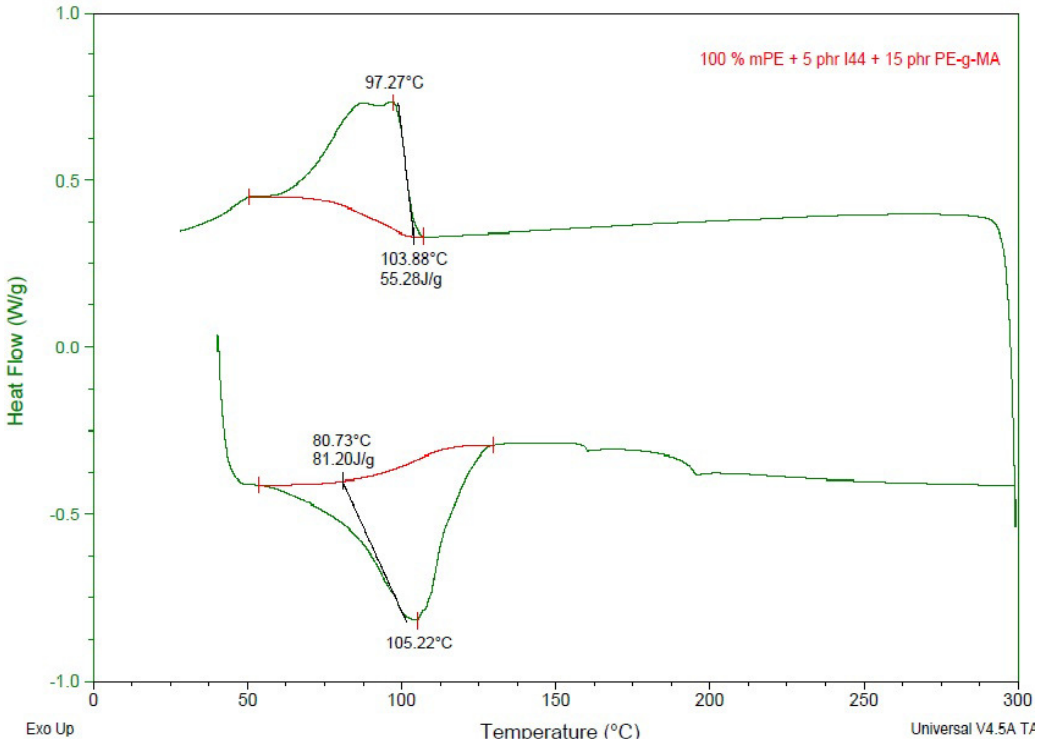

Figure A.2 : DSC diagram of 100% mPE, 5 phr O-MMT and 15 phr PE-g-MA containing sample (Sample 2).

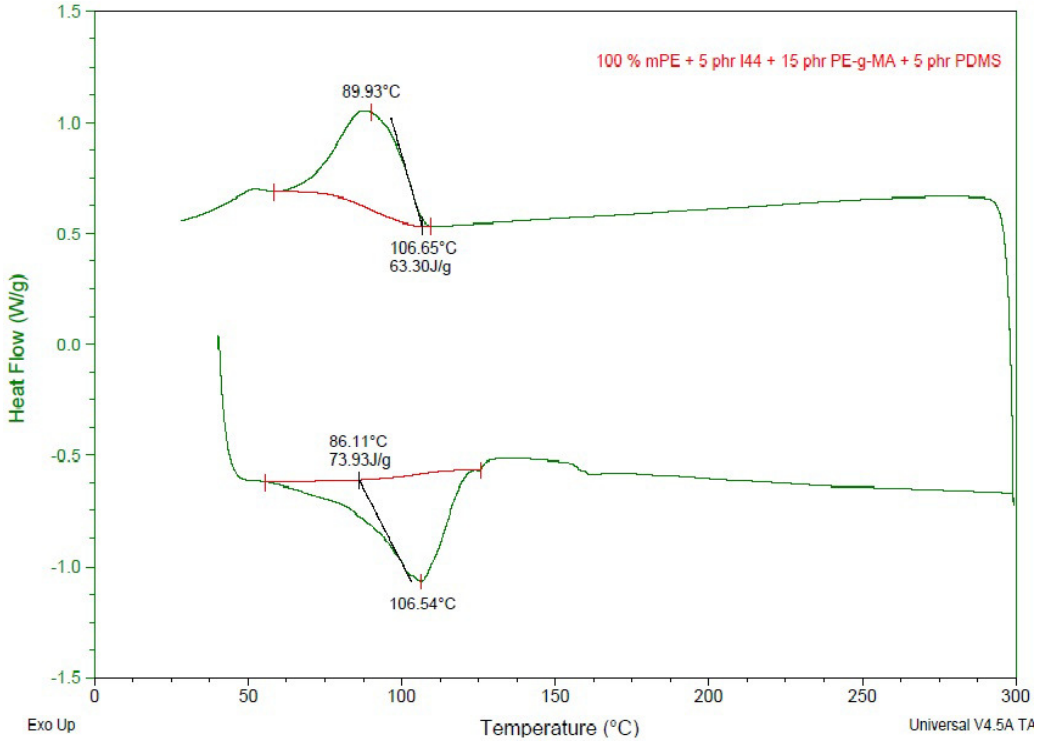

Figure A.3 : DSC diagram of 100% mPE, 5 phr O-MMT , 15 phr PE-g-MA, and 5 phr PDMS containing sample (Sample 3).

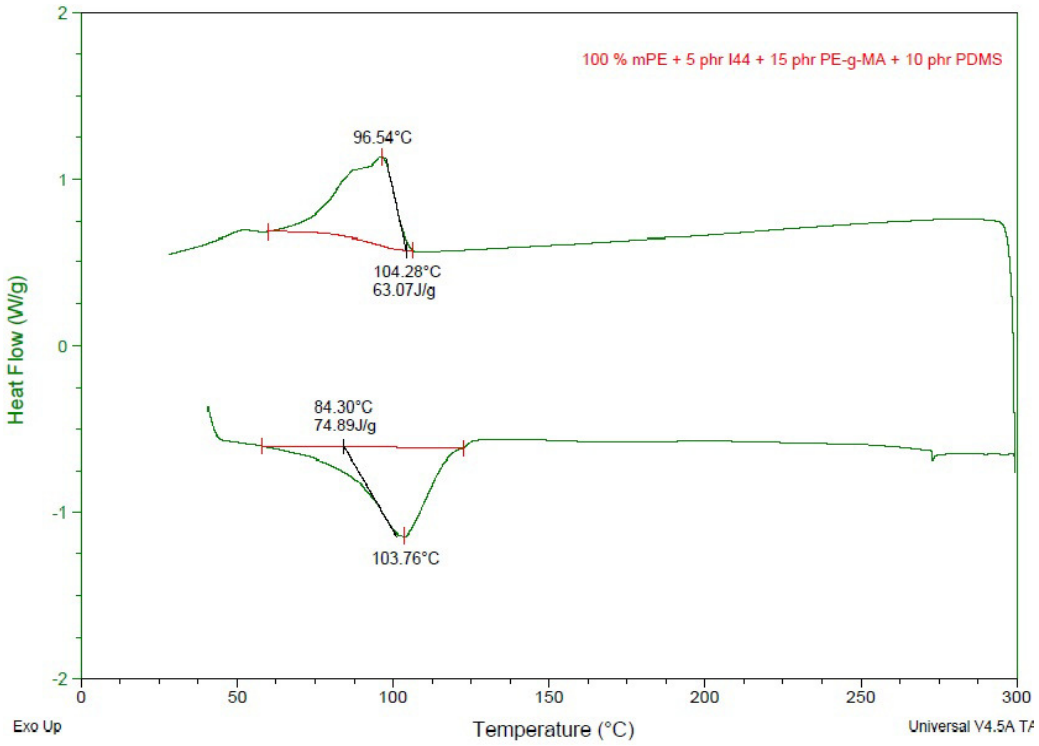

Figure A.4 : DSC diagram of 100% mPE, 5 phr O-MMT , 15 phr PE-g-MA, and 10 phr PDMS containing sample (Sample 4).

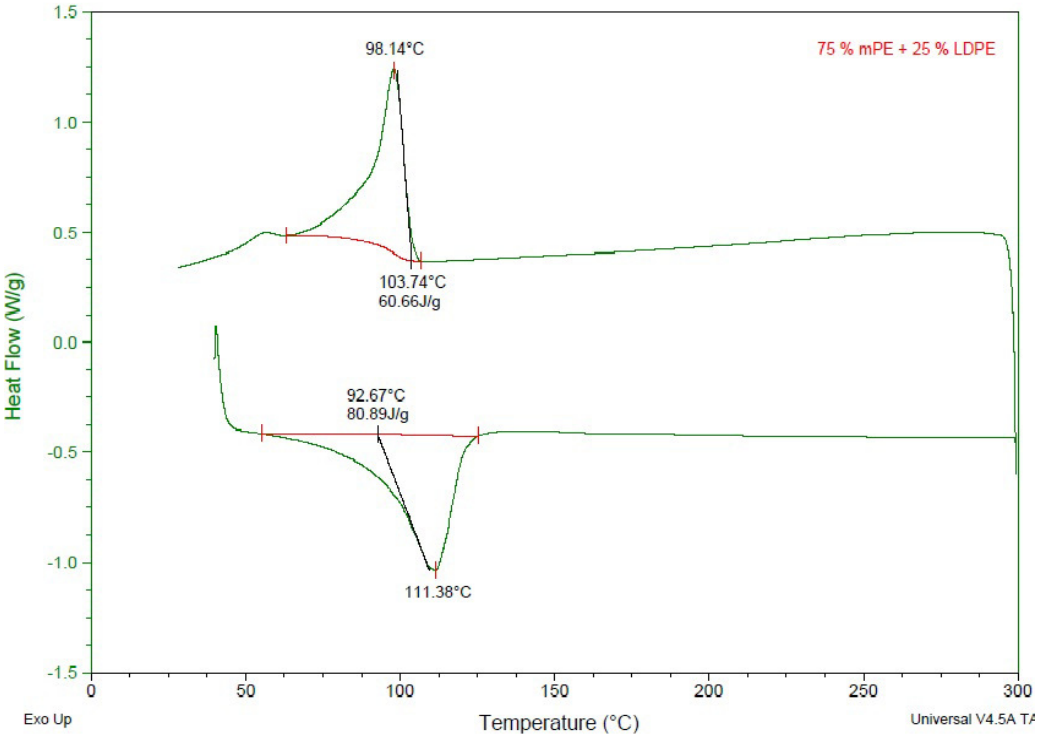

Figure A.5: DSC diagram of 75% mPE and 25% LDPE containing sample (Sample 5).

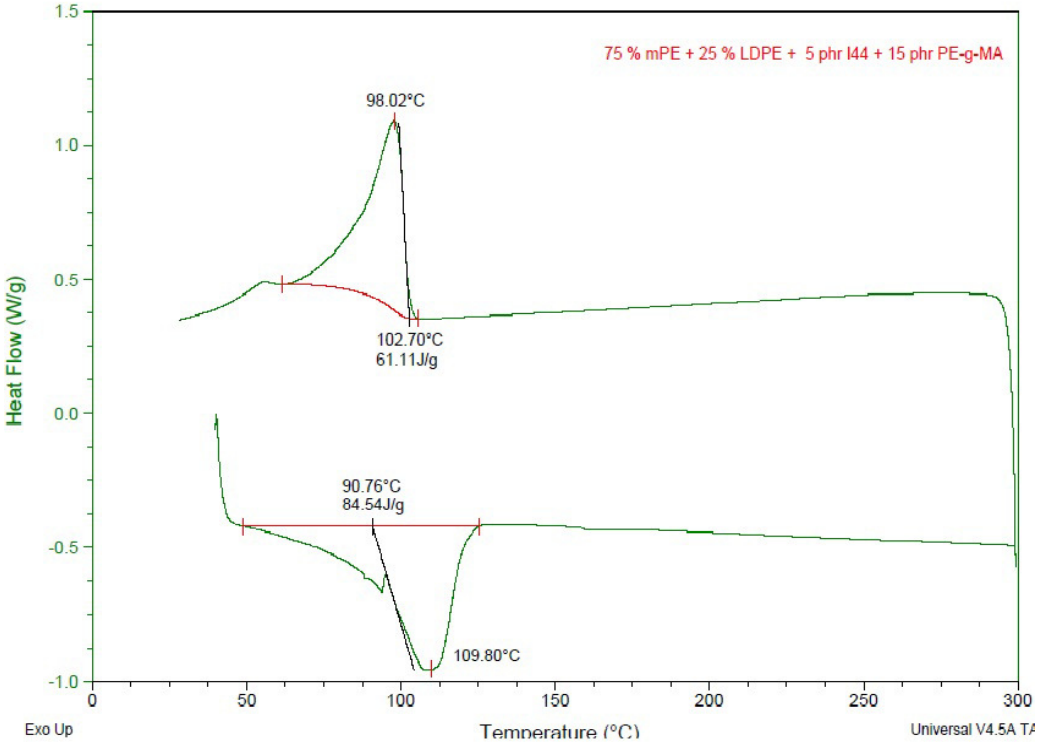

Figure A.6 : DSC diagram of 75% mPE, 25% LDPE, 5 phr O-MMT and 15 phr PE-g-MA containing sample (Sample 6).

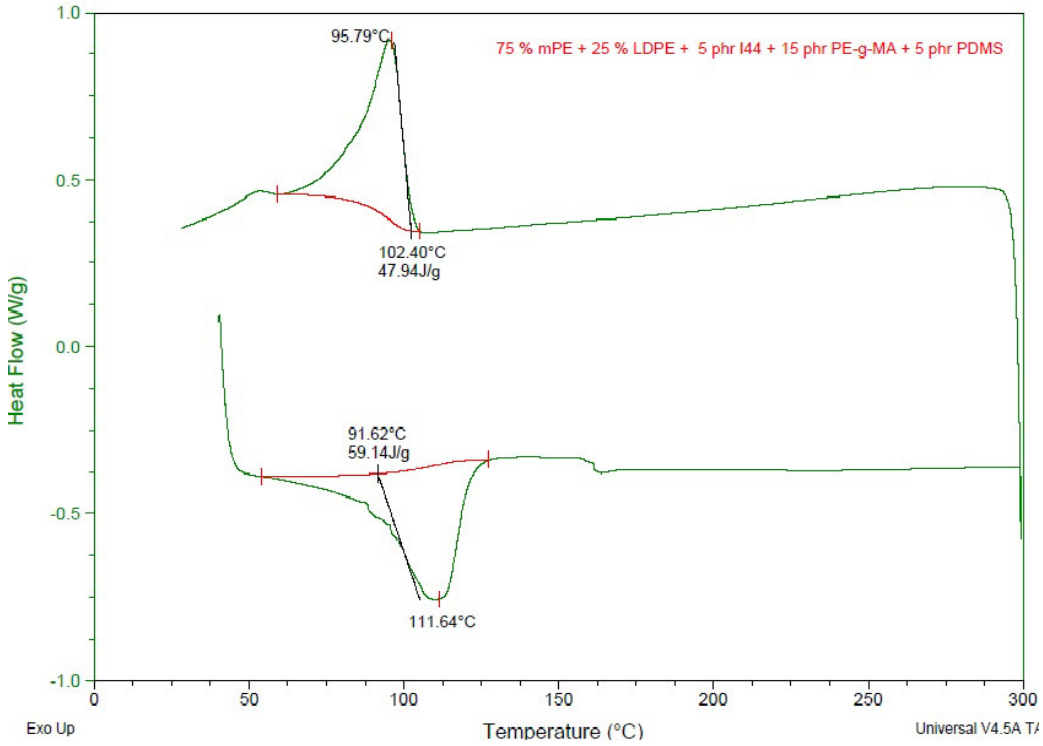

Figure A.7 : DSC diagram of 75% mPE, 25% LDPE, 5 phr O-MMT, 15 phr PE-g-MA, and 5 phr PDMS containing sample (Sample 7).

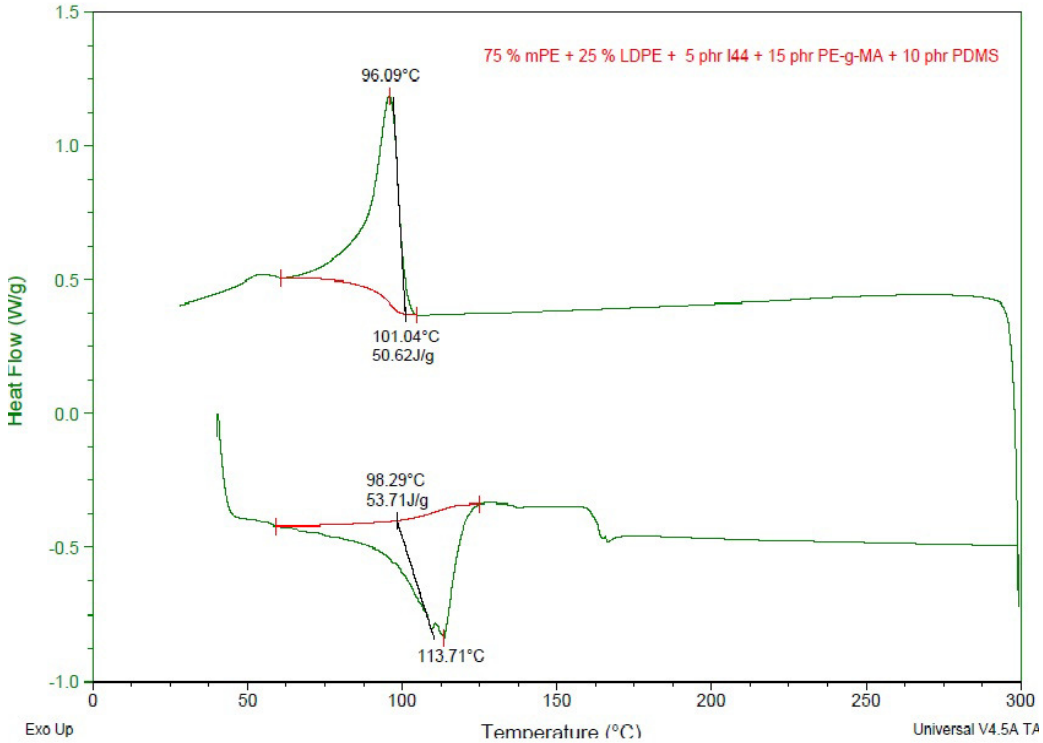

Figure A.8 : DSC diagram of 75% mPE, 25% LDPE, 5 phr O-MMT, 15 phr PE-g-MA, and 10 phr PDMS containing sample (Sample 8).

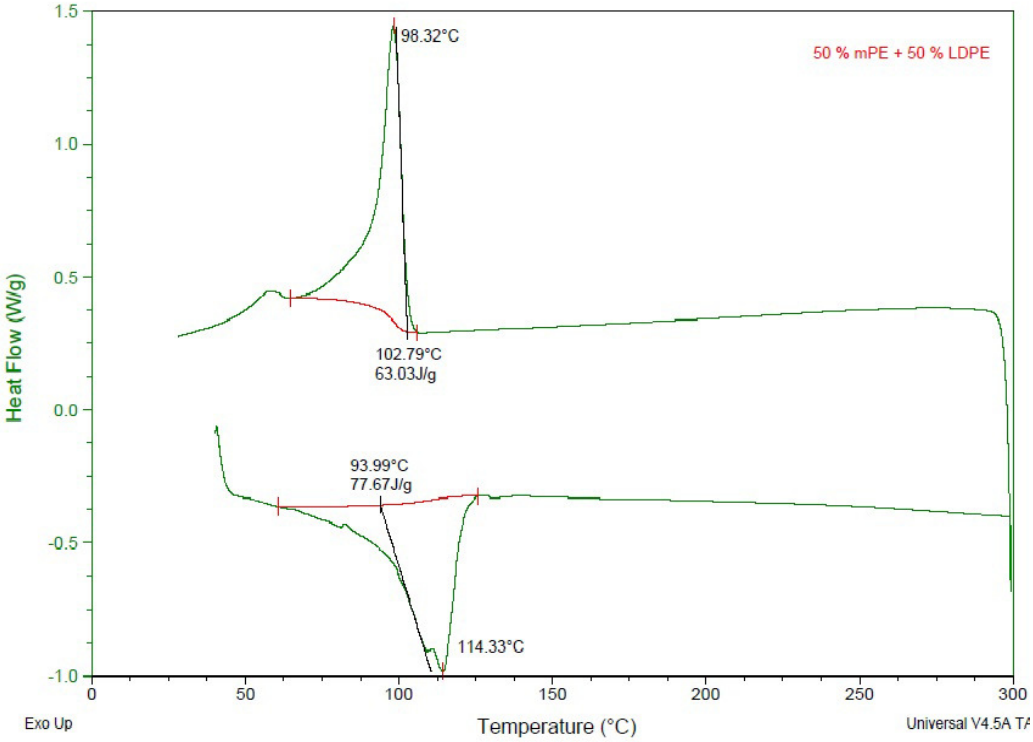

Figure A.9: DSC diagram of 50% mPE and 50% LDPE containing sample (Sample 9).

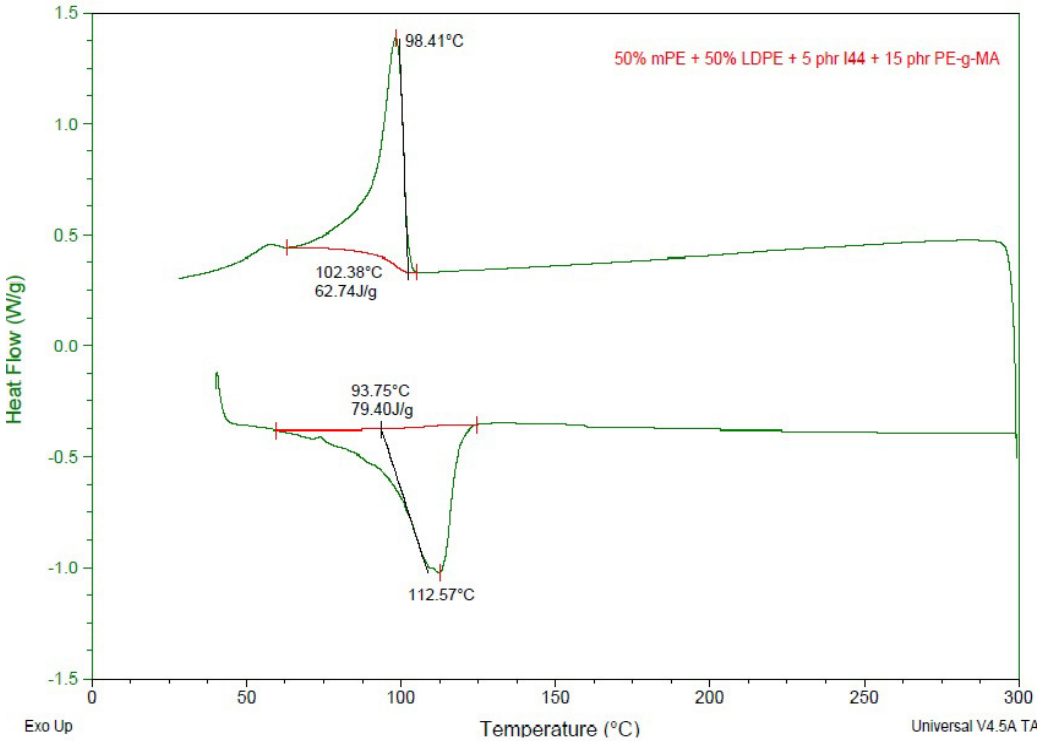

Figure A.10: DSC diagram of 50% mPE, 50% LDPE, 5 phr O-MMT and 15 phr PE-g-MA containing sample (Sample 10).

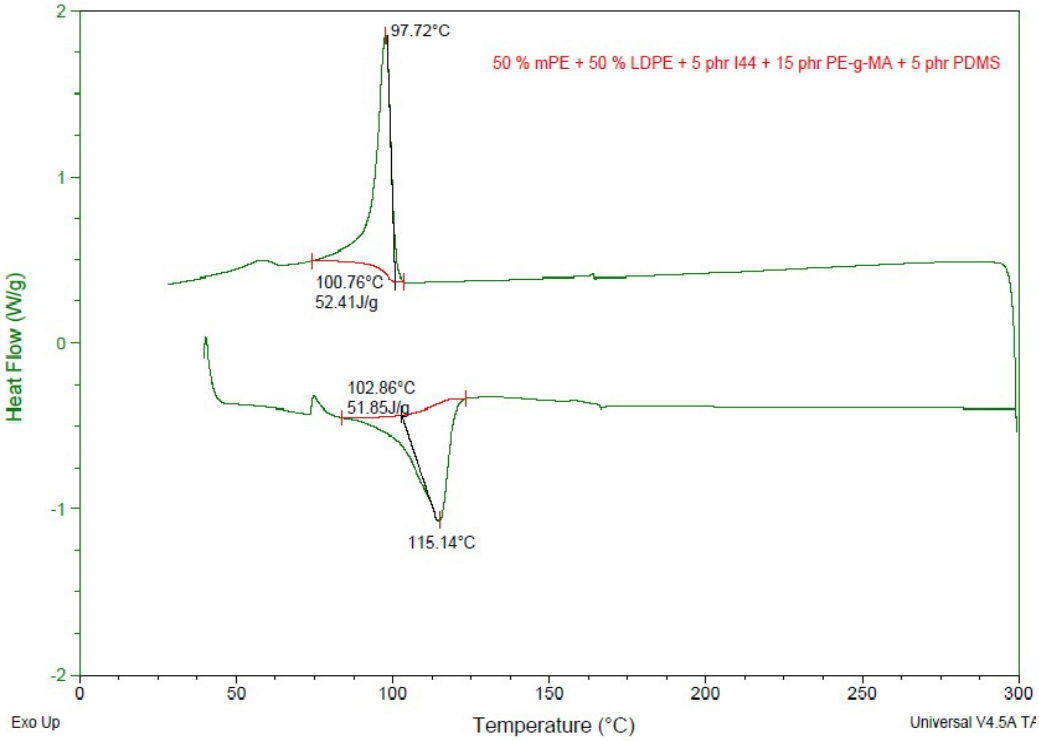

Figure A.11 : DSC diagram of 50% mPE, 50% LDPE, 5 phr O-MMT, 15 phr PE-g-MA, and 5 phr PDMS containing sample (Sample 11).

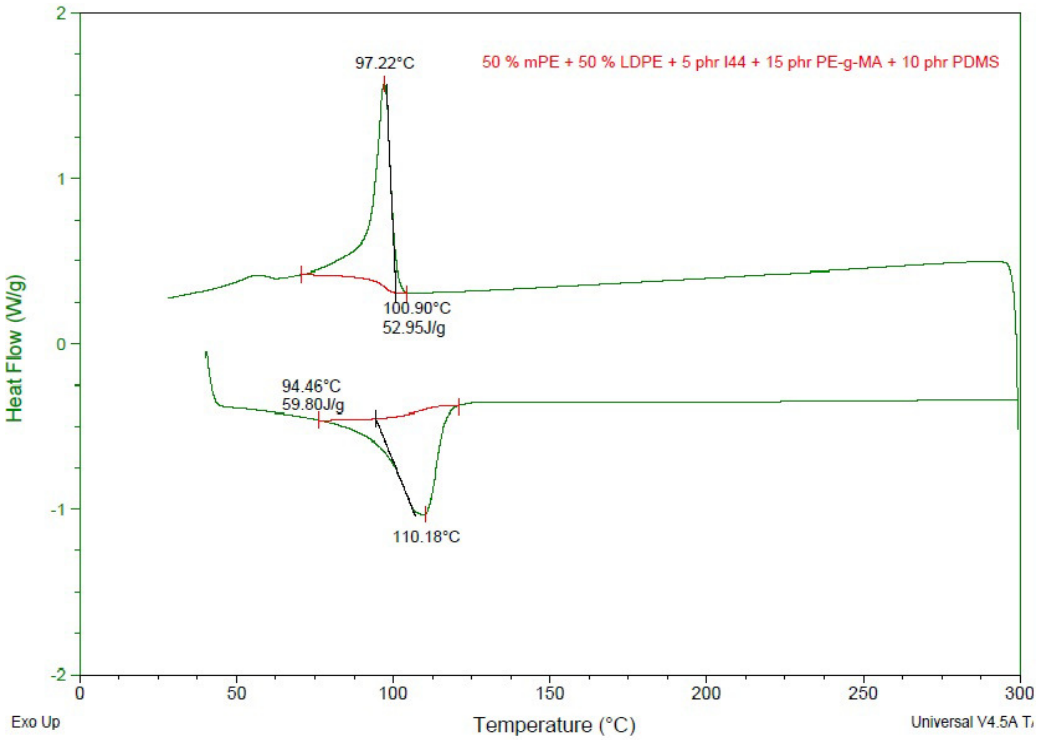

Figure A.12 : DSC diagram of 50% mPE, 50% LDPE, 5 phr O-MMT, 15 phr PE-g-MA, and 10 phr PDMS containing sample (Sample 12).

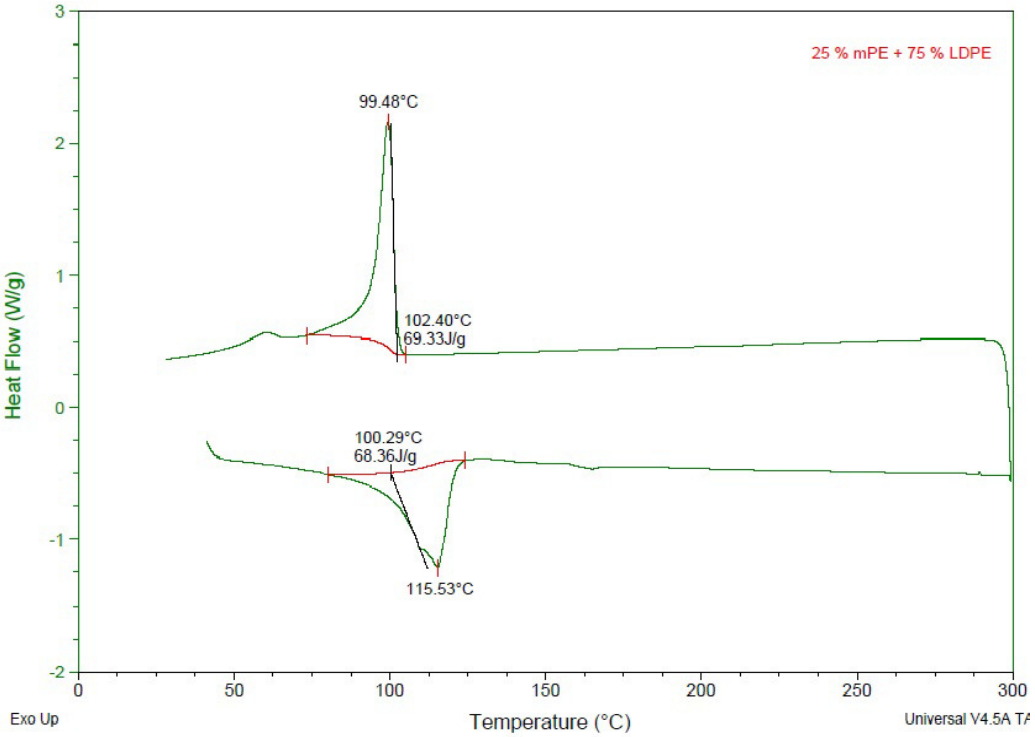

Figure A.13: DSC diagram of 25% mPE and 25% LDPE containing sample (Sample 13).

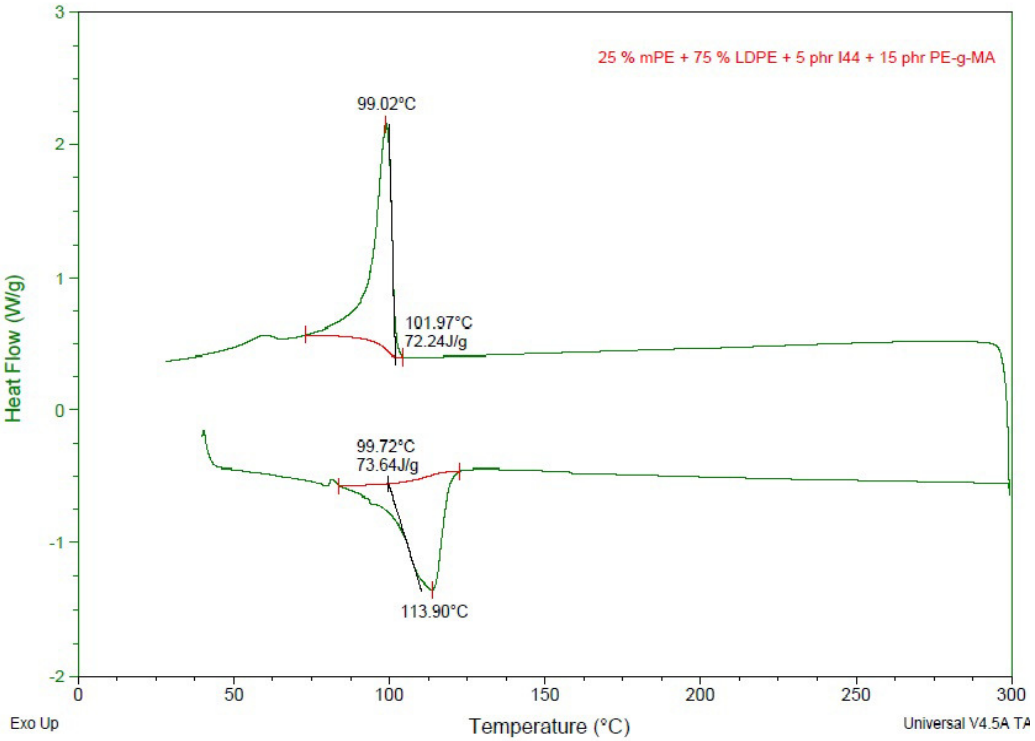

Figure A.14: DSC diagram of 25% mPE, 75% LDPE, 5 phr O-MMT and 15 phr PE-g-MA containing sample (Sample 14).

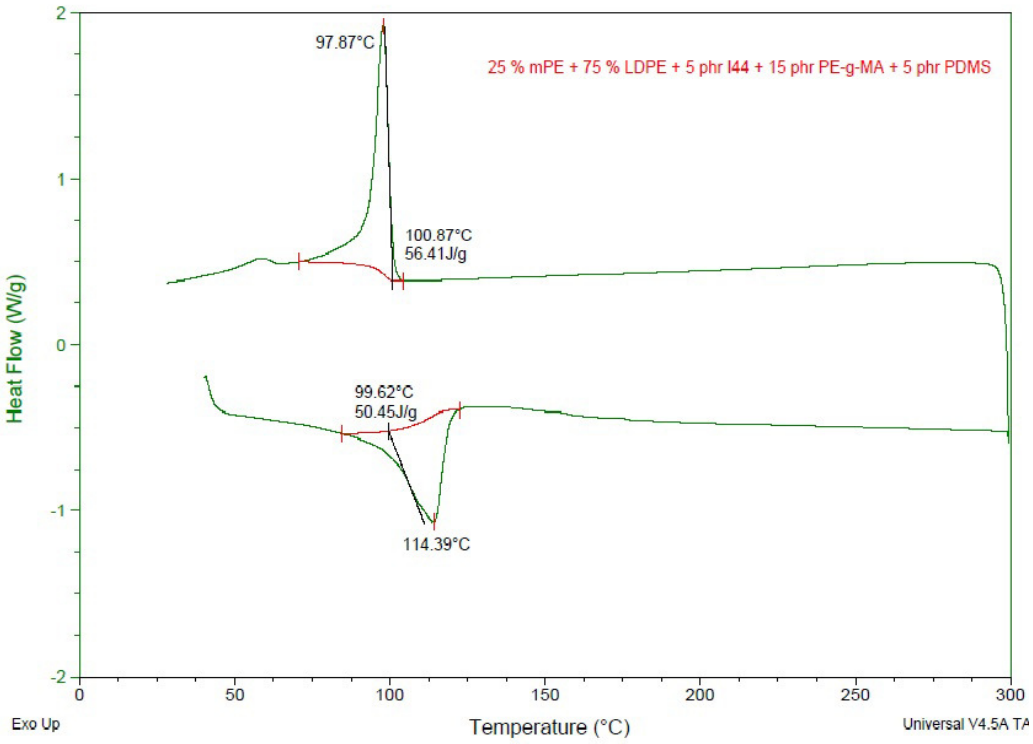

Figure A.15: DSC diagram of 25% mPE, 75% LDPE, 5 phr O-MMT, 15 phr PE-g-MA, and 5 phr PDMS containing sample (Sample 15).

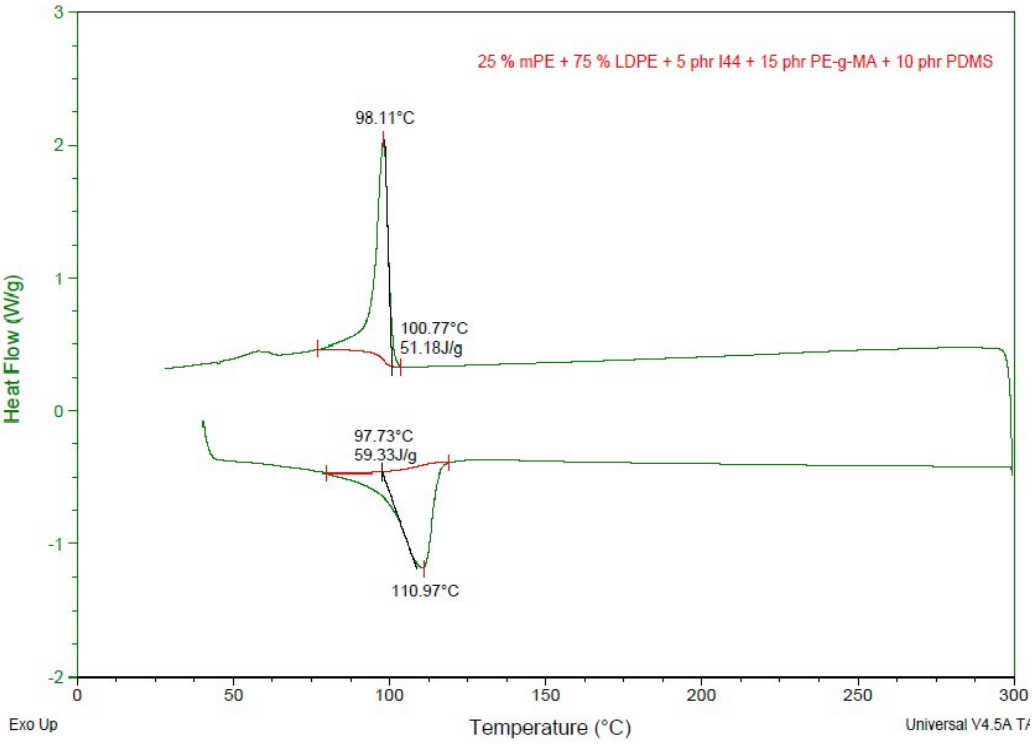

Figure A.16 : DSC diagram of 25% mPE, 75% LDPE, 5 phr O-MMT, 15 phr PE-g-MA, and 10 phr PDMS containing sample (Sample 16).

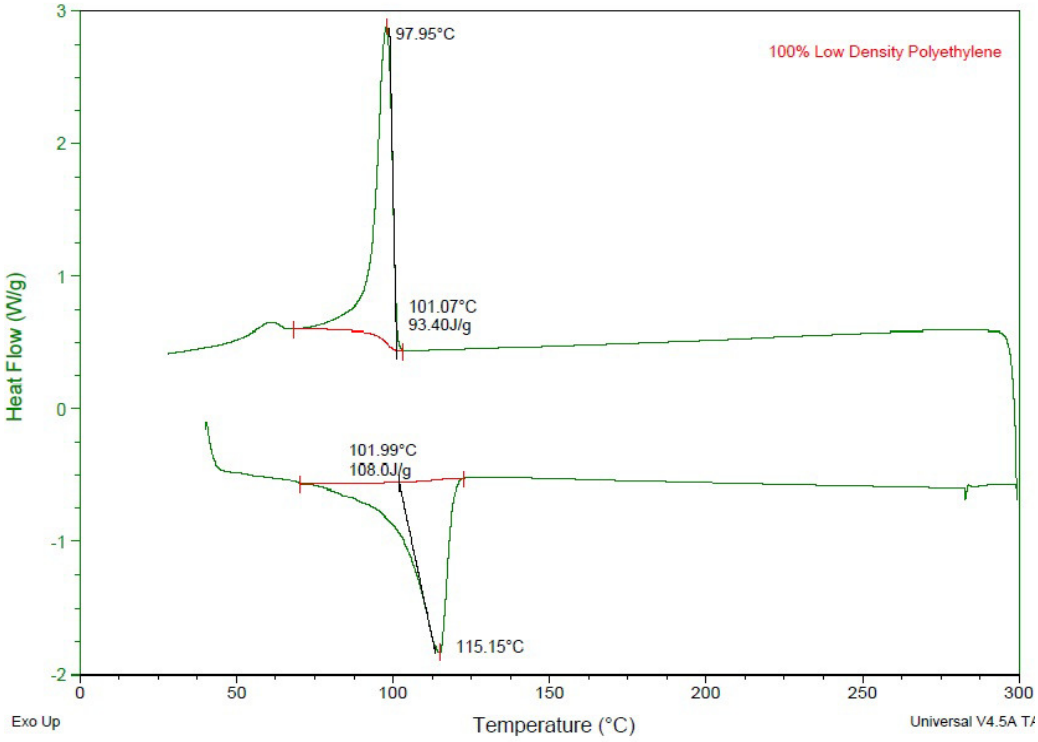

Figure A.17 : DSC diagram of 100% LDPE containing sample (Sample 17).

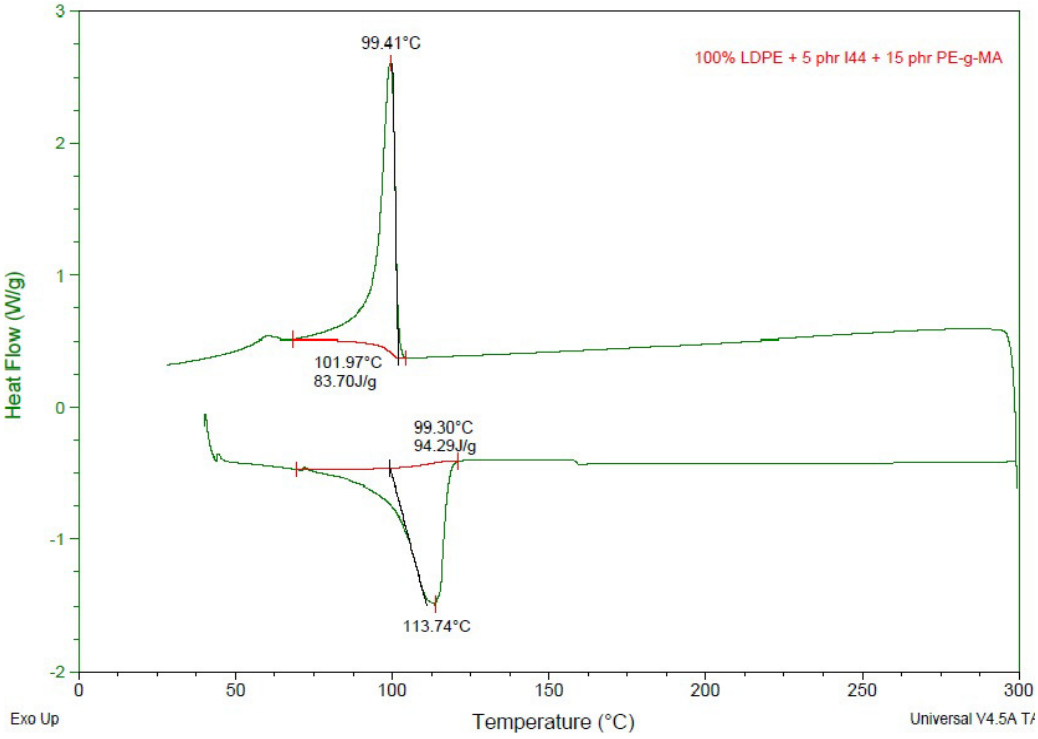

Figure A.18: DSC diagram of 100% LDPE, 5 phr O-MMT and 15 phr PE-g-MA containing sample (Sample 18).

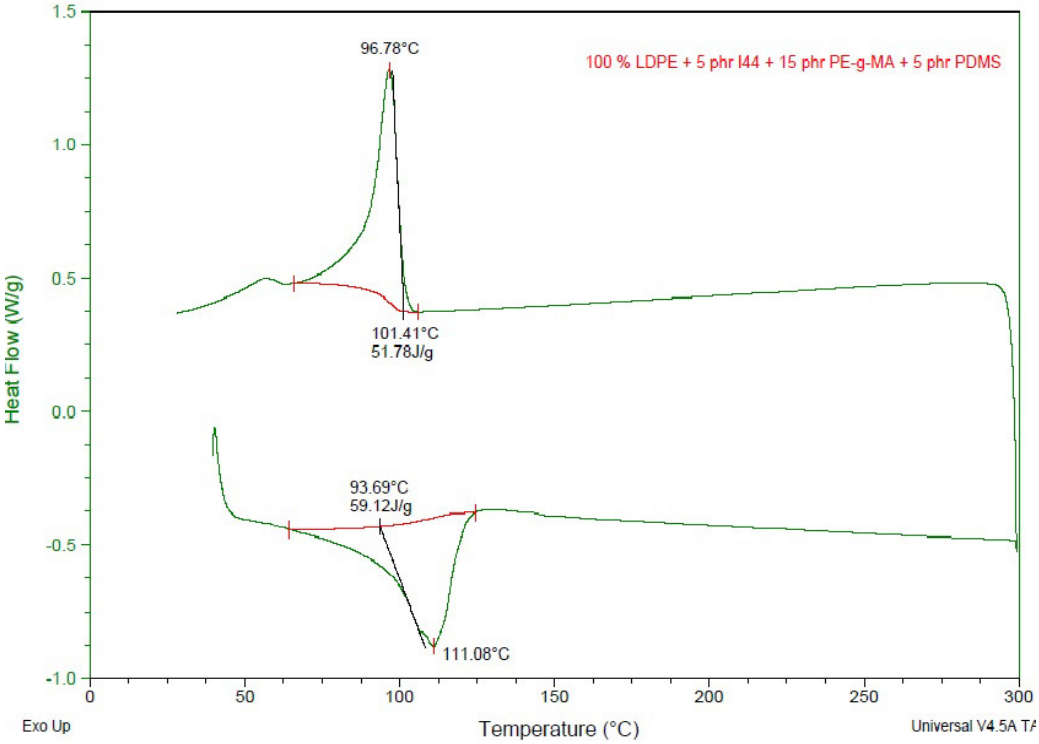

Figure A.19: DSC diagram of 100% LDPE, 5 phr O-MMT, 15 phr PE-g-MA and 5 phr PDMS containing sample (Sample 19).

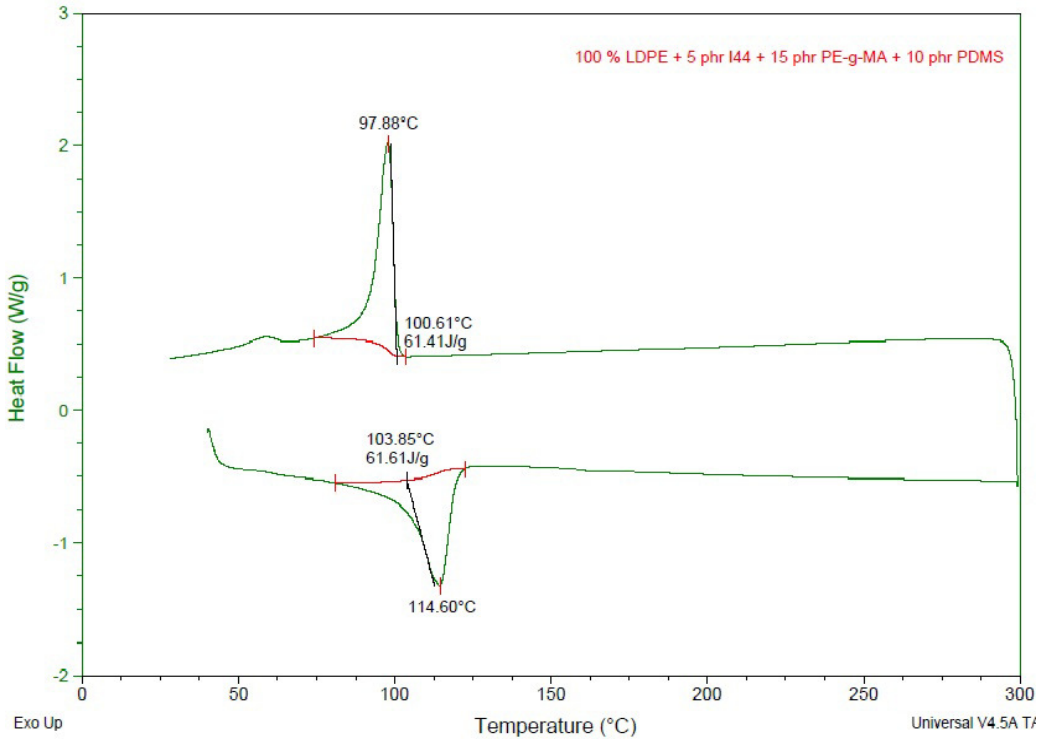

Figure A.20 : DSC diagram of 100% LDPE, 5 phr O-MMT, 15 phr PE-g-MA and 10 phr PDMS containing sample (Sample 20).

CURRICULUM VITAE

Name Surname: Duygu ÇAKIR

Place and Date of Birth: Rize –17.05.1988

Address: Şehit Filiz Soydemir Sok. Orkide Apt.No:4/15
Kozyatağı/Kadıköy/İSTANBUL

E-mail: dygcakir@hotmail.com

B.Sc.: Kocaeli University – Chemical Engineering